Regulation of neural stem cells

by a histone deacetylases inhibitor, valproic acid

（ヒストン脱アセチル化酵素阻害剤バルプロ酸による神経幹細胞制御）

Berry Juliandi

奈良先端科学技術大学院大学

バイオサイエンス研究科　分子神経分化制御研究室

（中島　欽一　教授）

平成 23 年 11 月 14 日提出

論 文 目 録

所　属 (主指導教員)	Molecular Neuroscience (Kinichi Nakashima)		
氏　名	Berry Juliandi	提　出	平成 23 年 10 月　25 日

学位論文の主たる部分を公表した論文
（題名、全著者名、公表時期、雑誌名、巻、ページ）

Induction of superficial cortical layer neurons from mouse embryonic stem cells by valproic acid. **Juliandi B**, Abematsu M, Sanosaka T, Tsujimura K, Smith A, Nakashima K. (2012) *Neurosci Res* 72: 23-31

参考論文
（題名、全著者名、公表時期、雑誌名、巻、ページ）

Chromatin remodeling in neural stem cell differentiation. **Juliandi B**, Abematsu M, Nakashima K. (2010). *Curr Opin Neurobiol* 20: 408-415.

Epigenetic regulation in neural stem cell differentiation. **Juliandi B**, Abematsu M, Nakashima K. (2010). *Develop Growth Differ* 52: 493-504.

Epigenetics, stem cells and cellular differentiation. *Handbook of Epigenetics: The New Molecular and Medical Genetics.* **Juliandi B**, Abematsu M, Nakashima K. (2010). Tollefsbol T, editor. Oxford: Elsevier Academic Press. pp. 315-328. ISBN 978-0-12-375709-8.

The ischial callosities of Sulawesi macaques. **Juliandi B**, Suryobroto B, Perwitasari-Farajallah D. (2009). *Am J Primatol* 71: 1021-1031.

所属 （主指導教員）	Molecular Neuroscience (Prof. Kinichi Nakashima)		
氏名	Berry Juliandi	提出	平成　23 年　11 月 04 日
題目	Regulation of neural stem cells by a histone deacetylases inhibitor, valproic acid （ヒストン脱アセチル化酵素阻害剤バルプロ酸による神経幹細胞制御）		

要旨

　　　Neural stem cells (NSCs) hold great promise for clinical treatment of neurological diseases and dysfunctions, owing to their ability to self-renew and their potential to generate various neural cell types. It is now established that epigenetic regulation contributes substantially, along with other mechanisms, to these properties of NSCs. However, our knowledge about the precise mechanisms that control NSCs differentiation is still in its infancy and many avenues remain to be explored.

　　　Histone deacetylases (HDACs) are the chromatin modifiers that can epigenetically regulate NSC fate choice. Activity of HDACs can be altered by chemicals such as valproic acid (VPA), a widely used anticonvulsant and mood stabilizer drug, which recently has been shown to have an HDACs inhibition properties. Although several studies have reported that taking VPA during early pregnancy could lead to developmental abnormalities of the future offspring, it is currently still allowed to be prescribed to pregnant patients if this drug is the only medication that adequately controls seizures.

　　　In the present study, I demonstrated that transient HDAC inhibition by VPA in mouse embryonic stem cell-derived NSCs enhances their neuronal differentiation. I further showed that the increasing neuronal population after VPA treatment includes a higher proportion of cut-like homeobox 1 (Cux1)-positive superficial-layer neurons, accompanied by a decreasing proportion of B-cell leukemia/lymphoma 11B (Bcl11b; also called Ctip2)-positive deep-layer neurons. Transient

prenatal exposure of VPA to mouse embryo during prominent neurogenic phase (embryonic day 12-14) also resulted in an enhancement of embryonic cortical neurogenesis. Neurogenesis was promoted using indirect pathway that form the intermediate progenitor cells, which mainly differentiated into Cux1-positive superficial-layer neurons, at the expense of direct pathway that generate Ctip2-positive deep-layer neurons. As a result, cortical laminarization at postnatal was disrupted, with an increase and decrease of superficial-layer (layer II-IV) and deep-layer (layer V-VI) thickness, respectively.

At their adult stages, I also found that VPA-treated mice showed poor performance in several learning and memory tasks. Further, I observed that prenatal VPA exposure impaired adult hippocampal NSC proliferation and differentiation, implying that these impairments contribute to those poor performances in learning and memory tasks. Interestingly, voluntary running improved adult hippocampal NSC proliferation and differentiation, and recovered some of the learning and memory deficiencies in VPA-treated mice.

VPA treatment also changes gene expression profile in embryonic telencephalon where NSCs reside. Similar change in gene expression profile was absent in embryo that was treated by VPA analog, valpromide, which is also an anticonvulsant and mood stabilizer drug but lack of HDACs inhibition properties, suggesting that the observed phenotypes found in this study were mainly caused by HDAC inhibition.

Taken together, these results imply that histone acetylation is an important factor for the NSC differentiation and developmental progression. It also suggests that epigenetic alteration in NSCs at embryonic stage can still persisted until adulthood, affecting learning and memory. Nevertheless, this alteration and its outcomes can be recovered, if not completely, by voluntary running.

List of contents

List of figures

List of tables

I. Introduction

I.1. Stem cells

Animal stem cell research began in the fields of embryology and of the biology of organs with inherent regenerative ability (Kempermann, 2006). Other organs with presumptive non-regenerative behavior, such as brain, heart, and lung, were thought to lack stem cells. However, there is increasing evidence that stem cells exist ubiquitously, from embryo to adult and in many organs of the body.

Embryogenesis in multicellular organisms starts with the fertilization of an ovum by a sperm to make a zygote. The zygote is totipotent: it has the potential to develop into a complete organism and also to make a trophoblast, a structure that will form the placenta. Initial divisions of the zygote yield the morulla and later on the blastocyst, which is composed of the trophoblast, inner cell mass, and blastocyst cavity (Keller, 2005). The inner cell mass can be isolated and cultured under specific conditions *in vitro* to generate embryonic stem cells (ESCs). ESCs are categorized as pluripotent cells, since they can generate cells of all body tissues except the trophoblast. This deficiency makes ESCs incapable of forming a complete organism upon implantation into the uterus. Nevertheless, ESCs have the capacity to generate somatic stem cells and subsequently differentiated cells of all three germ layers, ectoderm, mesoderm and endoderm, if they are pre-treated under optimal *in vitro* culture conditions (Fig. 1).

During subsequent developmental stages, each germ layer retains cells that possess stem cell features. These cells are described as being multipotent, because they can generate all progenitor and differentiated cell types within their particular restricted lineage. Neural

stem cells (NSCs) is an example of such multipotent cells. NSCs can differentiate into neurons, and glial cells (astrocytes and oligodendrocytes). The neuroepithelial cells lining the neural tube are considered as the primary NSCs. From this cell type, the central nervous system (CNS) develops in a sophisticated temporal and spatial sequence, governed in part by epigenetic mechanisms (Namihira et al., 2008; Okano & Temple, 2009; Juliandi et al., 2010a).
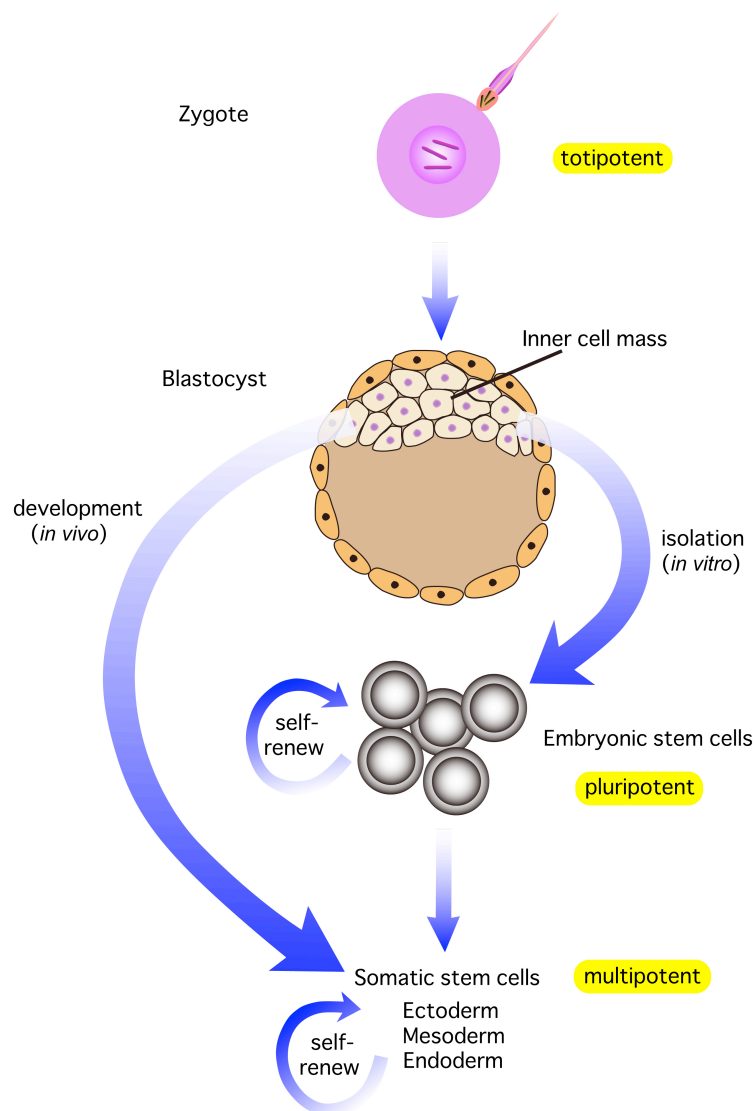
Fig. 1. Developmental potential of stem cells. The totipotent level exists after the egg is fertilized. After several mitotic divisions that lead to the blastocyst, the inner cell mass can be isolated *in vitro*, yielding pluripotent embryonic stem cells (ESCs). ESCs can self-renew and differentiate into multipotent somatic stem cells specific to each of the three germ layers.

I.2. Epigenetics of neural stem cells

The mammalian CNS consists of the brain and spinal cord, an organs which have a highly complex structure. These organs develop from common multipotent NSCs that line the neural tube. NSCs have the capacity to self-renew and to differentiate into distinct cell types such as neurons, astrocytes and oligodendrocytes. During the differentiation process, some NSCs can also produce immediate progeny that are known as neural progenitor cells (NPCs). NPCs have a more limited self-renewal capacity, and behave as transit amplifying cells that expand the number of newly differentiated cells owing to their higher rate proliferation than the more quiescent stem cells (Kempermann, 2006). Progression along the lineage from NSCs to its progenies is characterized by striking morphological and functional changes at each stage of lineage commitment. During brain development, NSCs in the ventricular zone (VZ) divide symmetrically in early gestation to increase their own numbers (Fujita 1963, 1986, 2003; Fig. 2). These cells then undergo neurogenesis through a mostly asymmetric division, giving rise to two distinct daughter cells: another NSC and a neuron (Noctor et al., 2001, 2004). As gestation proceeds, some NSCs can acquire the ability to divide asymmetrically to produce another NSC and a NPC, which then reside in the subventricular zone (SVZ) and almost all of these NPCs will subsequently divide symmetrically to produce two neurons (Noctor et al., 2004). Towards the end of the neurogenic phase, residual NSCs eventually acquire the multipotentiality to generate astrocytes and oligodendrocytes in addition to neurons (Qian et al., 2000; Fig. 2). Although the mechanisms of NSC fate determination are not yet fully understood, it is gradually becoming apparent that cell-intrinsic programmes such as epigenetic regulation, together with transcription factors (TFs) and extracellular cues, are deeply involved in this fate specification of NSCs.

3
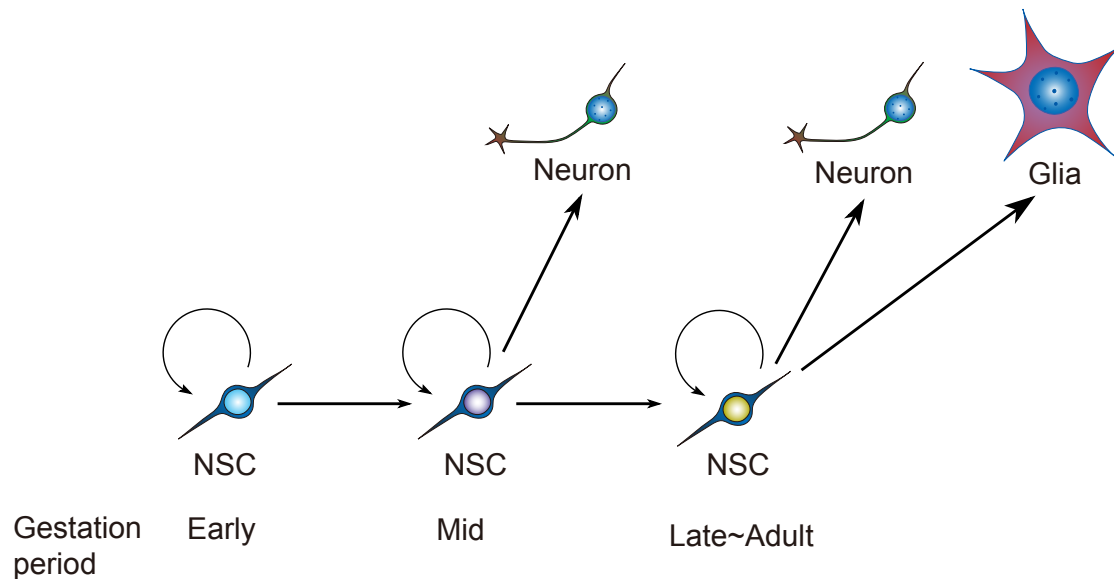
Fig. 2. Temporal development of neural stem cells (NSCs) exemplified by the ventricular zone of the cerebral cortex. Early-gestational NSCs divide symmetrically to increase their own number. These NSCs then undergo neurogenesis at midgestation, through mostly asymmetric divisions, each cell giving rise to two distinct daughter cells, another NSC and a neuron. As gestation proceeds, some NSCs can acquire the ability to divide asymmetrically to produce another NSC and a NPC (not depicted). Almost all of these NPCs will later divide symmetrically to produce two neurons. Towards the end of the gestational period, and perinatally, residual NSCs eventually acquire the multipotentiality to generate glia (astrocytes and oligodendrocytes) in addition to neurons.

The term 'epigenetic' refers to any heritable influence (in the progeny of cells or individuals) on chromosome or gene function that is not accompanied by a change in DNA sequence (Yoder et al., 1997). It includes processes such as DNA methylation, histone modification and noncoding RNA expression. Appropriate gene activation and/or silencing at each step of NSC progression is achieved by such epigenetic regulation. Several recent reports investigating the role of epigenetic mechanisms in the determination of NSC fate in the mammalian CNS, with a special emphasis on the developing forebrain, will be introduced below.

I.2.a. DNA methylation

One of the major epigenetic mechanisms in vertebrates, which regulates a diverse array of cellular events including developmental gene regulation, X chromosome inactivation, genome defense and genomic imprinting, is cytosine methylation of genomic DNA at CpG dinucleotides (Jaenisch & Bird, 2003). The DNA methylation pattern in the genome is established by a family of DNA methyltransferases (DNMTs). Maintenance of methylation patterns is achieved by a function of DNMT1 during DNA replication, while *de novo* methylation is primarily catalyzed by DNMT3a and DNMT3b. The DNMT family is essential for embryogenesis, as either single disruption of the *DNMT1* gene or compound disruption of *DNMT3a* and *DNMT3b* genes in mice led to drastic demethylation in the genome and the mice died at midgestation (Goto et al., 1994; Okano et al., 1999; Robertson & Wolffe, 2000).

Regulation of gene expression by DNA methylation can be achieved by two mechanisms. First, methylation of CpG dinucleotides affects DNA structure and can directly interfere with the binding of TFs to their target sequences (Takizawa et al., 2001); second, a more pervasive effect, methyl-CpG-binding domain (MBD)-containing protein family members can bind to genes with methylated CpG dinucleotides, thereby suppressing the genes' expression (Lewis et al., 1992; Cross et al., 1997; Nan et al., 1997).

The acquisition of multipotentiality in NSCs during development is tightly regulated by DNA methylation. As described above, NSCs at early gestation can only self-renew and then differentiate exclusively into neurons during midgestation (Fig. 2). Gradually, NSCs begin to differentiate into glia (astrocyte and oligodendrocyte) at late gestation (Fujita, 1986, 2003; Miller, 1996; Qian et al., 2000; Temple, 2001; Fig. 2). Two

5

well studied pathways that act synergistically to promote astrocytic differentiation are those activated by the interleukin-6 (IL-6) family of cytokines (such as leukaemia inhibitory factor (LIF), ciliary neurotrophic factor (CNTF) and cardiotrophin-1 (CT-1)) and bone morphogenetic protein (BMP) signaling (Bonni et al., 1997; Rajan & McKay, 1998; Nakashima et al., 1999a, 1999b; Sun et al., 2001; Barnabe-Heider et al., 2005; Fig. 3). LIF, CNTF and CT-1 can activate the Janus kinase (JAK)-signal transducer and activator of transcription (STAT) pathway upon binding to their cognate receptors (Stahl & Yancopoulos, 1994), while BMPs activate the downstream TF SMAD through their serine/threonine kinase type cognate receptors (Massague, 2000). Synergistic activation of astrocytic genes is achieved by the formation of a complex involving activated STAT3 and SMADs bridged by the transcriptional coactivator p300/CBP (Nakashima et al., 1999b; Fig. 3). It has been suggested that, in early- and midgestational NSCs, astrocytic gene promoters such as glial fibrillary acidic protein (*gfap*) are hypermethylated, a status which impedes binding of the STAT3-p300/CBP-SMADs complex to its target sequence and thus prevents these NSCs from differentiating into astrocytes even when the cells are stimulated by astrocyte-inducing cytokines (Takizawa et al., 2001; Fig. 4).

Mouse embryonic stem cells (mESCs) also do not express GFAP and remain in the undifferentiated state, even in the presence of LIF in its culture medium. Like NSCs at early- and midgestation, the *gfap* promoter is hypermethylated in mESCs (Shimozaki et al., 2005). Hypermethylation is maintained even after mESCs differentiate into endodermal and mesodermal lineages, and demethylation in this region only occurs when the cells are committed to a neural lineage that is capable of producing astrocytes (Shimozaki et al., 2005). *Gfap* promoter hypermethylation is also observed in adult tissues outside the nervous system,

6

such as liver, heart and femoral muscle (Takizawa et al., 2001). In contrast, the STAT3

binding site-containing *gfap* promoter in NSCs at late gestation is barely methylated, so that

upon LIF stimulation these NSCs can differentiate into astrocytes (Takizawa et al., 2001; Fig.

4).
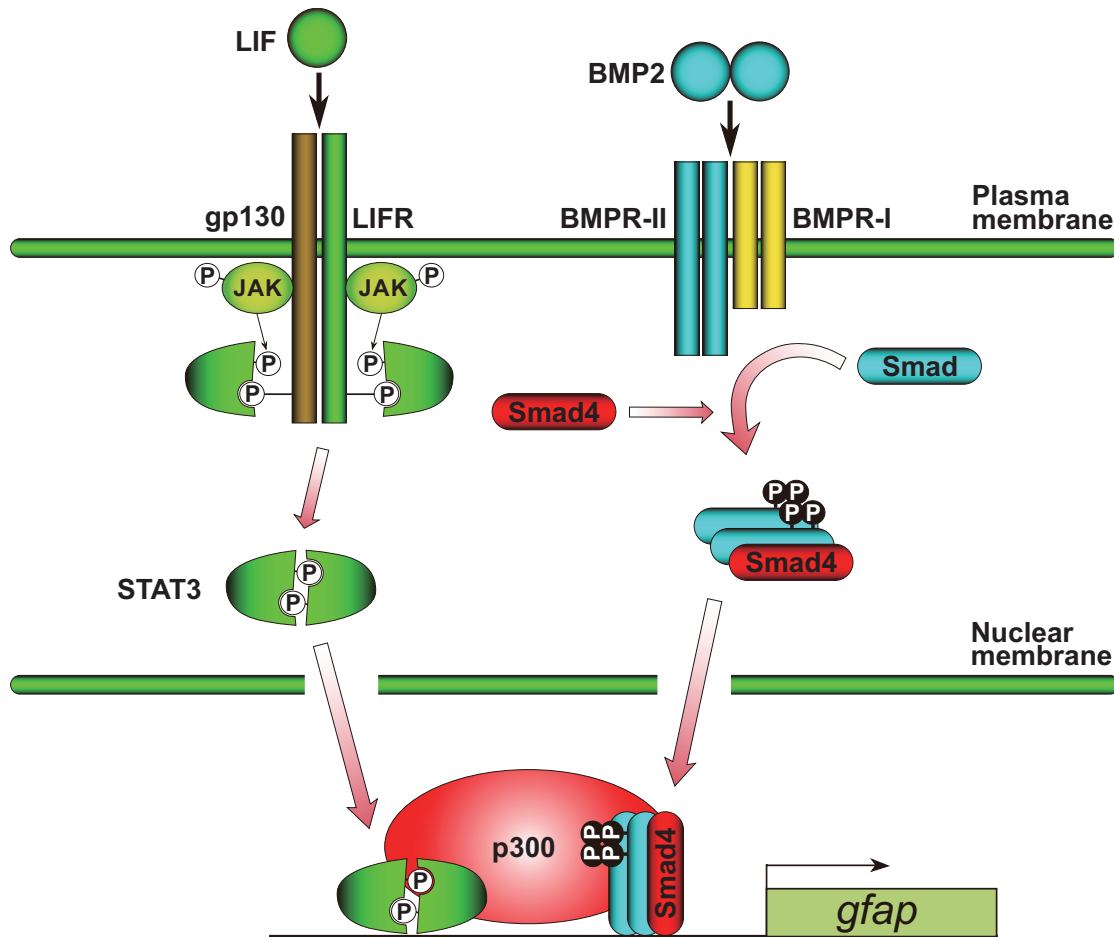
Fig. 3. Signaling crosstalk between two distinct cytokines to activate astrocytic genes. LIF, a member of the IL-6 cytokine family, binds to its specific receptor, LIFR, which dimerizes with a common signal transducer, gp130; this dimerization leads to activation of the JAK-STAT pathway. Activated STAT3 forms a homodimer and subsequently translocates into the nucleus. BMP2, a member of the TGF-β superfamily, signals through a heterotetrameric serine/threonine kinase receptor complex composed of two type I (BMPR-I) and two type II (BMPR-II) receptor molecules. Activated BMPRs phosporylate the downstream transcription factors Smad1, -5, and -8, which then bind to the common mediator Smad4 before accumulating in the nucleus. There, STAT3 and Smads form a complex bridged by the transcriptional coactivator p300/CBP to activate the transcription of astrocytic markers such as *gfap*.
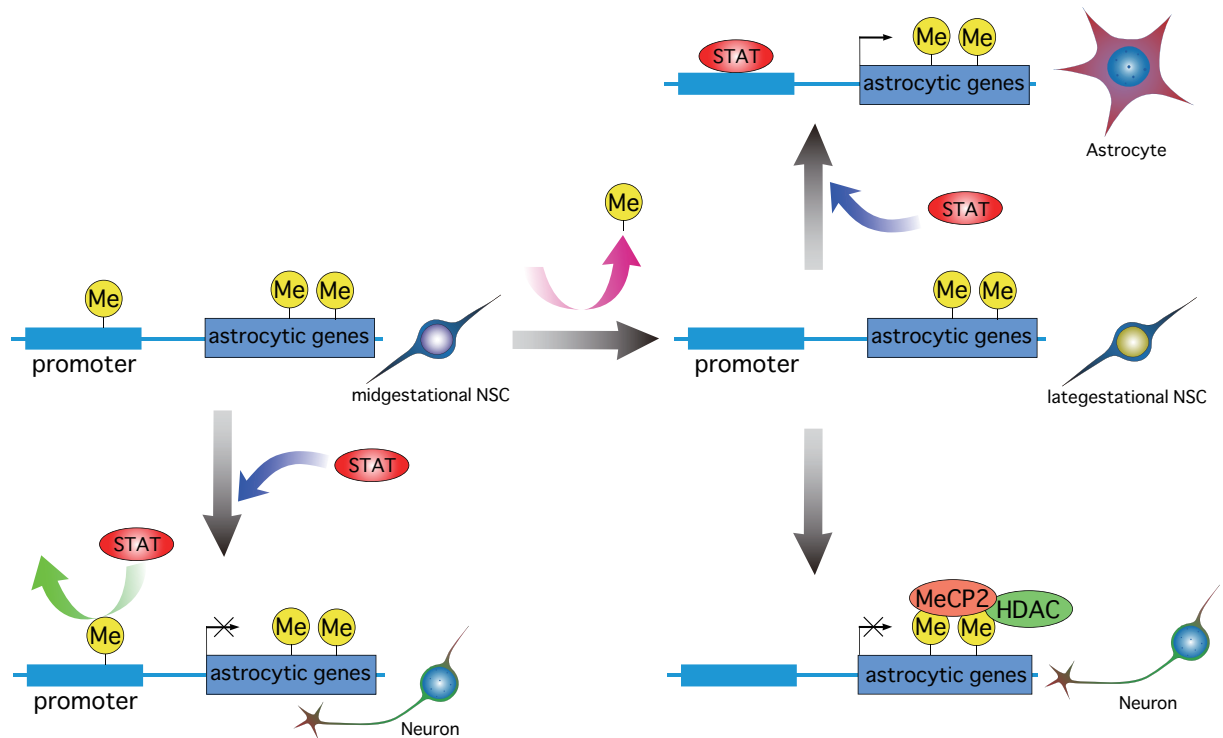
Fig. 4. Astrocytic gene methylation status during NSC development. Although STAT3 can be activated in midgestational NSCs, it cannot bind to astrocytic gene promoters such as *gfap* due to promoter hypermethylation, so these NSCs can only differentiate into neurons (left). As gestation proceeds, these promoters become demethylated, allowing STAT3 to bind and activate astrocytic genes, resulting in the differentiation of NSCs into astrocytes (upper right). MeCP2 blocks this activation in neurons (lower right).

DNA demethylation as gestation proceeds is not exclusive to the *gfap* promoter, but is common for astrocyte-specific genes. For example, the earlier astrocytic marker *S100β* also possesses a cytosine residue in its promoter which is highly methylated in mESCs but becomes demethylated as the cells differentiate into NSCs (Shimozaki et al., 2005). This demethylation also occurs at midgestation, coincident with the onset of *S100β* expression in the brain (Namihira et al., 2004). Furthermore, the genome-wide DNA methylation status of mid- and late gestational NSCs has recently been compared by a microarray profiling method (Hatada et al., 2008), confirming that many astrocytic genes become demethylated in late

stage NSCs (Fig. 4). Thus, it is apparent that DNA methylation plays an important role in defining the timing of NSC fate specification switch from neurogenesis to astrocytogenesis.

Although it is now clear that DNA demethylation determines the competency of astrocytic gene expression, the mechanisms underlying this process are not yet fully elucidated. The *gfap* promoter is hypermethylated at all developmental stages and in all lineages except for late-gestational NSCs and its progenies. Therefore, demethylation of the *gfap* promoter is temporally regulated and cell type-specific. The most likely candidate mechanism for DNA demethylation is the passive loss of CpG methylation due to successive rounds of DNA replication in the absence of DNMT1-catalyzed maintenance methylase activity (Bestor, 2000). After conditional deletion of *DNMT1* from the neural lineage in mouse, which led to hypomethylation of the genome, neural development was shown to be precociously shifted toward astroglial differentiation (Fan et al., 2005). Further, this precocious astrocytic differentiation was attributable not only of demethylation of the STAT3-binding site in the *gfap* promoter, but also of the elevation of overall JAK-STAT signaling activity, due to the rapid demethylation of gene promoters that are involved in the JAK-STAT pathway and consequent upregulation of the genes' expression. These data suggest that DNA methylation can regulate the timing and magnitude of astrocytic differentiation, through both direct inhibition of TFs binding to astrocytic genes promoter and modulation of JAK-STAT activity (Fan et al., 2005). However, recent studies suggest that active DNA demethylation occurs in vertebrates through DNA excision repair process which is medicated by several enzymatic machineries and non-enzymatic Gadd45 proteins (Ma et al., 2009).

Dynamic expression of the murine homologs of chicken ovalbumin upstream promoter transcription factors I and II (COUP-TFI/II) may also contribute to the demethylation of the astrocytic gene promoter. COUP-TFI/II expression is transiently upregulated in the early neurogenic period but decreases markedly before the onset of astrocytogenesis (Naka et al., 2008). Using a mESC-derived NSC culture which recapitulates *in vivo* mouse CNS development (Okada et al., 2008), Naka et al. (2008) showed that CpG methylation of the *gfap* promoter remained high after COUP-TFI/II composite knockdown and that the switch from neurogenesis to gliogenesis was thereby inhibited. COUP-TFI/II composite knockdown in the developing mouse forebrain also had the same effect. Taken together, these results indicate that COUP-TFI/II are important factors for *gfap* promoter demethylation, although the mechanism is not yet known.

Another contribution to *gfap* promoter demethylation might come from the progeny of early- and midgestational NSCs (Fig. 5). Several reports have indicated that neuronally committed NPCs and young neurons express Notch ligands (Campos et al., 2001; Kawaguchi et al., 2008; Yoon et al., 2008). Notch signaling is a conserved pathway from insects to mammals which contributes to cell-to-cell communication (Simpson, 1995; Nye & Kopan, 1995; Bray, 1998; Louvi & Artavanis-Tsakonas, 2006) and controls cell fate determination in the CNS (Lundkvist & Lendahl, 2001). Upon Notch activation by its ligands, the Notch intracellular domain (NICD) is released from the plasma membrane and translocates into the nucleus, where it converts a particular repressor complex into an activator complex (Wallberg et al., 2002; Nakayama et al., 2008). Namihira et al. (2009) confirmed that Notch ligands are indeed expressed in neuronally committed NPCs and young neurons, and that these ligands activate Nocth signaling in the residual NSCs (Fig. 5). Further, forced expression of NICD in

midgestational NSCs induced the upregulation of nuclear factor 1A (NF1A), which in turn accelerated demethylation of astrocytic gene promoters by preventing DNMT1 from binding to them (Fig. 5) and thus allowed precocious astrocytic differentiation in response to LIF stimulation (Namihira et al., 2009).
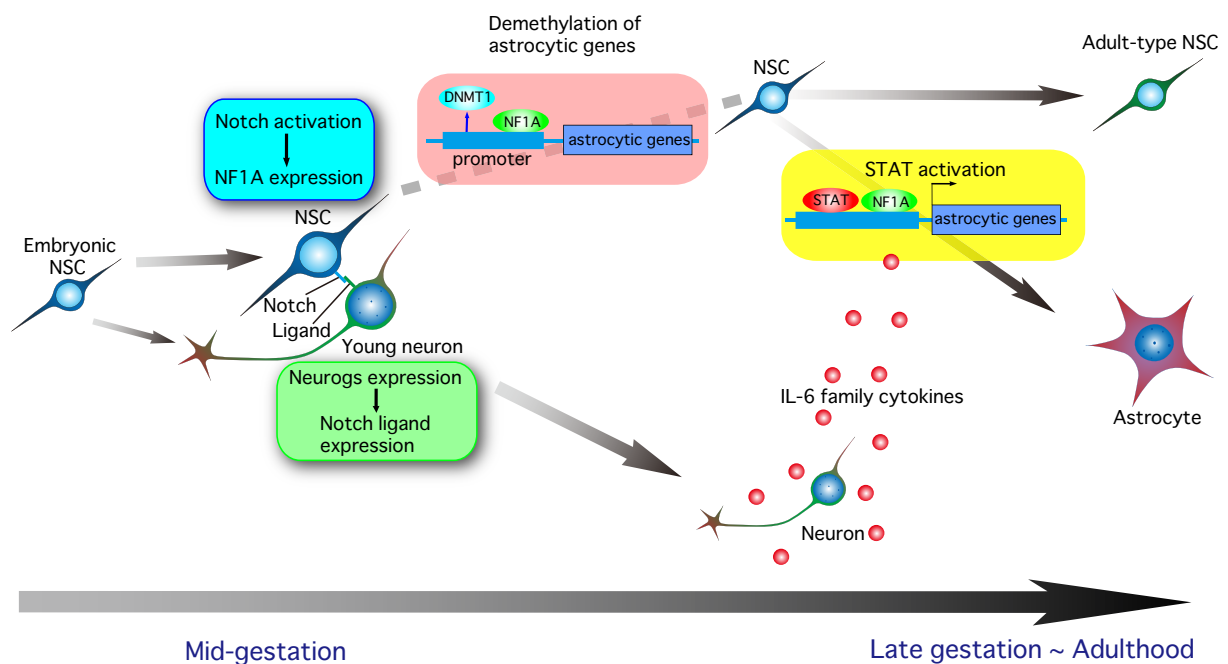
Fig. 5. Notch-induced demethylation of astrocytic genes. Activation of Notch signaling in residual NSCs by young neurons induces demethylation of astrocytic gene promoters by upregulation of NF1A and release of DNMT1 from astrocytic gene promoters. In turn, at late gestation, IL-6 family cytokines activate the STAT3 pathway and induce NSCs to differentiate into the astrocytic lineage.

Members of the MBD family have been also shown to influence NSC differentiation. MBD proteins are expressed predominantly in neurons, and not in astrocytes or oligodendrocytes, in the CNS (Coy et al., 1999; Jung et al., 2002; Shahbazian et al., 2002; Kishi & Macklis, 2004). As discussed above, late gestational NSCs have lost *gfap* promoter methylation and become competent to differentiate into astrocytes, in addition to neurons (Figs 2 and 4). However, it was later found that exon1 of *gfap* are hypermethylated in all

11

neural cell types - i.e., NSCs, neurons, astrocytes and oligodendrocytes, and only in neurons, methyl-CpG-binding protein 2 (MeCP2), a member of the MBD family, is highly expressed and binds to this methylated exon1 region of the gene (Setoguchi et al., 2006; Fig. 4). Therefore, even if STAT3 binds to the hypomethylated *gfap* promoter in neurons, GFAP expression and thus astrocyte differentiation is blocked by the presence of MeCP2 at exon1 (Setoguchi et al., 2006). In neurons, MeCP2 also binds to hypermethylated CpG sites around the transcription start site of *S100β*, thereby suppress its expression and consequently astrocyte differentiation. Although recent studies have shown that MeCP2 expression also occurs in astrocytes, it is at a very low level (Kohyama et al., 2008; Ballas et al., 2009). Indeed, ectopic expression of MeCP2 directs NSCs to become neurons and inhibits astrocytic differentiation, even in the presence of astrocyte-inducing cytokines such as LIF and BMP2 (Tsujimura et al., 2009). Interestingly, such cytokines, if applied simultaneously with ectopic expression of MeCP2, actually induce NSCs to produce more neurons by as yet unknown mechanisms. Ectopic expression of other MBD family members, such as MBD1, also inhibits astrocyte differentiation of NSCs, demonstrating some functional redundancy among MBD proteins (Setoguchi et al., 2006). Moreover, MBD1-deficient NSCs generate fewer neurons than do wild-type NSCs, suggesting an important role for MBD1 in neuronal fate specification (Zhao et al., 2003). Hypomethylated *gfap* promoter can be also found in oligodendrocytes but, unlike neurons, these cells do not express MeCP2 at high levels, and upon astrocyte-inducing cytokine stimulation can change their fate and become astrocytes (Kohyama et al., 2008).

I.2.b. Histone modification

Histone modification displays high levels of diversity and complexity compared

with DNA methylation. Two of the core histones, H3 and H4, have long amino-terminal tails that protrude out of the nucleosome and can be subjected to a variety of posttranslational modifications: methylation, acetylation, phosphorylation, ubiquitylation, sumoylation, glycosylation, biotinylation, carbonylation and ADP-ribosylation (Strahl & Allis, 2000). Among these, lysine (K) acetylation and methylation are the most studied and best understood histone modifications.

I.2.b.i. Acetylation

Acetylation and deacetylation of lysine residue in histone tails is mediated by histone acetyl transferases (HATs) and histone deacetylases (HDACs), respectively (Hsieh & Gage, 2005). In general, an increase of histone acetylation by HATs causes remodeling of chromatin from a tightly to a loosely packed configuration (euchromatin), which subsequently leads to transcriptional activation. Conversely, a decrease of histone acetylation by HDACs results in a condensed chromatin structure (heterochromatin) and finally transcriptional silencing (Juliandi et al., 2010b; Fig. 6).

Histone acetylation is at least partially involved in the differentiation of mESCs into NSCs and neurons. Mouse ESCs appear to have a higher global level of histone acetylation than lineage-restricted stem cells and differentiated cells, which is consistent with their higher levels of transcription and more open chromatin configuration (Efroni et al., 2008). In fact, heterochromatin markers such as HP1 are highly dynamic and dispersed in the nuclei of mESCs, and become more concentrated at specific loci as differentiation proceeds (Meshorer & Misteli, 2006; Meshorer et al., 2006).

In mESCs and non-neuronal cells, neuron-specific genes are repressed by the binding of neuron restricted silencing factor/RE-1 silencing transcription factor

(NRSF/REST) to its DNA response element (RE-1); this binding permits the formation of a repressor complex upon recruitment of HDAC1/2 and Sin3A (Rice & Allis, 2001; Lunyak et al., 2002; Lunyak & Rosenfeld, 2005; Ballas et al., 2005). As the cells differentiate into neuronal progenitors and neurons, this HDAC-containing repressor complex dissociates from neuron-specific genes due to the degradation of NRSF/REST (Ballas et al., 2005).
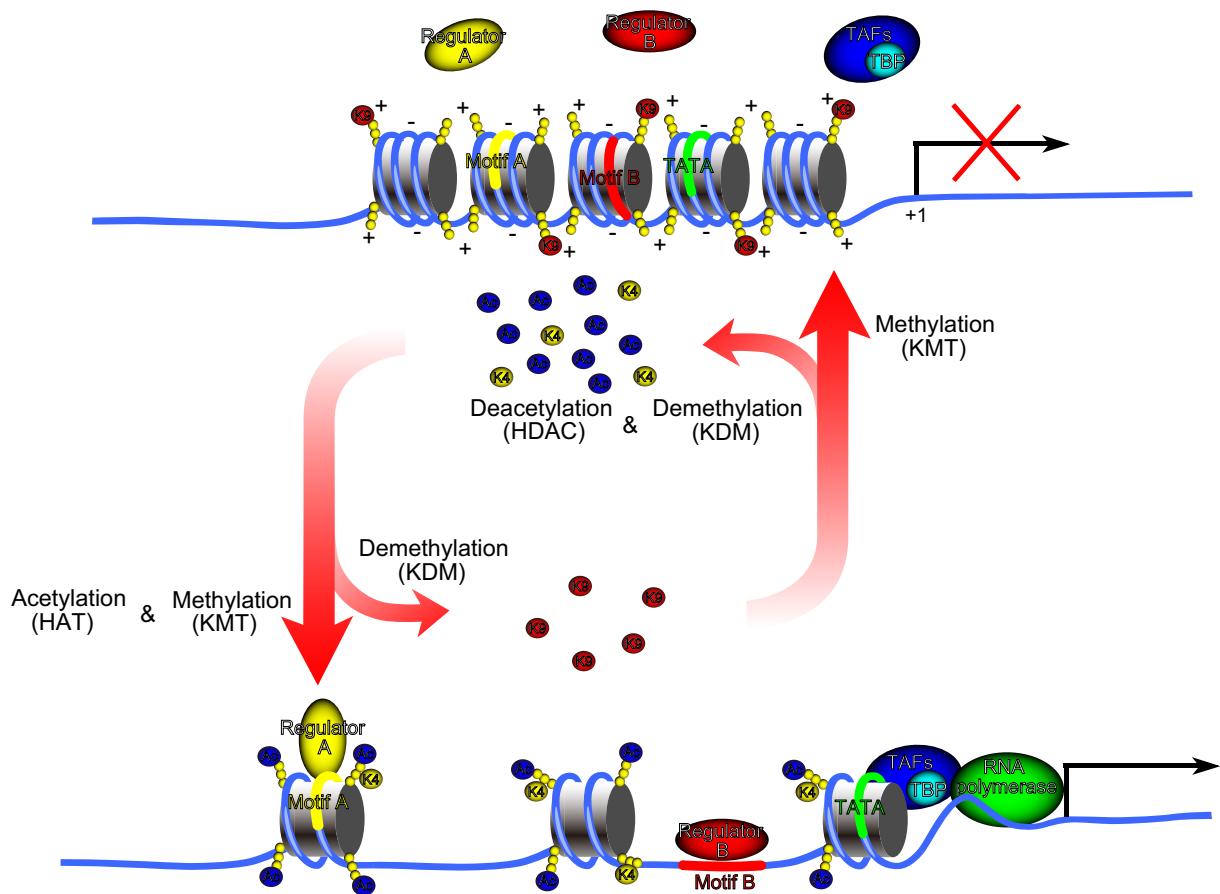
Fig. 6. Dynamic histone tail modifications convert chromatin structure from a repressive to an active state to regulate gene expression. Histone acetylation and H3K4 methylation allow relaxation of chromatin and enable RNA polymerase and specific regulators to access DNA and initiate transcription. Histone deacetylation and H3K9 methylation contribute to the formation of repressive chromatin. Ac, acetyl group; K4 and K9, lysine methyl group; HAT, histone acetyltransferase; HDAC, histone deacetylase; KMT, lysine methyltransferase; KDM, lysine demethylase; TBP, TATA-binding protein; TAF, TBP-associated factor.

Adult hippocampal-derived NSCs differentiate predominantly into neurons, at the expense of astrocytes and oligodendrocytes, when treated by the antiepileptic and HDAC inhibitor valproic acid (VPA) *in vitro*, even in conditions that favor glia-specific differentiation (Hsieh et al., 2004). VPA-mediated HDAC inhibition upregulates the neuron-specific gene *NeuroD*, a neurogenic basic helix-loop-helix TF, resulting in the induction and suppression, respectively, of neuronal and glial differentiation. In the developing rat brain and in cultured E14 NSCs, VPA treatment has also been shown to promote neurogenesis by activating the Ras-ERK pathway (Jung et al., 2008).

Progression of the oligodendrocyte lineage is also dependent on HDAC activity (Marin-Husstege et al., 2002). Postnatal administration of VPA was shown to delay the timing of NSC differentiation into myelin-forming oligodendrocytes in the developing forebrain (Shen et al., 2005); significant hypomyelination in the developing corpus callosum, together with sustained expression of progenitor markers and delayed expression of late differentiation markers, were observed in this study. However, HDAC inhibition by VPA after the onset of myelination resulted in comparable myelin gene expression to that seen in VPA-untreated rats, which was attributed to further transitions in nucleosomal histones from a state of reversible deacetylation to a more stably repressed state by histone methylation. It has also recently been shown that HDAC1/2 contribute to the progression of murine oligodendrocyte differentiation by disrupting the β-catenin-TCF activator complex at *id2/4*, inhibitor of differentiation genes, thereby preventing the synthesis of Id2/4 proteins which can inhibit myelin gene expression (Ye et al., 2009).

I.2.b.ii. Methylation

Histones are methylated and demethylated at lysine residues by histone methyl transferases (KMTs) and histone demethylases (KDMs), respectively (Fig. 6). Methylation can result in either activation or repression of gene transcription, depending on which residue is methylated (Yoo & Jones, 2006). For example, histone H3 lysine 4 (H3K4) methylation is a well-known marker for transcriptionally active chromatin, whereas methylated H3K9 and H3K27 mark transcriptionally inactive chromatin.

Several extrinsic factors affect the histone methylation status of NSCs. For example, it has been suggested that fibroblast growth factor 2 (FGF2) signaling is directly responsible for the acquisition of glial competency during NSC culture by increasing H3K4 and reducing H3K9 methylation around the STAT3-binding sites of the *gfap* and *S100β* promoters so that, upon CNTF stimulation, NSCs can differentiate into astrocytes (Song & Ghosh, 2004). However, FGF2 is a common factor, when used either alone or together with epidermal growth factor (EGF), for maintaining NSCs in culture. Early gestational NSCs are initially responsive only to FGF2, and this signal then primes NSCs to become responsive to EGF later during development or culture *in vitro* (Tropepe et al., 1999; Lillien & Raphael, 2000; Ciccolini, 2001). How FGF2 and/or EGF signaling might influence KMTs and KDMs, resulting in the aforementioned changes in histone methylation, therefore remains an open question.

Mixed-lineage leukemia (MLL), a member of the trithorax group (trxG) gene family, can either specifically methylate H3K4 for gene activation, by recruiting HATs such as MOF and CBP in various cell lines (Ernst et al., 2001; Milne et al., 2002; Dou et al., 2005), or repress target genes by recruiting polycomb group (PcG) proteins, HDACs and/or

SUV39H1 (Xia et al., 2003). In the postnatal mouse brain, MLL1 is required for neurogenesis and its deficiency in NSCs in the subventricular zone (SVZ) leads to a glial lineage preference (Lim et al., 2009). One of the key downstream regulators of SVZ neurogenesis, *Dlx2*, is not expressed in MLL1-deficient NSCs. This is due to a change in histone methylation of *Dlx2*, from a single high level of H3K4 trimethylation (H3K4me3) to a bivalent poised state marked by both activating H3K4me3 and repressive H3K27me3 (Lim et al., 2009).

The existence of both activating and repressive histone methylation marks is necessary for the rapid activation of genes during differentiation. In mESCs, while pluripotency-associated genes are marked by active H3K4me3, those that are necessary for differentiation are marked by both active H3K4me3 and repressive H3K27me3 (Azuara et al., 2006; Bernstein et al., 2006; Fig. 7). It has been shown that a specific KDM, Jmjd3 (an H3K27me3 demethylase) which belongs to the jumonji protein family, can resolve the bivalent state of NSC marker genes promoter such as *nestin*, and thereby lead mESCs to NSC commitment (Burgold, 2008). Eventually, in mESC derived-NSCs, the ESC pluripotency-associated genes are repressed by H3K9 methylation and the bivalent state exists on neuronal and glial differentiation genes (Fig. 7). Thus, it is conceivable that the bivalent state generated by trxG and PcG proteins is a common mechanism for the maintenance of differentiation potential in many stem/progenitor cell types (Mikkelsen et al., 2007).

PcG proteins have also been shown to participate in NSC differentiation by establishing the H3K27me3 repressive mark at proneuronal basic helix-loop-helix (bHLH) genes, such as Neurogenin1 (*Neurog1*) (Hirabayashi et al., 2009). Neurog1 expression *in vitro* and *in vivo* can suppress astrocytic differentiation of NSCs in part because Neurog1 sequesters the p300/CBP-Smads complex from STAT3, leading to suppression of STAT3

target genes (Cai et al., 2000; Sun et al., 2001; Guillemot, 2007). Since Neurog1 is expressed solely during the neurogenic and not the astrocytic period of neocortical development (Sun et al., 2001), *neurog1* repression, by means of an H3K27me3 mark applied by PcG proteins in late gestational NSCs, provides a mechanism for a switch in NSC differentiation from neurogenic to astrogenic (Fig. 7).
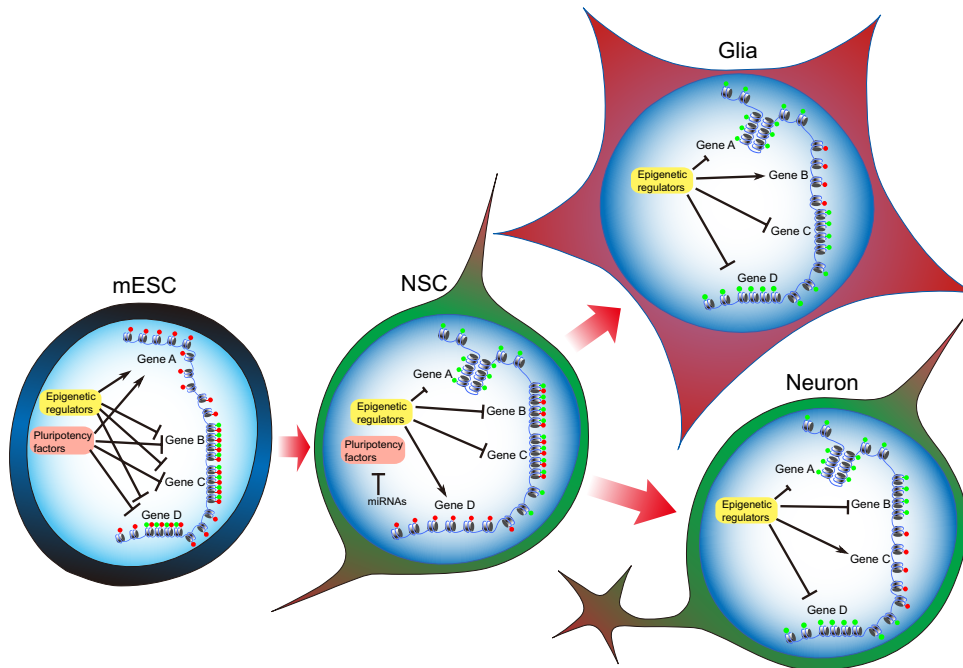
Fig. 7. Chromatin dynamics and histone modification status during stem cell development. Chromatin status changes from a highly to a less dynamic form during differentiation of mESCs into NSCs and neural lineage cells. Genes associated with pluripotency (Gene A) are actively transcribed in pluripotent mESCs, while NSC multipotency- (Gene D) and differentiation-associated genes (Genes B, glial differentiation; Gene C, neuronal differentiation) are kept in a silent poised state. Several epigenetic regulators and pluripotency factors regulate this state, in part by a combination of the activating H3K4me3 (red circles) and the repressive H3K27me3 (green circles) methylation marks. In mESCs, only H3K4me3 is present at pluripotency-associated genes, while both H3K4me3 and H3K27me3 mark NSC multipotency- and differentiation-associated genes (bivalent marks). Upon progression to NSCs, miRNAs downregulate pluripotency factors. NSC multipotency genes, such as *nestin*, resolve bivalent marks into the single activating H3K4me3, while differentiation-associated genes retain their bivalent marks. During NSC differentiation to each neural lineage, NSC multipotency genes are kept silenced with H3K27me3, and differential methylation status in genes specific for each lineage determines NSC fate.

Noncoding RNAs are increasingly recognized as exerting epigenetic effects on gene regulation (Grewal & Moazed, 2003; He & Hannon, 2004). Among several types of such RNAs, microRNA (miRNA) has been studied intensively in the context of its role in NSC differentiation. miRNA is a 20-25-nucleotide single-stranded RNA that can bind to the 3' untranslated region (UTR) of target mRNAs, by an imperfect sequence match, to repress their translation and stability (Rana, 2007) through the formation of a structure called the RNA-induced silencing complex (RISC). As well as the 3' UTR, miRNA may also target the coding region and the 5' UTR of target mRNAs (Lytle et al., 2007; Orom et al., 2008).

miR-124a is expressed predominantly in neural tissues and has been shown to participate in the *in vitro* differentiation of NSCs into neurons by mediating degradation of non-neuronal gene transcripts (Conaco et al., 2006). miR-124a expression is regulated by NRSF/REST, which is expressed only in NSCs and non-neuronal cells including mESCs (Fig. 8). In NSCs, therefore, since expression of the *miR-124a* gene is suppressed by NRSF/REST, the stability of non-neuronal gene transcripts can be increased, thus preventing NSCs from differentiating into neurons. When NRSF/REST is absent, the expression of *miR-124a* and neuronal genes is upregulated, leading to a preference for neuronal lineage differentiation (Fig. 8). miR-124a can also target small carboxy-terminal domain phosphatase 1 (SCP1), which, like NRSF/REST, is an anti-neuronal factor in non-neural tissues and is recruited to RE1-containing gene promoters by NRSF/REST (Yeo et al., 2005), thus providing another mechanism to induce neurogenesis (Visvanathan et al., 2007). Interestingly, NRSF/REST can also be down-regulated by two other neural tissue-specific miRNAs, miR-9 and miR-9*, which target NRSF/REST and its cofactor CoREST, respectively (Packer et al., 2008; Fig. 8).

Moreover, it has been shown that overexpression of both miR-124 and miR-9 promotes neuronal differentiation, while their down-regulation has the opposite effect (Conaco et al., 2006).
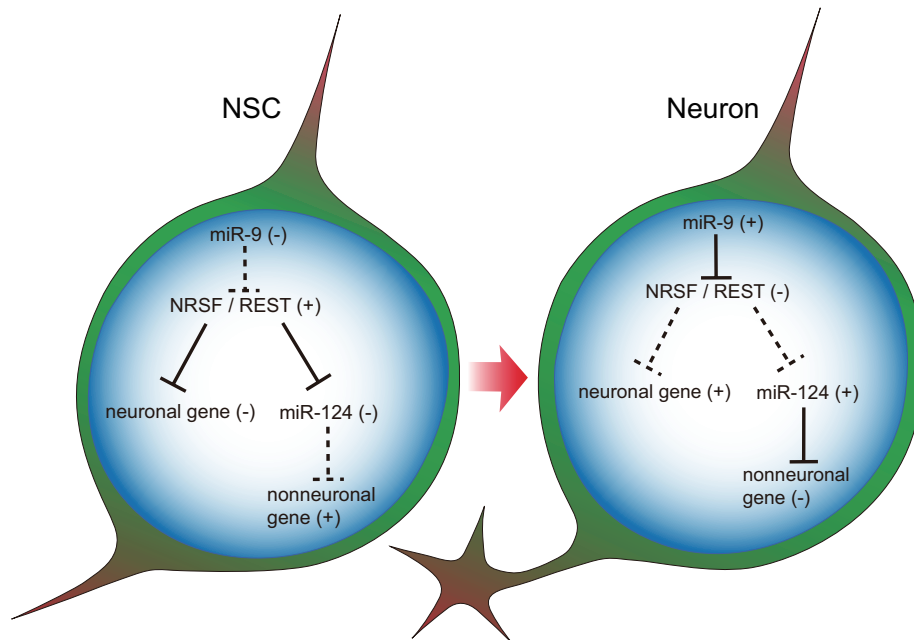
Fig. 8. Regulation of neurogenesis by miRNA and NRSF/REST. In NSCs, NRSF/REST is expressed and inhibits neuronal genes and miR-124 expression, allowing non-neuronal transcripts to persist. When NSCs differentiate into neurons, downregulation of NRSF/REST by miR-9 derepresses neuronal and miR-124 gene loci, resulting in the selective degradation of non-neuronal gene transcripts.

Promotion of neurogenesis by miR-124 and miR-9 might also involve other mechanisms. Both of these miRNAs can stimulate neurogenesis *via* inhibition of STAT3 activation, which is responsible for astrocytogenesis (Krichevsky et al., 2006). miR-124 has also been shown to repress *Sox9*, a SRY-box TF that is important for glial cell specification, during the transition of NPCs to neuroblasts in the adult subventricular zone (Cheng et al., 2009). miR-124 can also reduce the levels of polypyrimidine tract binding protein 1 (PTBP1), a global repressor of alternative pre-mRNA splicing, leading to a switch from non-neuronal to neuronal alternative splicing patterns (Makeyev et al., 2007). In the case of miR-9, several

studies have shown that it can form a regulatory loop with *Tlx*, a self-renewal gene in NSCs, that is critical for neurogenesis by each regulating the other's transcript (Shi et al., 2004; Zhao et al., 2009). miR-9 has also been shown to modulate Cajal-Retzius cell differentiation by targeting transcripts of *Foxg1*, which encodes a winged helix transcriptional repressor, in mouse medial pallium (Shibata et al., 2008). How these known mechanisms are coordinated and integrated during neurogenesis is an important topic for future studies.

Other miRNAs, such as miR-128, miR-129 and miR-298, are also expressed exclusively in the neuronal lineage (Lau et al., 2008), while miR-23 is restricted to the glial lineage, and miR-26 and miR-29 are more strongly expressed in glia than in neurons (Smirnova et al., 2005; Lau et al., 2008). Interestingly, during oligodendrocyte lineage progression, miR-124a is also down-regulated, as it is in neuronal differentiation (Lau et al., 2008). Therefore, it is tempting to conclude that modulation of the expression of individual miRNAs may be cellular context dependent and crucial for cell fate choice.

I.3. HDAC expression and function during NSC differentiation

More than a dozen of HDACs have been characterized to date, and they can be classified into at least three major classes. In particular, HDAC1 and HDAC2, belonging to the class I group, are clearly implicated in NSC differentiation. NSCs and their lineage-commited progenitor cells express high levels of HDAC1, while only some of them express low levels of HDAC2 (MacDonald & Roskams, 2008; Figure 9). Interestingly, as NSCs commit to the neuronal lineage, expression of HDAC2 is upregulated but that of HDAC1 is down-regulated to the extent that in most post-mitotic neurons it becomes

undetectable, except only in some types of neurons (MacDonald et al., 2005; MacDonald & Roskams, 2008). On the other hand, HDAC1 expression is sustained in the majority of glial lineage cells (astrocytes and oligodendrocytes), in which HDAC2 is not detected (Shen et al., 2005; MacDonald & Roskams, 2008; Figure 9). Moreover, HDAC2, but not HDAC1, was found to inhibit astrocytic differentiation (Humphrey et al., 2008). Intriguingly, despite the abundance of HDAC1 in NSCs, the level of histone acetylation in these cells is actually higher than that in their differentiated progeny (Hsieh et al., 2004). HDAC1 may begin to deacetylate histones, and thus to compact chromatin structure, at the onset of gliogenesis, as mature glial cells eventually display a very low level of global histone acetylation (Hsieh et al., 2004). The effect of HDAC1 on cell proliferation also probably differs among brain regions where NSCs reside, as HDAC inhibition using VPA has been reported both to inhibit (Hsieh et al., 2004; Jessberger et al., 2007) and to stimulate NSC proliferation (Higashi et al., 2008).

I.4. Cortical layer neurons generation in the cerebral cortex

The cerebral cortex is composed of two main populations of neurons: projection (or pyramidal) neurons which are glutamatergic and excitatory, and interneurons which are GABAergic and inhibitory. In rodents, the projection neurons originate from NSCs in the cortical VZ, and in contrast, almost all interneurons originate from NSCs located outside the cortex (Marin & Rubenstein, 2001; Gorski et al., 2002). It has been long time appreciated that the cerebral cortex is organized in layers that are defined by the densities and morphologies of these neurons.
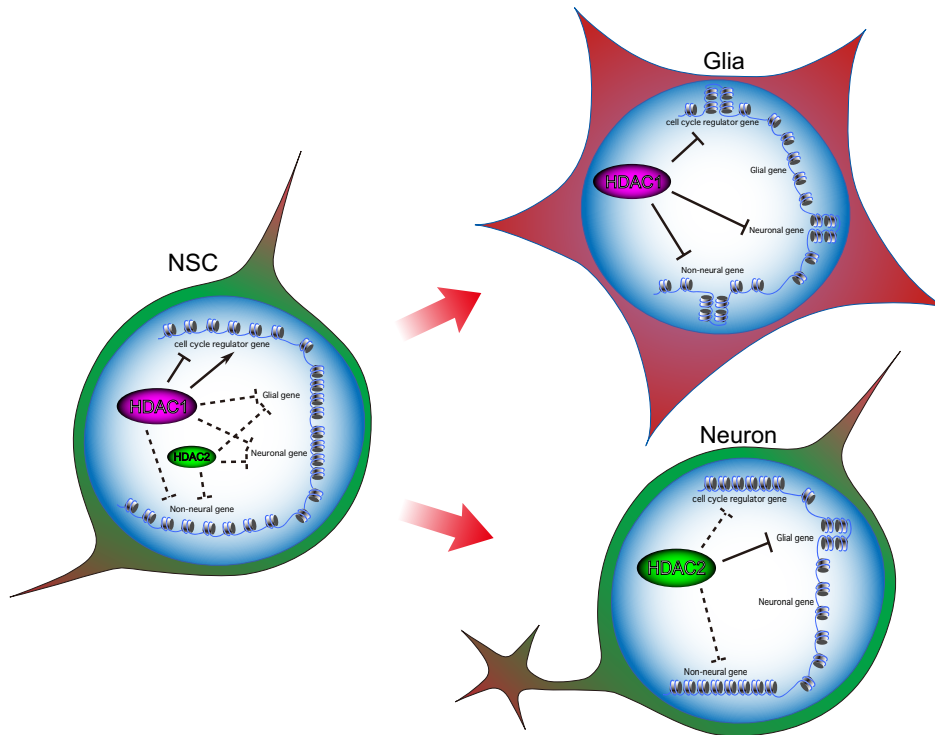
Fig. 9. A model of HDAC expression and function during NSC differentiation. In NSCs, HDAC1 (purple oval) is more abundant than HDAC2 (green oval) and probably functions mainly as a regulator of the cell cycle. During glial differentiation, global histone acetylation and the amount of HDAC2 are reduced dramatically. In contrast, only a slight decrease of global histone acetylation occurs during neuronal differentiation with a persistent abundance of HDAC2. HDAC1 may contribute to global histone deacetylation in glial cells, while HDAC2 may have a specific function to repress glial genes in neurons. Solid and broken lines represent strong and moderate regulation of histone acetylation, respectively.

Cortical projection neurons of different layers are generated in a temporal sequence during development (Molyneaux et al., 2007). The first neurons to exit cell cycle and migrate out of the VZ occupy the preplate, which is subsequently split into two zones by the arrival of later neurons that will form the cortical plate (CP). The upper zone of the splitted preplate (also known as marginal zone, and later become layer I) is populated by Cajal-Retzius neurons which are derived mostly from cortical hem (Zhao et al., 2006), while the deeper zone becomes subplate which functions mainly in axon targeting during development (Kanold & Shatz, 2006). In the newly formed CP, neurons of the deep layers (layer V and VI) are

generated earlier than neurons of the superficial layers (layer II-IV), and these superficial-layer neurons migrate past the deep-layer neurons in the CP, in such process called an inside-out fashion (Molyneaux et al., 2007).

The fate determination of deep-layer neurons has been attributed to the zinc-finger transcription factor *Fezf2* (Leone et al., 2008). *Fezf2* is expressed in NSCs and its progenitors starting on E8.5 and its expression is retained by deep-layer neurons during corticogenesis (Chen et al., 2005; 2008). Later on, deep-layer neurons acquire the expression of the second zinc-finger transcription factor *Ctip2* during postmitotic differentiation (Arlotta et al., 2005; Chen et al., 2008). Several studies have indicated that *Fezf2* expression in NSCs and its progenitors may promotes the expression of *Ctip2* in young neurons, and together these genes confer a deep-layer neuronal fate during differentiation (Leone et al., 2008).

In the case of superficial-layer neurons, its fate determination requires the chromatin remodeling protein Satb2 (Britanova et al., 2008; Leone et al., 2008). Fezf2 has been suggested to repress *Satb2* (directly or indirectly) thereby inhibiting generation of superficial-layer neurons (Chen et al., 2008). Satb2 has been also reported to inhibit *Ctip2* expression by direct binding to the matrix attachment regions in *Ctip2* locus (Britanova et al., 2008). At later times during corticogenesis, when superficial-layer neurons are generated, Fezf2 expression is absent which relieves the repression of *Satb2* (Chen et al., 2008). This, in turn, enables Satb2 to actively represses *Ctip2* expression and promotes the adoption of superficial-layer neurons identity.

I.5. Adult hippocampal neurogenesis

Neurogenesis in the brain of adult mammals occurs throughout life, and has been clearly demonstrated at two locations under physiological condition: the subventricular zone (SVZ) of the lateral ventricles and the subgranular zone (SGZ) of the dentate gyrus (DG) in the hippocampus (Kempermann, 2006). Neurons born in the adult SVZ migrate over a great distance through the rostral migratory stream, and become granule neurons and periglomerular neurons in the olfactory bulb. Neurons born in the adult SGZ migrate in short distance into granule cell layer (GCL) of DG and become dentate granule cells. Recent studies showed that newborn neurons in the adult brain integrate into the existing circuitry and receive functional input (Zhao et al., 2008).

The adult-born neurons in the hippocampus can be identified by many approaches, such as by incorporation of nucleotide analogues (ex: bromodeoxyuridine (BrdU)), by virus-mediated labelling, and by genetically engineered reporter genes (Kempermann, 2006; Deng et al., 2008). Several research have shown that neurogenesis in this area is regulated both by physiological and pathological activities at all stages, including: (i) the proliferation of adult NSCs and its progenitors, (ii) differentiation and fate determination of progenitor cells, and (iii) the survival, maturation, and integration of newborn neurons (Zhao et al., 2008). Furthermore, each of these processes is subject to regulation by numerous intrinsic and extrinsic factors (Suh et al., 2009).

Adult hippocampal neurogenesis begins with the proliferation of NSCs in the SGZ. Two types of NSCs can be found according to their specific morphologies and expression of unique sets of molecular markers (Kempermann, 2006; Zhao et al., 2008). Type 1 have a

radial process spanning the entire GCL and ramify in the inner molecular layer. These cells express nestin, GFAP, and the Sry-related HMG box transcription factor Sox2 (Fukuda et al., 2003; Garcia et al., 2004; Suh et al., 2007). Type 2 has only short processes, express nestin and Sox2 but do not express GFAP, and start to express neuronal transcription factors Prox1 and NeuroD1, and structural protein doublecortin (DCX) (Seri et al., 2001; Kempermann et al., 2004; Steiner et al., 2008). Type 2 cells may arise from type 1 cells, but direct evidence delineating this lineage relationship is still lacking (Zhao et al., 2008). Interestingly, the relationship between these two NSCs types could be also reciprocal, as one type has been observed to generate the other type (Suh et al., 2007). From type 2 cells, migratory neuroblasts (also called type 3 cells) are generated. This cell type express Prox1, DCX and calretinin, can still proliferate, but exit cell cycle before full maturation into granule neurons (Kempermann et al., 2004). Mature granule neurons eventually express NeuN and calbindin, while retaining Prox1 expression (Kempermann et al., 2004; Kempermann, 2006; Zhao et al., 2008).

Evidence increasingly indicates that adult neurogenesis is important for hippocampal function, although the exact function of new neurons is unclear (Aimone et al., 2010). Hippocampus is a crucial structure for the formation of certain types of memory, such as episodic memory and spatial memory (Squire, 1992). Genetic and environmental factors that affect adult hippocampal neurogenesis also cause corresponding changes in cognitive performance, suggesting the putative function of adult hippocampal neurogenesis in learning and memory (Zhao et al., 2008).

One of the implications of a role for adult hippocampal neurogenesis in learning and memory is that neurogenesis can be regulated by numerous factors associated with behavioral and cognitive states. Hippocampus-dependent learning is one of the major positive regulators of hippocampal neurogenesis (Gould et al., 1999). Living in an enriched environment, which presumably provides a larger opportunities for learning than standard laboratory housing (van Praag et al., 2000), can also enhances hippocampal neurogenesis by increasing the survival of adult-born DG neurons (Kempermann et al., 1997). Physical exercice not only improves the physical health but also being reported to improve cognition and other brain functions (Hillman et al., 2008; van Praag, 2009). In rodents, voluntary running significantly increases the proliferation of NSCs in SGZ of both young and aged animals (van Praag et al., 1999a; 2005). Voluntary running also interacts with other stimuli, such as stress and social interactions, to regulate neurogenesis (Snyder et al., 2009; Leasure & Decker, 2009). Although physical exercise can induce angiogenesis and expression of neurotrophic factors such as brain-derived neurotrophic factor (BDNF) in the brain (van Praag, 2009), the molecular mechanisms responsible for exercise-induced neurogenesis remain undetermined (Deng et al., 2010).

I.6. Objectives of the research

NSCs hold great promise for clinical treatment of neurological diseases and dysfunctions, owing to their ability to self-renew and their potential to generate various neural cell types. It is now established that epigenetic regulation contributes substantially, along with other mechanisms, to these properties of NSCs. However, our knowledge about the precise

mechanisms that control NSC differentiation is still in its infancy and many avenues remain to be explored.

In this study, I investigated the role of histone acetylation, by means of HDAC inhibition, in the regulation of NSCs. In order to inhibit HDAC, I used VPA which is an established drug for epilepsy, and now in clinical trials for therapeutic application on several CNS disorders and diseases (Kazantsev & Thompson, 2008). Previous studies have found that taking VPA for anti-epileptic drug at early pregnancy can lead to severe developmental defects (DiLiberti et al., 1984; Nau et al., 1991), so that it must not be taken at this period. Nevertheless, it can be prescribed at later periods where VPA is considered to be safe. The effect of VPA during later pregnancy period is elusive, and children of mothers who take VPA at this period show no significant defects during their development. Taken together these facts, I also investigated the consequences of VPA treatment during mid-gestation and its outcomes after postnatal, and searched for the appropriate treatments to recover those consequences and outcomes.

II. Materials and Methods

II.1. Maintenance of mESCs

The mESC line 46C (*Sox1*-GFP-IRES-pac knock-in) was routinely propagated without feeder cells as described previously (Ying et al., 2003; Conti et al., 2005). mESCs were grown at 37 °C in a 5% (v/v) CO_2 incubator in ESC medium (ESM) containing Glasgow Minimum Essential Medium (Invitrogen), supplemented with 10% (v/v) fetal bovine serum (Biowest), 1 mM sodium pyruvate (Invitrogen), 0.1 mM MEM non-essential amino acids (Invitrogen), 0.1 mM 2-mercaptoethanol (Sigma), 1,000 U/ml murine leukemia inhibitory factor (Millipore), and 0.5x antibiotic-antimycotic (Invitrogen), on 0.1% (v/v) gelatin-coated (Sigma) 9-cm dishes (Nunc). Medium was changed every day, and when the cells reached 60-70% confluence they were passaged onto new dishes at a plating density of 1×10^6 cells per 9-cm dish.

II.2. Neural differentiation

mESCs were induced to differentiate to the neural lineage as described previously (Ying et al., 2003; Conti et al., 2005; Gaspard et al., 2008, 2009). In brief, mESCs were trypsinized, dissociated and plated on 0.1% (v/v) gelatin-coated (Sigma) dishes at a density of 0.3×10^6 cells per 9-cm dish (Nunc) in ESM. One day later, the medium was replaced with DDM, which is composed of DMEM/F12 (Invitrogen) supplemented with freshly prepared modified N2-supplement (Ying & Smith, 2003), 1 mM sodium pyruvate (Invitrogen), 0.1 mM MEM non-essential amino acids (Invitrogen), 0.1 mM 2-mercaptoethanol (Sigma), 0.5 mg/ml bovine serum albumin fraction V (Invitrogen), 1x GlutaMAX (Invitrogen) and 0.5x

antibiotic-antimycotic (Invitrogen). This day was designated as differentiation day 0. Cyclopamine (Calbiochem) was added to a final concentration of 1 μM from differentiation day 2 to day 10. On differentiation day 10, the medium was replaced with DDM only (without cyclopamine). For selection of Sox1-expressing neural progenitor cells, from differentiation day 8 to day 10, puromycin (Sigma) was added to a final concentration of 0.5 μg/ml. The culture was maintained until differentiation day 12 and the medium was changed every 2 days during day 0 to day 12.

At differentiation day 12, mESC-derived NPCs were trypsinized, dissociated and plated on poly-L-lysine/laminin-coated (Sigma, Becton Dickinson) dishes at a density of 0.5 x 10^6 cells per 3.5-cm dish (Nunc) in N2/B27 medium, which consists of a 1:1 mixture of DDM (without sodium pyruvate and MEM non-essential amino acids) and Neurobasal/B27 medium (Neurobasal, 1x B27 supplement without vitamin A, 1x GlutaMAX and 0.5x antibiotic-antimycotic (all from Invitrogen)). Valproic acid (Sigma) was added one time to the culture medium to a final concentration of 0.5 mM at differentiation day 12 where appropriate. Culture was maintained until differentiation day 14 or 21, and the medium was changed every 2 days during day 12 to day 21.

II.3. Immunocytochemistry

Medium was removed and cells were washed with phosphate buffered saline (PBS) and then fixed with 4% paraformaldehyde in PBS for 15 min. After 3 washes with PBS, the cells were incubated for 1 h at room temperature (RT) in blocking solution (PBS containing 3% FBS and 0.1% Triton X-100). They were then incubated overnight at 4 °C with the appropriate primary antibodies. The following primary antibodies were used: chick anti-GFP

(1:500, Aves Labs), rabbit anti-β-tubulin isotype III (Tuj1; 1:1000, Covance), mouse anti-nestin (1:250, Millipore), rabbit anti-Pax6 (1:500, Covance), mouse anti-Map2ab (1:1000, Sigma), rat anti-Ctip2 (1:1000, Abcam), mouse anti-reelin (1:1000, MBL), and rabbit anti-Cux1 (1:500, Santa Cruz). After 3 washes with PBS, the cells were incubated for 2 h at RT with the appropriate secondary antibodies. The following secondary antibodies were used: FITC-conjugated donkey anti-chick, Cy5-conjugated donkey anti-rabbit, Cy3-conjugated donkey anti-rabbit, Cy5-conjugated donkey anti-mouse, Cy3-conjugated donkey anti-mouse (all 1:500, Jackson ImmunoResearch), Alexa Fluor 488-conjugated donkey anti-mouse, Alexa Fluor 488-conjugated donkey anti-rabbit, and Alexa Fluor 488-conjugated donkey anti-rat (all 1:500, Invitrogen). After 3 washes with PBS, nuclei were stained for 15 min at RT with Hoechst 33258 (Nacalai Tesque). Cells were washed with PBS, mounted on cover slips with Immu-Mount (Thermo Scientific), and examined and photographed using a fluorescence microscope (Axiovert 200M, Zeiss) equipped with a camera and appropriate epifluorescence filters.

II.4. Animal treatment

All experiments were carried out according to the animal experimentation guidelines of Nara Institute of Science and Technology that comply with National Institutes of Health Guide for Care and Use of Laboratory Animals. All efforts were made to minimize the number of animals used and their suffering. Pregnant C57BL/6 mice were individually housed in plastic breeding cages with free access to water and pellet diet in a 12 h light-dark cycle. Three groups were designated as valproic acid (VPA), valpromide (VPM) and methylcellulose (MC) group on gestation period. VPA and VPM group received an oral

administration of 300 mg/kg VPA (Sigma) and VPM (Wako), respectively, once a day on three consecutive embryonic day (E)12.5, E13.5, and E14.5. MC group received an oral administration of identical volumes of 0.5% (w/v) MC (Wako) once a day on the same days.

Pregnant mice from MC and VPA group received a single intraperitoneal (i.p.) injection of 150 mg/kg 5-bromo-2-deoxyuridine (BrdU) on E14.5. These mice were then sacrificed on E15.5 for cell cycle exit analysis or on P7 and P56 for differentiation and migration analysis. For proliferation analysis, mice were injected by 150 mg/kg BrdU i.p. 30 min before sacrifice on E15.5. For histone acetylation analysis during cortical NSCs development, mice at E11.5 and E16.5 were sacrificed and used.

Another set of pregnant mice in MC and VPA group were allowed to give birth and their pups were weaned at 4 weeks of age. Four male mice per liter were randomly selected and housed in one cage. Four groups were designated on weaning period as MC (pups from MC-treated mother), MC+RW (pups from MC-treated mother with running wheel), VPA (pups from VPA-treated mother), and VPA+RW (pups from VPA-treated mother with running wheel). Mice in MC+RW and VPA+RW were introduced to running wheel and were freely to run in their cage immediately after weaning. To analyze adult neurogenesis, 100 mg/kg BrdU were i.p. injected for 5 or 7 consecutive days starting on 12 weeks of age. Mice were sacrificed one day (proliferation group) and 4 weeks (differentiation group) after the last BrdU injection. For behavior and electrophysiology analysis, the same groups of mice 11-12 weeks of age were used.

II.5. Immunohistochemistry

Mice were anesthesized and perfused with PBS followed by 4% PFA in PBS on the indicated times. The brain was dissected, and postfixed overnight in the same fixative at 4 °C. For cryosectioning, fixed tissue were cryoprotected in 10% sucrose in PBS overnight at 4 °C, then in 20% sucrose in PBS overnight at 4 °C, and embedded in OCT compound (Tissue Tek). Cryostat sections of embryonic and P7 brains (15 μm) were cut and affixed to MAS-coated glass slides (Matsunami Glass), while other postnatal brains (40 μm) were cut and floated with PBS in 6-well or 12-well chamber slides (Nunc, Greiner). For some antibodies, antigen retrieval were conducted either by incubation in L.A.B. Solution (Polysciences Inc.) for 15 min at RT or by autoclave in Target Retrieval Solution (Dako) for 15 min at 105 °C. For BrdU-immunostaining, sections were incubated with 2N HCl for 30 min at 37 °C. After 3 washes with PBS, the sections were incubated for 1 h at room temperature (RT) in blocking solution (PBS containing 3% FBS and 0.1% Triton X-100). They were then incubated overnight at 4 °C with the appropriate primary antibodies. The following primary antibodies were used: rabbit anti-acetyl-histone H3 (1:1000, Millipore), rabbit anti-acetyl-histone H4 (1:1000, Millipore), rabbit anti-β-tubulin isotype III (Tuj1; 1:1000, Covance), mouse anti-nestin (1:250, Millipore), goat anti-doublecortin (DCX; 1:500, Santa Cruz), rabbit anti-doublecortin (DCX; 1:1000, Abcam), mouse anti-human Ki67 (1:500, BD Pharmingen), rat anti-BrdU (1:1000, AbD Serotec), rat anti-Ctip2 (1:1000, Abcam), rabbit anti-Tbr2 (1:500, Abcam), mouse anti-phospo-histone H3 (PH3; 1:1000, Cell Signaling), rabbit anti-Tbr1 (1:500, Abcam), rat anti-Ctip2 (1:1000, Abcam), rabbit anti-cleaved caspase 3 (1:1000, Cell Signaling), mouse anti-NeuN (1:100, Millipore), rabbit anti-S100b (1:500, Swant), rabbit anti-Sox2 (1:500, Millipore), and rabbit anti-Cux1 (1:500, Santa Cruz). After 3 washes with

PBS, the sections were incubated for 2 h at RT with the appropriate secondary antibodies. The following secondary antibodies were used: FITC-conjugated donkey anti-chick, Cy3-conjugated donkey anti-rabbit, Cy3-conjugated donkey anti-mouse, Cy3-conjugated donkey anti-goat, Cy3-conjugated donkey anti-rat, Cy5-conjugated donkey anti-rabbit, Cy5-conjugated donkey anti-mouse (all 1:500, Jackson ImmunoResearch), Alexa Fluor 488-conjugated donkey anti-mouse, and Alexa Fluor 488-conjugated donkey anti-rabbit (all 1:500, Invitrogen). After 3 washes with PBS, nuclei were stained for 15 min at RT with Hoechst 33258 (Nacalai Tesque). For floating postnatal sections, after washed with PBS, sections were affixed to MAS-coated glass slides (Matsunami Glass). Sections mounted on cover slips with Immu-Mount (Thermo Scientific), and examined and photographed using a fluorescence microscope Axiovert 200M (Zeiss) or confocal microscope LSM 710 (Zeiss), equipped with a camera and appropriate epifluorescence filters.

II.6. Cell counts and volume measurements

Cell counting was conducted manually by using a fluorescence microscope Axiovert 200M (Zeiss) equipped with a camera and appropriate epifluorescence filters, within the indicated areas.

For BrdU counting in adult neurogenesis experiment, the total number of BrdU-positive cells was counted using every 6th section (240 μm apart). BrdU-positive cells were counted throughout the rostrocaudal extent of the granule cell layer (GCL) using a 20x objective and a fluorescence microscope Axiovert 200M (Zeiss). Derived numbers were multiplied by 6 (slice series) to obtain total cell numbers per GCL. For BrdU double (or triple) immunostaining with other markers, 1-in-12 series of sections (480 μm apart) from the

proliferation and the differentiation group were used and double (or triple) labeling was confirmed by three-dimensional reconstructions of z-series. From each mouse, 50 BrdU-positive cells were randomly picked throughout the GCL and analyzed for double (or triple) immunopositive.

Volume measurement of hippocampus and its parts was done using every 6th section (240 μm apart). Area of interest was traced using ImageJ software, and the derived number was multiplied by 240 (the distance between section sampled) to obtain the estimated volume.

Granule cell number was estimated by using every 6th section (240 μm apart). Systematic sampling was done using a three-dimensional counting box, 15 μm on each side, in a variant of the optical dissector principle (Gundersen et al., 1988; Williams & Rakic, 1988). Nuclei of granule cells were stained with Hoechst 33258 (Nacalai Tesque). Nuclei intersecting the uppermost focal plane (exclusion plane) and those that intersected the exclusion boundaries of the counting box were excluded from the count. The average (mean) granule cell number per dissector volume was multiplied by the granule cell layer volume (see volume measurement above) to estimate the absolute granule cell count.

II.7. Behavioral test

Experimental apparatuses and image analyzing software were obtained from O'Hara & Co., Ltd., Japan. Image analyzing software (Image OF4, Image LD2, Image EP2 and Image FZ2) were developed from the public domain ImageJ software. All experiments were done with 12 mice per group and were conducted between 13:30 and 16:30. The level of

background noise during behavioral testing was about 50 dB. After each trial, the apparatuses were wiped and cleaned.

II.7.a. Open field test

The locomotor activity was measured for 10 min using an open field apparatus made of white plastic (50 x 50 x 40 (H) cm). An LED light system was positioned 50 cm above the centre of the field (50 lux at the centre of the field). Total distance travelled (cm), time spent in the central area (30% of the field)(sec), and the frequencies of movement were measured (Tanemura et al., 2002).

II.7.b. Light/dark transition test

The apparatus used for the light/dark transition test consisted of a cage (21 x 42 x 25 (H) cm) divided into two chambers by a partition with an opening. One chamber was brightly illuminated (250 lux), whereas the other chamber was dark (2 lux). A mouse was placed into the dark area and allowed to move freely between the two chambers through the opening for 5 min. The latency for the first move to the light area, the total number of transitions and the time spent on each side were measured.

II.7.c. Elevated plus maze test

The plus-shaped apparatus consisted of four arms (25 x 5 cm) connected to a central square area (5 x 5 cm). Opposite two arms were enclosed with 20 cm-high transparent walls and other two were left open. The floor of the maze was made of white plastic plate and was elevated 60 cm above the room floor (200 lux at the centre of the apparatus). A mouse was

placed to the central square area of the maze, facing one arms, and the behavior was recorded for 10 min: total distance traveled (cm), total time on open arms and central square area (sec) and the total number of entry to any of the arms (Tanemura et al., 2002).

II.7.d. Contextual/cued fear conditioning test

The apparatus consists of a conditioning chamber (or a test chamber) (17 x 10 x 10 (H) cm) made of clear plastic with ceiling and placed in a sound proof box. The chamber floor has stainless steel rods (2-mm diameter) spaced 5 mm apart for electric foot shock (0.1 mA, 3 sec duration) to the mouse. The sound proof box consists of white-coloured wood, and was equipped with an audio speaker and light source (35 lux at the centre of the floor). A CCD camera was positioned 20 cm above the ceiling of the chamber. During the conditioning trial (Day 1), mice were placed individually into the conditioning chamber in the sound proof box and, after 90 sec, they were given three tone-shock pairings (30 sec of tone, 75 dB, 10 KHz followed by 3 sec of electric shock at the end of the tone, 0.1 mA) separated by 90 sec. Then they were returned to their home cage. Next day (Day 2), as a "contextual fear test", they were returned to the conditioning chamber without tone and shock for a 6-min. On the third day (Day 3), they were brought to a novel chamber of different make without stainless steel rods place in the sound proof box and, after a period of 3 min, only the conditioning tone was presented for 3 min (no shock was presented, 35 lux at the centre of the floor). The freezing response of mice was defined as a consecutive 2 sec period of immobility. Freezing rate (%) was calculated as [time freezing/session time] x 100 (Tatebayashi et al., 2002)

II.7.e. Prepulse inhibition test

A startle reflex measurement system was used. A test session was started by placing a mouse in a Plexiglas cylinder, where it was left undisturbed for 10 min. The duration of white noise that was used as the startle stimulus was 40 msec for all trial types. The startle response was recorded by accelerometer for 140 msec (measuring the response every 1 msec) starting with the onset of the prepulse stimulus. The background noise level in each chamber was 70 dB. The peak startle amplitude recorded during the 140 msec sampling window was used as the dependent variable. A test session consisted of 6 trial types (i.e. two types for startle stimulus-only trials, and four types for prepulse inhibition trials). The intensity of the startle stimulus was 120 dB. The prepulse sound was presented 100 msec before the startle stimulus, and its intensity was 90 and 95 dB. Two combinations of prepulse and startle stimuli were employed (90-120 and 95-120). Six blocks of the 6 trial types were presented in pseudorandom order such that each trial type was presented once within a block. The average inter-trial interval was 15 sec (range: 10-20 sec).

II.7.f. Tail suspension test

Mice were suspended above the floor (60 cm) for 3 min by holding their tail. The immobility time during this period was scored. Immobility was defined as the absence of all movement except for those required for respiration.

II.7.g. Y-maze alternation test

The Y-maze is made of clear plastic. The maze has 3 identical arms (40 x 9 x 16 cm) placed at 120° from each others. The centre platform is a triangle with 9 cm side-length.

Each mouse is placed at the end of one arm, the head directed to the walls and allowed to explore freely the apparatus for 5 min. Sequential alternations in entering the arms were recorded.

II.8. Golgi-Cox staining and dendrite analysis

Golgi-Cox staining was done using Rapid GolgiStain Kit (FD NeuroTechnologies) according to the protocol suggested by the manufacturer with some modifications. Brain was removed from the skull without any perfusion, and later sectioned on a cryostat with 100 μm thickness. After sections were mounted on cover slips, they were examined and photographed using microscope Axiovert 40 CFL (Zeiss) equipped with a camera.

Dendrites of granule cell neurons were designated as molecular layer (ML)-oriented if they falled under 60 degree area which was drawed vertically from hilus to ML in the photograph. Other dendrites outside this area were designated as non ML-oriented.

II.9. Voltage-sensitive dye imaging

II.9.a. Slice preparation

Hippocampal slices (400 μm thick) were prepared from 12- to 13-week-old male mice, decapitated under deep ether or isoflurane anesthesia. The brains were quickly removed and cooled in ice-cold artificial cerebrospinal fluid (ACSF; 124 mM NaCl, 2.5 mM KCl, 2 mM $CaCl_2$, 2 mM $MgSO_4$, 1.25 mM NaH_2PO_4, 26 mM $NaHCO_3$, and 10 mM glucose, pH 7.4) bubbled with 95:5% O_2/CO_2 gas. After cooling for 5 min, the hippocampus was dissected out along with the surrounding cortex and sliced into 400-μm-thick transverse sections with a vibratome (Leica VT-1000). A cut was made through the slices at the CA3/CA1 border to

prevent seizure propagation from the CA3 region. Following incubation in gassed ACSF for 3–5 min, each slice was transferred onto a fine-mesh membrane filter (Omni Pore membrane filter, JHWP01300; Millipore Corp.), held in place by a thin Plexiglas ring (inner diameter, 11 mm; outer diameter, 15 mm; thickness, 1–2 mm). These slices were transferred to a moist chamber continuously supplied with a humidified O_2/CO_2 gas mixture. The temperature was held at 32°C for 1 h and then maintained at room temperature thereafter. After 1 h incubation, each slice was stained for 25 min with 100 μl of the VSD solution, containing 0.2 mM di-4-ANEPPS (Molecular Probes) in 2.5% ethanol, 0.13% Cremaphor EL (Sigma), 1.17% distilled water, 48.1% fetal bovine serum (Sigma), and 48.1% ACSF. The slices were subjected to experiments after at least a 1 h incubation at room temperature after the washout of VSD.

II.9.b. Optical recording

The Plexiglas ring supporting each slice was placed in an immersion-type recording chamber. Slices were continuously perfused with prewarmed (31°C) and oxygenated ACSF (bubbled with a 95:5% O_2/CO_2 gas mixture) at a rate of 1 ml/min. Custom laboratory-designed epifluorescence optics consisting of two principal lenses were used to view the slices during experiments. The optics consisted of a modified 35-mm camera lens (f=50 mm F/1.4, Nikon; the final magnification of the system was x1.5) and another lens (f=55 mm x1.0 Leica Microsystems MZ-APO) as the projection lens. Excitation light was provided by a halogen lamp source (150 W; MHW-G150LR; Moritex Corp.) projected through an excitation filter ($\lambda = 530 \pm 10$ nm) and reflected onto the hippocampal slice by a dichroic mirror ($\lambda = 575$ nm). Emission fluorescence from the slice was passed through an

emission filter ($\lambda > 590$ nm) and projected onto a CCD camera (MiCAM01; BrainVision). The high-speed imaging system provided a spatial resolution of approximately 22 x 22 μm at the objective plane (96 x 64 pixels resolution) and a temporal resolution of 0.7 ms/frame.

The intensity of fluorescence emitted by the slice prior to stimulation (a prestimulation period usually lasted from 100 to 740 frames) was averaged and used as a reference intensity (F_0). The fractional change in fluorescence [$\Delta F_{(t)} = F_{(t)} - F_0$] was normalized by the F_0 ($\Delta F/F_0$), and this value was used as the optical signal. Optical signals referred to in the following sections represent signals filtered in spatial and temporal dimensions with a digital Gaussian kernel of 5x5x3 (horizontal x vertical x temporal; $\sigma \approx 1$). In some experiments, we observed a slow drift of the baseline signal; in these cases, the drift was compensated for by subtracting a normalized smooth spline curve, obtained from optical signals recorded at pixels where no response was observed (e.g., optical signals in the hilus). We confirmed that this procedure produced steady and flat baseline signals and did not cause an artificial drift in the absence of stimulation.

We analyzed optical signals offline using a procedure developed for Igor Pro (WaveMetrics Inc.). At a wavelength of 610 nm, VSD fluorescence decreases in response to the depolarization of the membrane. To fit the polarity of the response to conventional membrane potential changes, we expressed the optical signal in a polarity that matched the membrane potential change. For example, decreased fluorescence, which corresponds to depolarization, was represented as a positive deflection.

We used tetanic stimulation consisted of 40 stimuli at 100 Hz instead of "classical" 100 stimuli to record the signal at higher frame rate within a fixed maximum frame length. The response was not qualitatively different in these protocols.

II.10. GeneChip analysis

These procedures were conducted according to the Percellome method (Kanno et al., 2006) to normalize mRNA expression values to sample cell numbers by adding external spike mRNAs to the sample in proportion to the genomic DNA concentration and utilizing the spike RNA quantity data as a dose-response standard curve for each sample. Brain samples were prepared from E14.5 (3 h after oral treatment), E18.5, and 12 weeks of age mice of MC, VPA, and VPM groups. Samples were homogenized and lysed in 500 ml of RLT buffer (Qiagen) and transferred to a 1.5-ml tube. Two separate 10 μl aliquots were treated with DNAse-free RNase A (Nippon Gene) for 30 min at 37 °C, followed by proteinase K (Roche) for 3 h at 55 °C, and then transferred to a 96-well black plate. PicoGreen fluorescent dye (Molecular Probes) was added to each well, and then incubated for 2 min at 30 °C. The DNA concentration was measured using a 96-well fluorescence plate reader with excitation at 485 nm and emission at 538 nm. Lamda phage DNA (PicoGreen kit, Molecular Probes) was used as standard. The appropriate amount of spike RNA cocktail was added to the sample homogenates in proportion to their DNA concentration. Five independent *Bacillus subtilis* poly-A RNAs were included in the grade-dosed spike cocktail. Total RNAs were purified using an RNeasy Mini kit (Qiagen), according to the manufacturer's instructions. First-strand cDNAs were synthesized by incubating 5 μg of total RNA with 200 U SuperScript II reverse transcriptase (Invitrogen) and 100 pmol T7-$(dT)_{24}$ primer [5'-GGCCAGTGAATTGTAATACGACTCACTATAGGGAGGCGG-$(dT)_{24}$-3']. After second-strand synthesis, the double-stranded cDNAs were purified using a GeneChip Sample Cleanup Module (Affymetrix), according to the manufacturer's instructions, and labeled by *in*

vitro transcription using a BioArray HighYield RNA transcript labeling kit (Enzo Life Sciences). The labeled cRNA was then purified using a GeneChip Sample Cleanup Module (Affymetrix) and treated with fragmentation buffer at 94 °C for 35 min. For hybridization to a GeneChip Mouse Genome 430 2.0 Array (Affymetrix), 15 μg of fragmented cRNA probe was incubated with 50 pM control oligonucleotide B2, 1x eukaryotic hybridization control (1.5 pM BioB, 5 pM BioC, 25 pM BioD and 100 pM Cre), 0.1 mg/ml herring sperm DNA, 0.5 mg/ml acetylated BSA and 1x manufacturer-recommended hybridization buffer in a 45 °C rotisserie oven for 16 h. Washing and staining were performed in a GeneChip Fluidics Station (Affymetrix) using the appropriate antibody amplification, washing and staining protocols. The phycoerythrin-stained arrays were scanned as digital image files, which were analyzed with GeneChip Operating Software (Affymetrix). The expression data were converted to copy numbers of mRNA per cell by the Percellome method, quality controlled, and analyzed using Percellome software (Kanno et al., 2006).

II.11. Quantitative real-time RT-PCR

Quantitative real-time PCR was performed to confirm the results of GeneChip analysis. RNAs from mESC-derived NPCs were reverse transcribed using Superscript II (Invitrogen) and amplified by PCR, with a specific pair of primers for each gene, using the Mx3000P system (Stratagene). The expression of target genes was normalized to that of glyceraldehyde-3-phosphate dehydrogenase (Gapdh). The gene-specific primers were as follows: mouse Fezf2: Fezf2-S, 5'-ggctacaagcccttcgtctg-3'; Fezf2-AS, 5'-gtgcatttgtactgcttctc-3'; mouse Gapdh: Gapdh-S, 5'-accacagtccatgccatcac-3'; Gapdh-AS, 5'-tccaccaccctgttgctgta-3'.

III. Results

III.1. 46C mESCs differentiate into the neuroectodermal lineage under Shh inhibition

Inhibition of HDAC activity by valproic acid (VPA), a widely used anticonvulsant and mood-stabilizing drug, has been shown to drive mESCs to differentiate into the ectodermal lineage at the expense of mesodermal and endodermal lineages (Murabe et al., 2007). This ectodermal lineage differentiation is further biased in favor of neuronal rather than glial fates by the VPA treatment (Murabe et al., 2007). Prior to this finding in mESCs, Hsieh et al. (2004) and Balasubramaniyan et al. (2006) had also found a similar tendency for neuronal over glial fate preference when they cultured neural progenitor cells (NPCs) in the presence of HDAC inhibitors such as VPA and trichostatin A. The types of neurons produced in these studies were not examined in detail, however, and the effects of HDAC inhibition on the differentiation of mESC-derived NPCs generated from culture condition for cortical projection neurons production (Gaspard et al., 2008, 2009) have not yet been studied.

I used 46C mESCs, one of whose characteristic features is the replacement of the *Sox1* open reading frame with that encoding green fluorescent protein (GFP) (Ying et al., 2003). Since *Sox1* is the earliest known neuroectodermal marker in the mouse embryo (Pevny et al., 1998; Wood & Episkopou, 1999), we could follow neural commitment of 46C mESCs in culture by monitoring their GFP expression.

46C mESCs can differentiate efficiently into the neural lineage in feeder-free adherent monolayer culture supplemented with serum-free medium (Ying et al., 2003; Conti et al., 2005; Abranches et al., 2009). *Sox1*-GFP-expressing NPCs can be detected from differentiation day 2, and composed more than 75% of the total cell population at

differentiation day 4 in N2/B27 medium (Ying et al., 2003). To assess the neural commitment of 46C mESCs in the adherent monolayer culture system proposed by Gaspard et al. (2008), I cultured these cells at low density in a chemically defined default medium (DDM) for 10 days (Fig. 10A). I monitored *Sox1*-GFP expression and neuronal differentiation (as judged by Tuj1 immunostaining) each day during this period. I found that 46C mESCs differentiated more slowly into the neural lineage in DDM than in N2/B27. Although *Sox1*-GFP-positive NPCs could already be observed from differentiation day 3, they reached 80% of the total cell population only after differentiation day 8 (Fig. 10B,D,D',F,F'). I also observed that starting from differentiation day 4, some of the NPCs had already differentiated into neurons (Fig. 10B,E,E',F,F').

I next examined the effects of the Shh inhibitor cyclopamine on 46C mESC survival and neural commitment. mESC-derived NPCs in DDM reportedly tend to possess ventral forebrain-like identity, and the addition of cyclopamine converts most of them into dorsal forebrain-like cells without affecting their proliferative pattern (Gaspard et al., 2008). I observed a similar pattern of neural commitment when I cultured 46C mESCs in DDM with or without cyclopamine, and found no significant difference in terms of cell survival (Fig. 10C,G-I,G'-I'). Thus, I conclude that 46C mESCs can survive and differentiate into the neural lineage in DDM with cyclopamine.
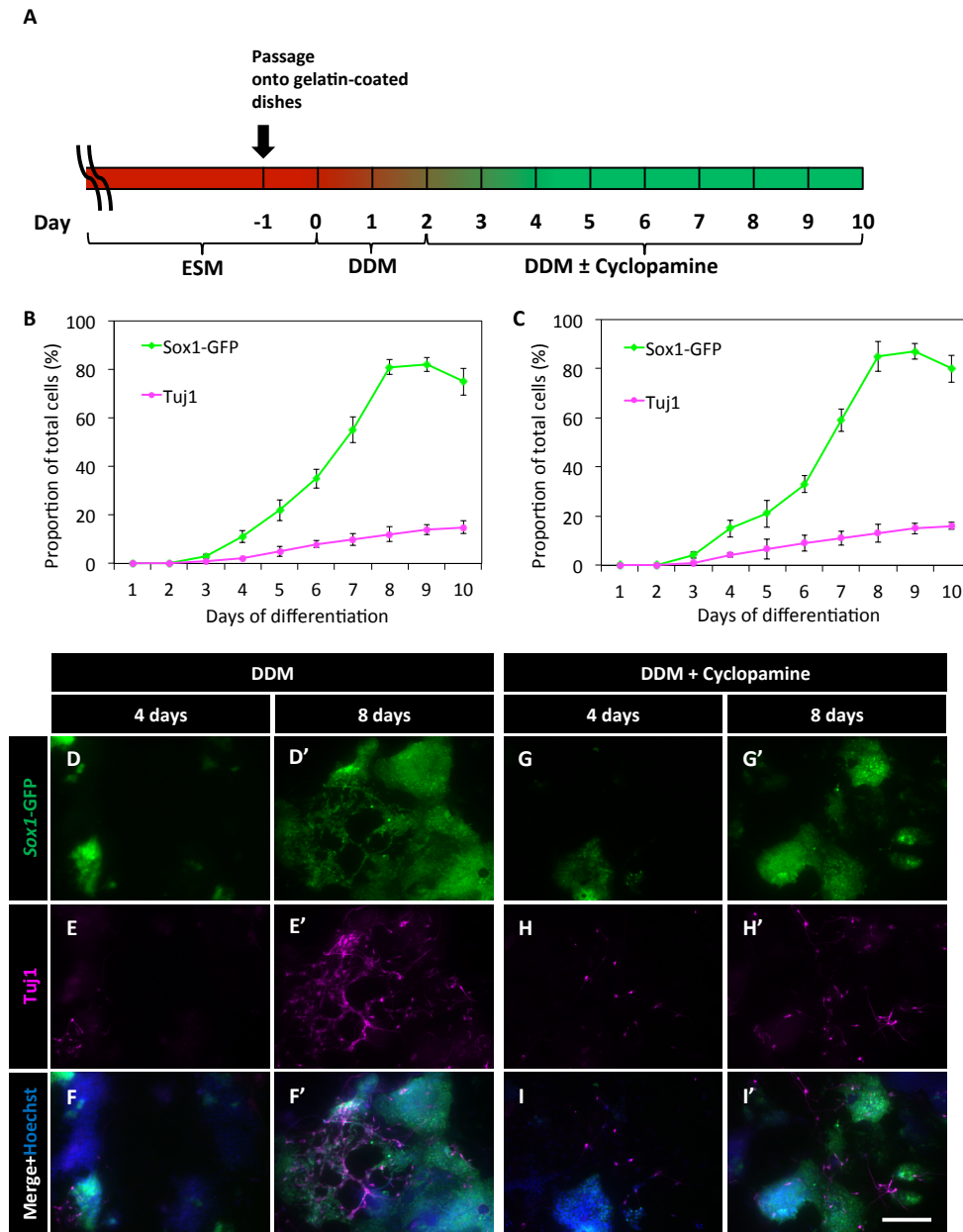
Fig. 10. 46C mESCs differentiate to the neuroectodermal lineage. (A) Timeline of the neural induction protocol using chemically defined default medium (DDM). mESCs were routinely propagated and then passaged to gelatin-coated dishes in embryonic stem cell medium (ESM) 1 day before neural induction (day -1). The next day (day 0), the medium was changed to DDM, and cyclopamine was added where appropriate from differentiation day 2 to day 10. The proportions of *Sox1*-GFP+ NPCs and Tuj1+ neurons did not differ in DDM (B) and in DDM with cyclopamine (C) during the culture period. Data are mean ± SD from at least three independent experiments. (D-I) Representative immunostaining images from differentiation day 4 and day 8 of *Sox1*-GFP-expressing (green in D,D',G,G') and Tuj1-expressing (magenta in E,E',H,H') cells, used for the quantitative data shown in B and C. Merged images with Hoechst (blue in F,F',I,I') are also shown. Scale bar is 100 μm.

III.2. VPA enhances neurogenesis of 46C mESC-derived NPCs

Another advantage of using 46C mESCs is the existence of an internal ribosome entry site (IRES)-linked puromycin resistance gene which was also knocked-in together with GFP-encoding sequence to replace the *Sox1* gene's open reading frame (Ying et al, 2003). Hence, we can enrich the resulting NPCs by addition of puromycin to the medium. Because I found that the majority of 46C mESCs (>80%) had already differentiated into NPCs by differentiation day 8 (Fig. 10B,C), I added puromycin from differentiation day 8 to day 10 for our subsequent analysis.

Next, I examined the differentiation potential of enriched NPCs which were derived from 46C mESCs. I adopted the differentiation protocol of Gaspard et al. (2008; 2009) for making cortical neurons (Figs. 11A, 12A). At differentiation day 14 (Fig. 11A), I found that more than 80% of the cells were nestin- and Pax6-positive, indicating that they were mostly still NPCs (Fig. 11B,C). VPA treatment for 2 days reduced the proportion of cells positive for both markers (Fig. 11B,C). This reduction was accompanied by an increase of Map2ab- and Tuj1-positive neuronal cells (Fig. 11D,E). I then conducted the same analysis for a longer culture period, up to differentiation day 21 (Fig. 12A). I still found higher proportion of neuronal marker-positive (Map2ab+, Tuj1+) cells in the VPA-treated dishes compared with control (Fig. 12B,C). These results indicate that the enrichment of NPCs by puromycin was successful and that VPA treatment enhances neuronal differentiation of these NPCs.
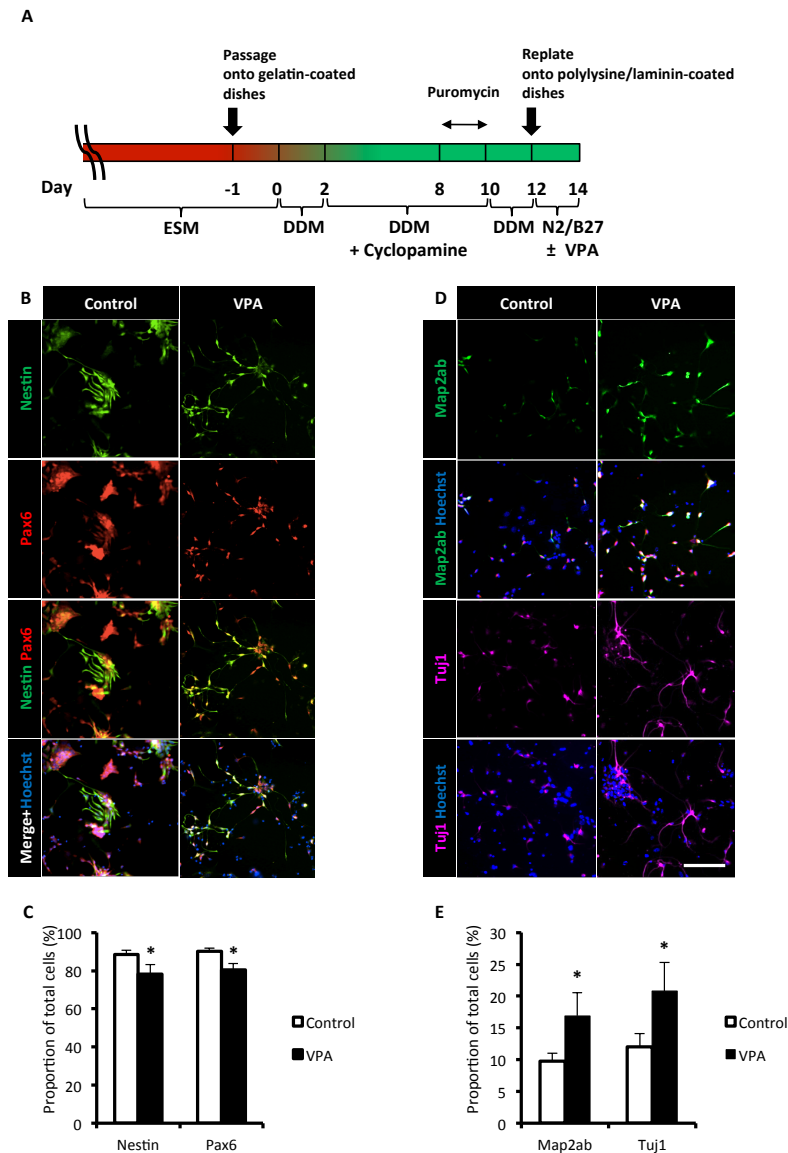
Fig. 11. VPA enhances neurogenesis of 46C mESC-derived NPCs. (A) Timeline of the corticogenesis protocol used for early differentiation analysis. mESCs were routinely propagated and passaged to gelatin-coated dishes in embryonic stem cells medium (ESM) 1 day before neural induction (day -1). The next day (day 0), medium was changed to chemically defined default medium (DDM) and cyclopamine was added from differentiation day 2 to day 10. At differentiation day 12, mESC-derived NPCs were replated to polylysine/laminin-coated dishes in N2/B27 (1:1 mixture of DDM and Neurobasal+B27). Valproic acid (VPA) was added where appropriate at differentiation day 12 and cells were harvested at differentiation day 14. (B-E) Representative immunostaining images from differentiation day 14 of nestin- and Pax6-expressing (green and red, respectively, in B), or Map2ab- and Tuj1-expressing (green and magenta, respectively, in D) cells and their quantification (C and E). Merged images with and without Hoechst (blue in B and D) are also shown. Tuj1 images in D were derived from the triple immunostaining data of Fig. 13A. Data are mean ± SD from at least three independent experiments. * $P < 0.05$ (Student's t-test). Scale bar is 100 μm.
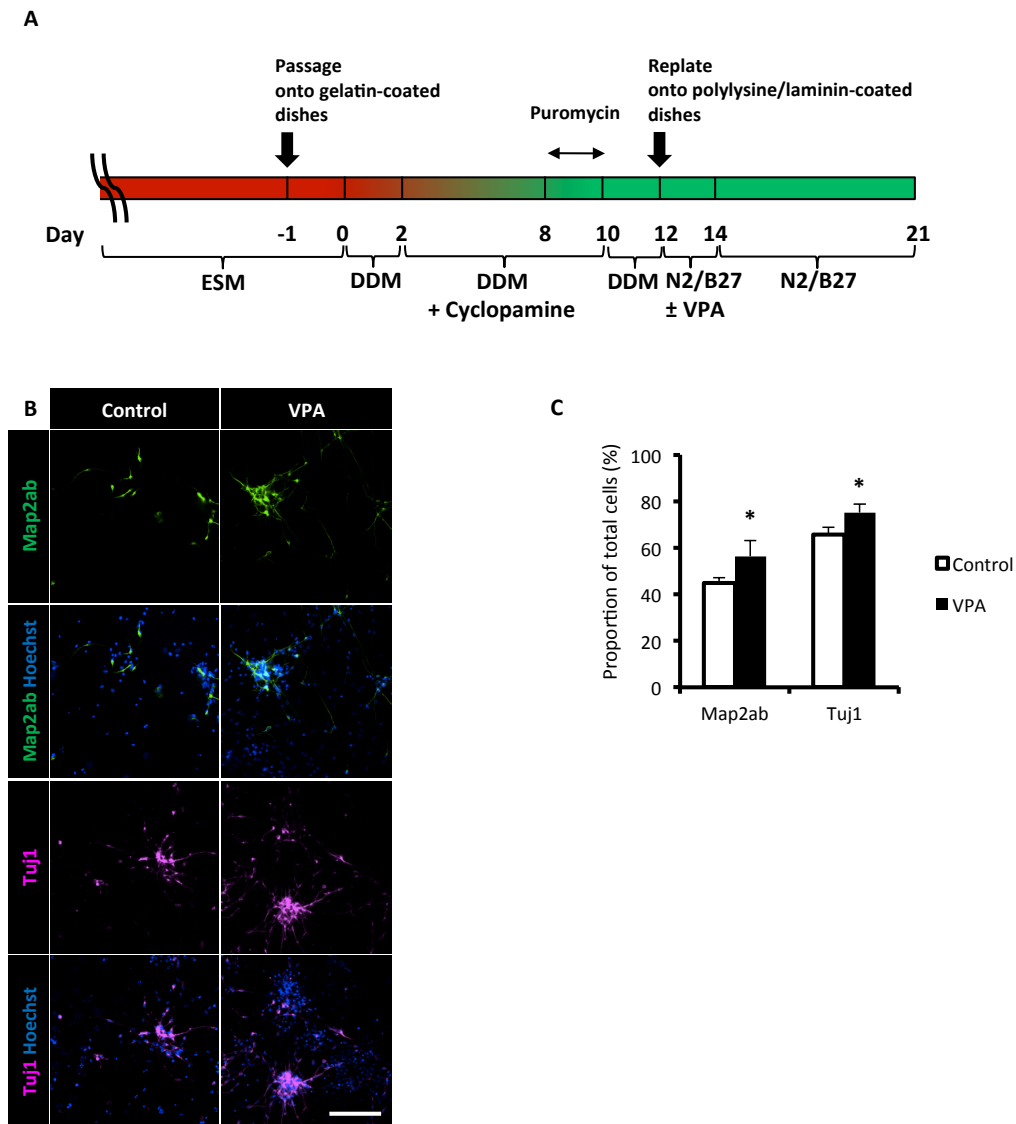
Fig. 12. Increased neurogenesis by VPA is observed even in prolonged culture. (A) Timeline of corticogenesis protocol used for late differentiation analysis. mESCs were routinely propagated and passaged to gelatin-coated dishes in embryonic stem cells medium (ESM) 1 day before neural induction (day -1). The next day (day 0), medium was changed to chemically defined default medium (DDM) and cyclopamine was added from differentiation day 2 to day 10. At differentiation day 12, mESC-derived NPCs were replated to polylysine/laminin-coated dishes in N2/B27 (1:1 mixture of DDM and Neurobasal+B27). Valproic acid (VPA) was added where appropriate at differentiation day 12 and cells were harvested at differentiation day 21. (B) Representative immunostaining images from differentiation day 21 of Map2ab- and Tuj1-expressing (green and magenta, respectively) cells. Merged images with Hoechst (blue) are also shown. Map2ab and Tuj1 images were derived from double- and triple-immunostaining data of Fig. 14A,B, respectively. (C) Quantification of neuronal marker-positive cells found in B. Data are mean ± SD from at least three independent experiments. * $P < 0.05$ (Student's t-test).

49

III.3. VPA induces the generation of superficial-layer neurons from 46C mESC-derived NPCs

Given that neurogenesis was enhanced by VPA treatment, I then looked at the cortical types of these neurons at differentiation day 14 (after two days exposure to VPA; Fig. 11A). I first found a decreased proportion of early born and deep-layer neuron markers. The proportions of reelin- and Ctip2-positive cells among Tuj1-positive cells were significantly decreased by VPA treatment (Fig. 13A,C). Next, I found an increased proportion of superficial-layer marker (Cux1)-positive cells among Map2ab-positive cells after VPA treatment (Fig. 13B,D). When I prolonged the culture until differentiation day 21 (Fig. 12A), I obtained similar results. The proportions of cells positive for early born or deep-layer markers (reelin+, Ctip2+) among Tuj1-positive neuronal cells were still lower (Fig. 14A,C), while that for cells expressing the superficial-layer marker (Cux1+) was also higher, after VPA treatment (Fig. 14B,D).

When I compared the proportions of neurons in control and VPA-treated cell populations at day 14 with those at day 21, I saw a 3-fold increase during this period under both conditions (Figs. 11E, 12C). In control cells, I observed an increased proportion of Ctip2-positive cells among Tuj1-positive cells during this period (Figs. 13C, 14C). In contrast, the proportions of reelin- or Cux1-positive cells among neuronal marker-positive cells remained unchanged (Figs. 13C,D, 14C,D). These results indicate that in control cells, the majority of neurons produced during this period were Ctip2-positive, even though some of the NPCs still generated reelin- and Cux1-positive neurons.
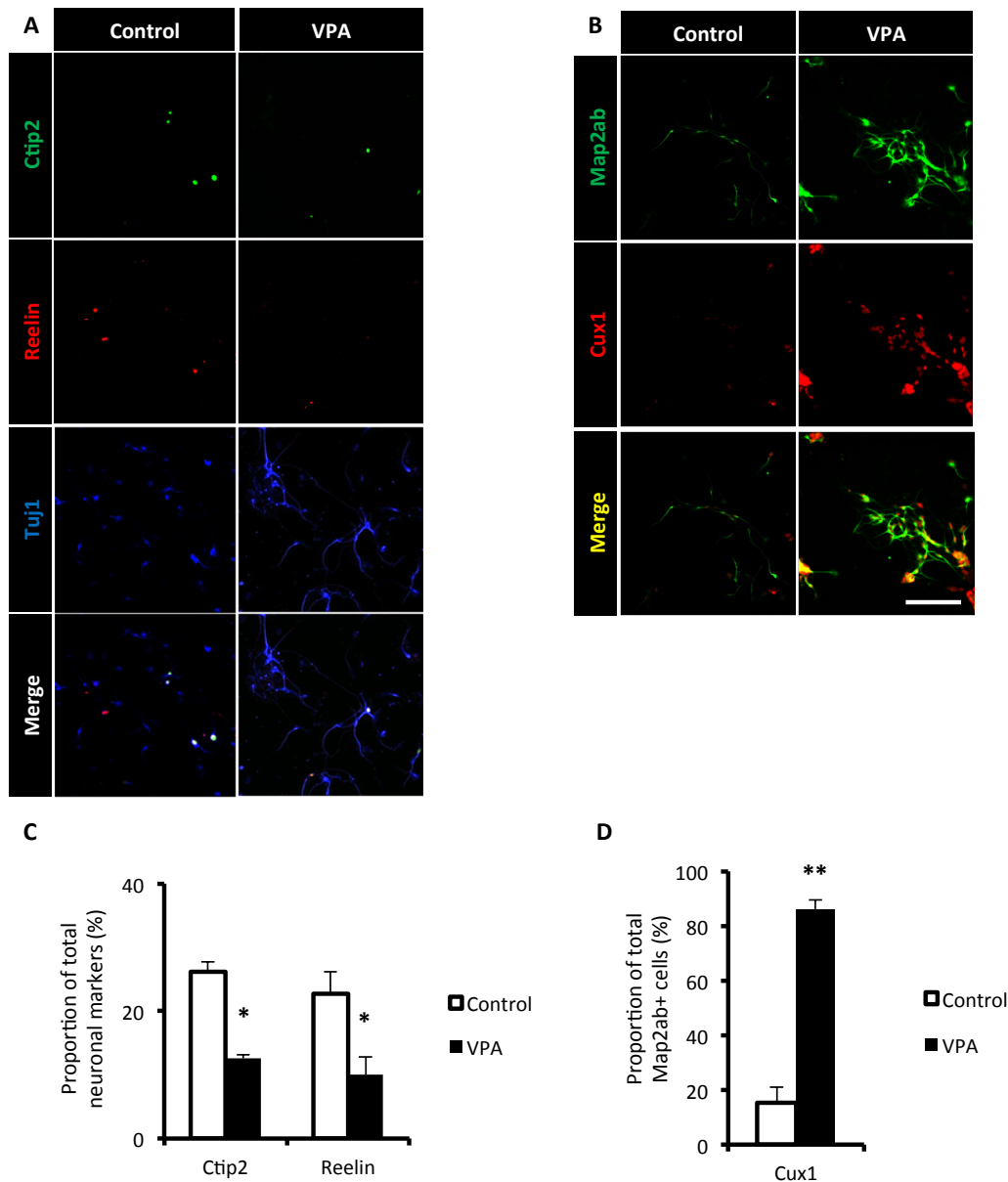
Fig. 13. VPA induces the production of superficial-layer neurons. (A,B) Representative immunostaining images from differentiation day 14, as in Fig. 11A, for Ctip2-, reelin- and Tuj1-expressing (green, red, and blue, respectively, in A), and Map2ab- and Cux1-expressing (green and red, respectively, in B) cells. Merged images are also shown. Hoechst staining can be found in Fig. 11D. Quantification of cortical layer marker-positive cells among neuronal marker-expressing cells for early-born or deep-layer (C) and superficial-layer neurons (D). Data are mean ± SD from at least three independent experiments. * $P < 0.05$, ** $P < 0.001$ (Student's t-test). Scale bar is 100 μm.
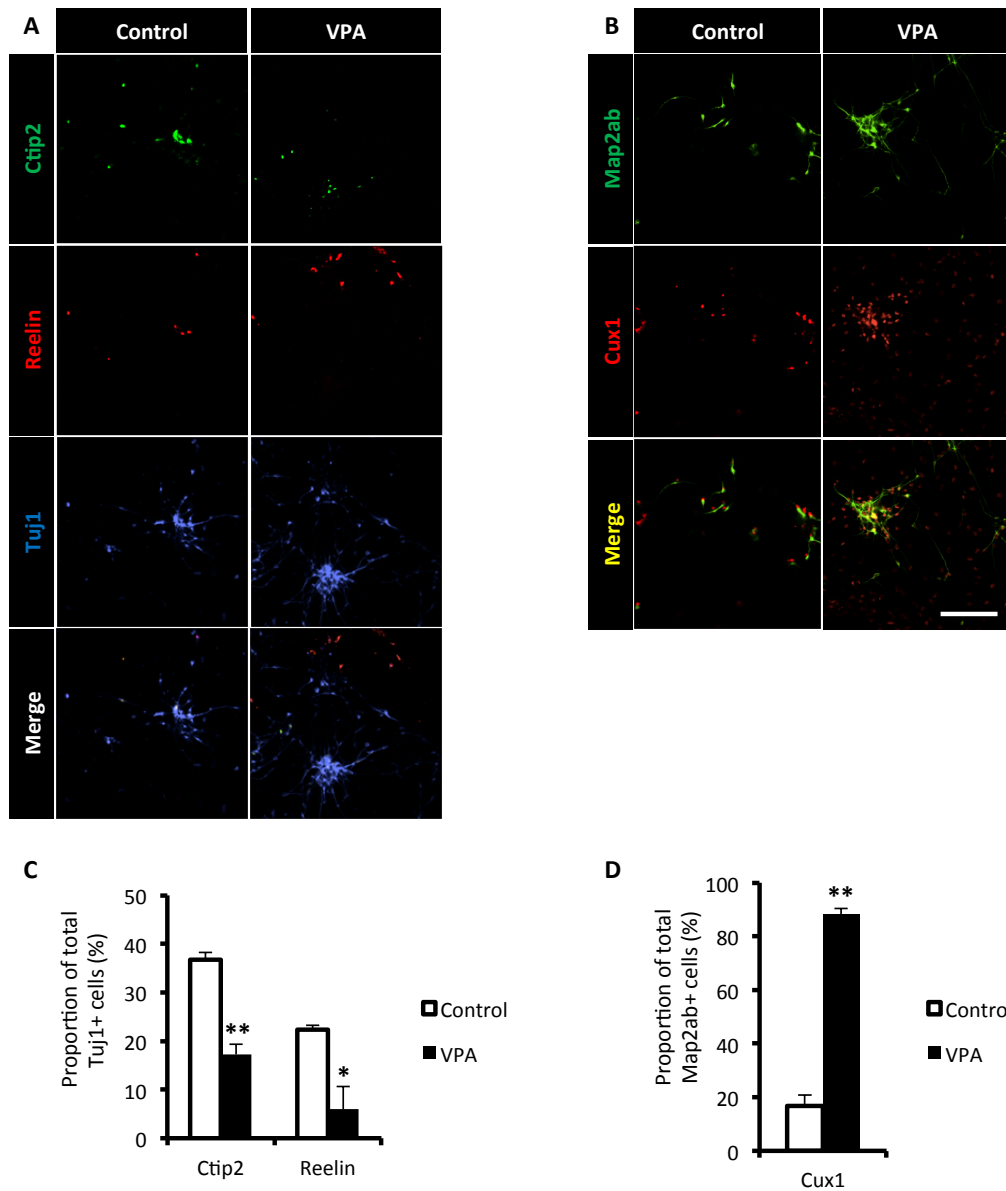
Fig. 14. Increased generation of superficial-layer neurons by VPA is observed even in prolonged culture. (A,B) Representative immunostaining images from differentiation day 21, as in Fig. 3A, for Ctip2-, reelin- and Tuj1-expressing (green, red, and blue, respectively, in A), and Map2ab- and Cux1-expressing (green and red, respectively, in B) cells. Merged images are also shown. Hoechst staining can be found in Fig. 12B. Quantification of cortical layer marker-positive cells among neuronal marker-expressing cells for early-born or deep-layer (C) and superficial-layer neurons (D). Data are mean ± SD from at least three independent experiments. * $P < 0.05$, ** $P < 0.001$ (Student's t-test). Scale bar is 100 μm.

On the other hand, the proportion of cells positive for the cortical markers I tested among neuronal marker-positive cells after VPA treatment did not change during the extended culture period (Figs. 13C,D, 14C,D). This indicates that VPA enhanced the production of Cux1-positive neurons only while it was being applied to the culture (differentiation day 12 to day 14). Nevertheless, the production of Ctip2-positive neurons in VPA treatment diminished compared to that in control cells during the extended culture period. These results suggest that transient VPA treatment enhances the temporal progression of some deep-layer-producing NPCs into superficial-layer-producing types during the treatment period, whereafter the residual NPCs retain this temporal progression even when VPA has been withdrawn from the culture.

III.4. VPA enhances embryonic cortical neurogenesis

Having found that HDAC inhibition by VPA enhances neurogenesis of mESC-derived NPCs, I further checked whether the same phenotype could be observed *in vivo*. After oral administration of VPA to pregnant mice on embryonic day (E)12.5 to E14.5 (Fig. 15A), where cortical neurogenesis is prominent, I found that the level of global histone acetylation in VPA-treated mice cortex was higher than methylcellulose (MC)-treated mice (control) for both histone H3 and H4 on E15.5 (Fig. 15B,C). To investigate whether this increasing histone acetylation was also accompanied by an enhancement of neurogenesis, embryonic cortex was subjected to immunohistochemistry using immature neuronal markers, Tuj1 and DCX (Fig. 16A,C). Both markers staining showed brighter signal in VPA-treated than MC-treated mice cortex; the stained-neurons were more abundant and have longer neuronal processes in VPA-treated mice. The cortical plate and intermediate zone, two areas

53

where most of the neurons reside, were thicker in VPA-treated mice. Moreover, a higher number of Tuj1 positive cells can be found in ventricular zone (VZ) and subventricular zone (SVZ) of VPA-treated mice indicating that differentiation to neuronal lineage was enhanced by VPA (Fig. 16B).
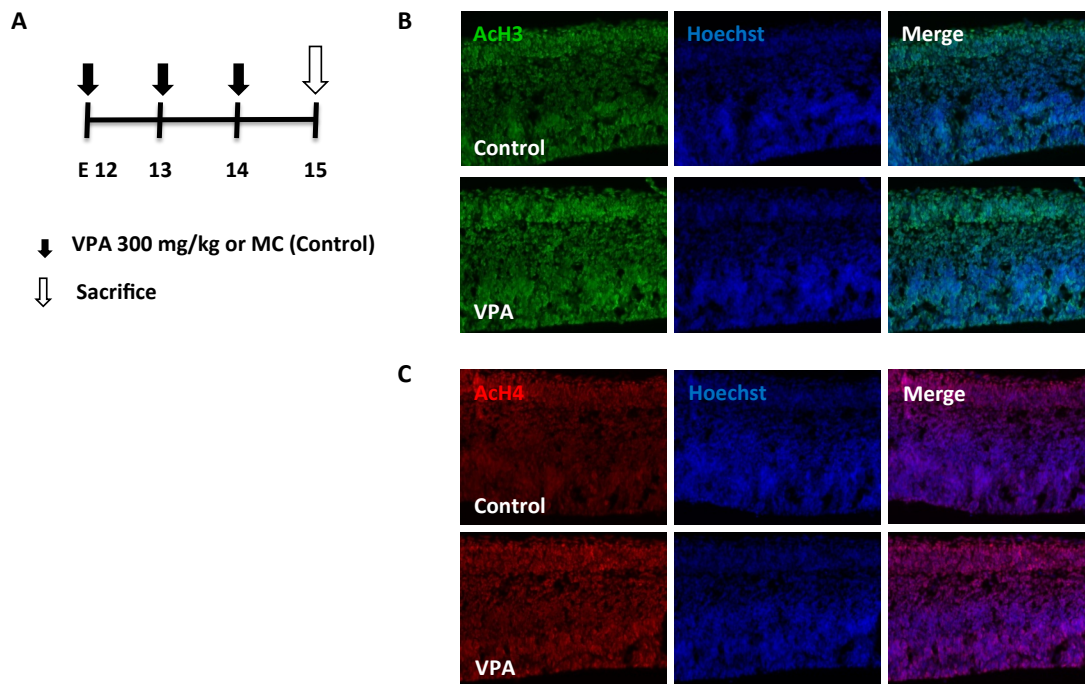

Fig. 15. VPA increases histone acetylation of embryonic cortex. (A) Valproic acid (VPA) or methyl-cellulose (MC; Control) was orally administered to pregnant mice from embryonic day (E)12.5 until E14.5 and sacrificed at E15.5. (B,C) Immunostaining signal of acetylated-histone H3 (B) and acetylated-histone H4 (C) of E15.5 cortex are higher in VPA-treated mice.

The enhancement of neurogenesis, or differentiation in general, usually coupled with the reduction of NSCs number because these cells have to exit cell cycle before they differentiate. I found that the expression of NSCs marker, Nestin, was lower in VPA-treated mice compared with control, indicating that the number of NSCs in VZ and SVZ were reduced (Fig. 16A). In order to check cell cycle exit, mice were given a single injection of BrdU on E14.5, one day before they were sacrificed (E15.5). Fraction of BrdU-positive cells

which were negative for Ki67, a marker for cell that is in cell cycle, were higher after VPA treatment (Fig. 17). These results suggest that VPA treatment enhances neurogenesis of NSCs and forces them to exit cell cycle, which results in a reduction of NSCs number in embryonic cortex.
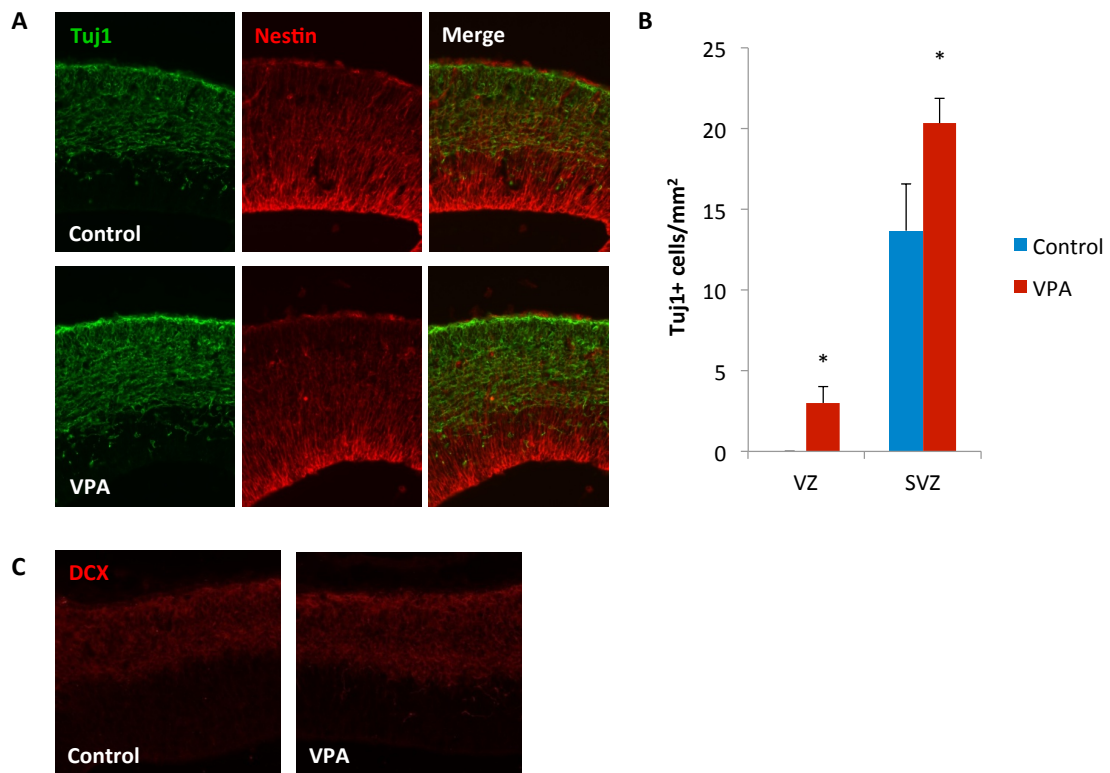

Fig. 16. VPA increases neurogenesis of embryonic NSCs. Increase immunostaining signal of neuronal markers, Tuj1 (green, A) and DCX (C), and decrease signal of NSCs marker, Nestin (red, A), can be observed in VPA-treated mice. (B) Quantification of Tuj1+ cells at ventricular zone (VZ) and subventricular zone (SVZ). * $P < 0.05$ (Student t-test).
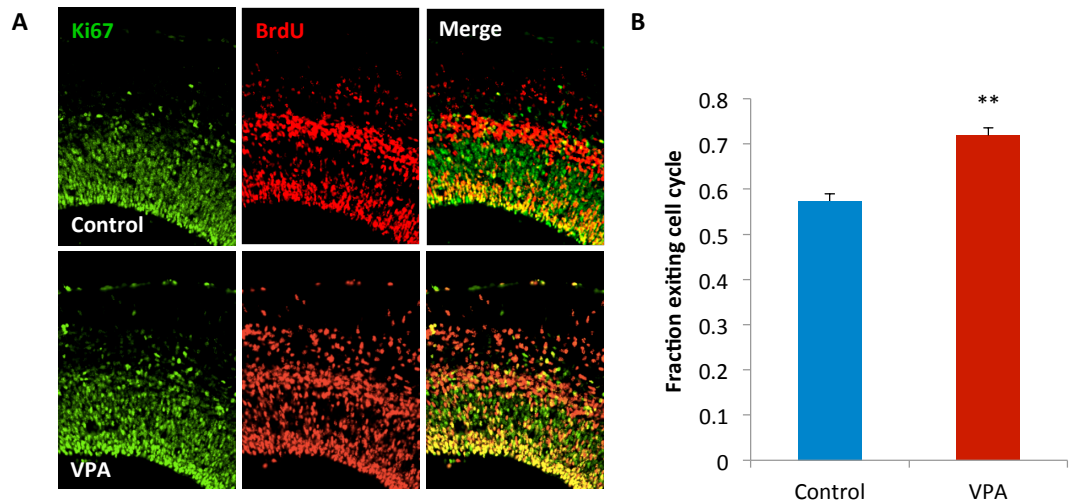
Fig. 17. VPA promotes cell cycle exit. (A) Ki67, BrdU double staining following BrdU pulse labeling 24 h before sacrifice, reveals increase rate of cell cycle exit in VPA-treated mice. (B) The fraction of cells labeled only with BrdU (BrdU+/Ki67-, no longer dividing) as compared with BrdU+/Ki67+ cells (re-entered cell cycle). ** $P < 0.001$ (Student t-test).
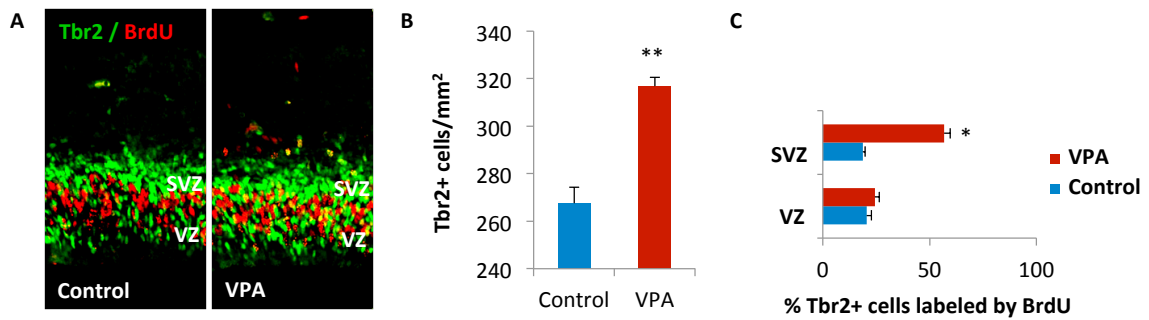

Fig. 18. VPA increases number of proliferating IPCs. Immunostaining images (A) and quantification (B) of intermediate progenitor cells (IPCs) marker, Tbr2 (green in A), and single pulse labeling of BrdU, 30 min before sacrifice (C) show an increase number of proliferating IPCs in VPA-treated mice. * $P < 0.05$, ** $P < 0.001$ (Student t-test).

Embryonic NSCs differentiate into neurons by two pathways: direct neurogenesis by forming neurons, and indirect neurogenesis by forming intermediate progenitor cells (IPCs) (Noctor et al., 2008). These IPCs are highly proliferative and express T-box transcription factor Tbr2 (Englund et al., 2005). Given that VPA enhances neurogenesis, I investigated which pathway was being used dominantly by NSCs to form neurons after VPA treatment. I found that on E15.5, the number of Tbr2-positive IPCs was increased by VPA treatment (Fig. 18A,B). These Tbr2-positive IPCs were more proliferative, as percentage of Tbr2-positive cells being labeled by BrdU in VPA-treated mice was higher than control (30 min pulse labeling before sacrificed, Fig. 18A,C). This result was intriguing because VPA has been reported previously both to inhibit (Hsieh et al., 2004; Jessberger et al., 2007) and to stimulate NSCs proliferation (Higashi et al., 2008). To check proliferation status of NSCs and to confirm the increase number of proliferating IPCs after VPA treatment, I counted the number of mitotic cells which showed phosporilated histone H3 (PH3) in embryonic cortex. I found that at VZ where NSCs reside, PH3-positive cells number was reduced by VPA treatment (Fig. 19). On the other hand, the number of PH3-positive cells at SVZ and percentage of Tbr2-positive cells colabeled by PH3 were increase by VPA treatment (Fig. 19). Taken together these results suggest that VPA enhances indirect neurogenesis of NSCs, inhibits proliferation of residual NSCs, and stimulates proliferation of IPCs.

III.5. Cortical laminarization is perturbed in VPA-treated mice

The increase proliferation of IPCs in VPA-treated mice might result in the pertubation of cortex laminarization. Previous studies have revealed that IPCs will differentiate mostly into superficial layer neurons of the postnatal cortex (Tarabykin et al.,

2001). This is intriguing because I have shown earlier that VPA treatment to the mESC-derived NPCs could induced higher generation of superficial layer neurons (Figs. 13B,D, 14B,D). To examine a possibility that the increase proportion of proliferating Tbr2-positive IPCs in VPA-treated mice could results in an increase generation of superficial layer neurons, I injected BrdU on E14.5 and analyzed the position of BrdU-retaining cells on P7 cortex. I found that cell density in superficial layer was more dense in VPA-treated mice (Fig. 20A,B). Moreover, the percentage of cells in superficial layer that retained BrdU was also higher in VPA-treated mice (Fig. 20A,C). Further, thickness of Cux1-positive superficial layer neurons-area was also increase in VPA-treated mice P7 cortex (Fig. 21A). The increase of superficial layer thickness in VPA-treated mice was also accompanied by a decreased thickness of deep layer neurons area, in particular layer V, as shown by a decrease of cell number, lower percentage of cells retaining BrdU, and thinner Ctip2-positive deep layer neurons-area in this layer (Figs. 20, 21B). Together these results suggest that VPA treatment increases the generation of proliferating IPCs from NSCs in the embryonic brain, thereby induces higher generation of superficial layer neurons and suppresses the generation of deep layer neurons.
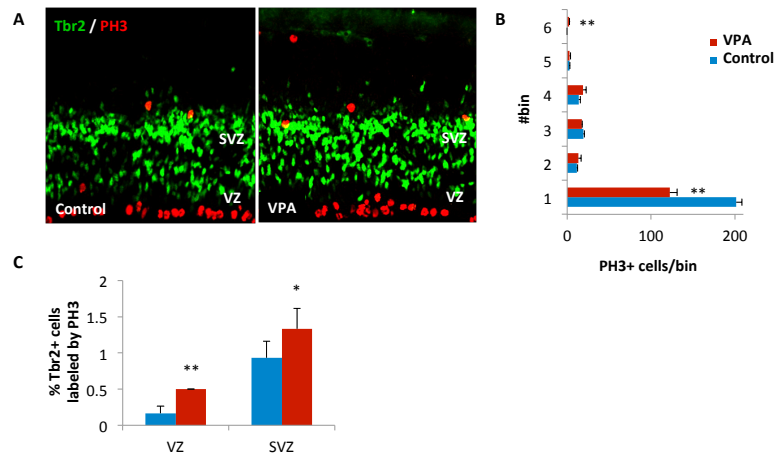
Fig. 19. VPA inhibits and stimulates NSCs and IPCs proliferation, respectively. (A) Immunostaining of IPCs (Tbr2+) and M-phase dividing cells (PH3+). Apical and basal PH3+ cells is decrease and increase in VPA-treated mice, respectively. (B) IPCs divide more intensively in VPA-treated mice as shown by an increase of Tbr2+/PH3+ cells. $* P < 0.05$, $** P < 0.001$ (Student t-test).
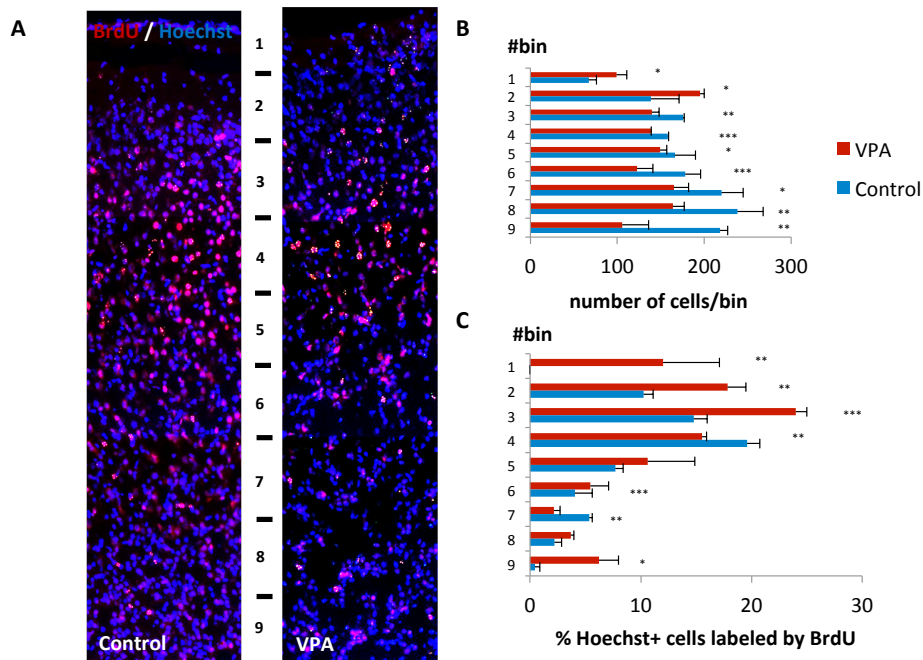

Fig. 20. VPA changes laminar positioning of neural cells. (A-C) Position of cells that were born at E14.5 is changing in VPA-treated mice as shown by BrdU single pulse labeling at E14.5 and sacrificed at P7. Quantitative data are shown for cell density (B) and BrdU+ cells labeling (C). $* P < 0.1$, $** P < 0.05$, $*** P < 0.001$ (Student t-test).
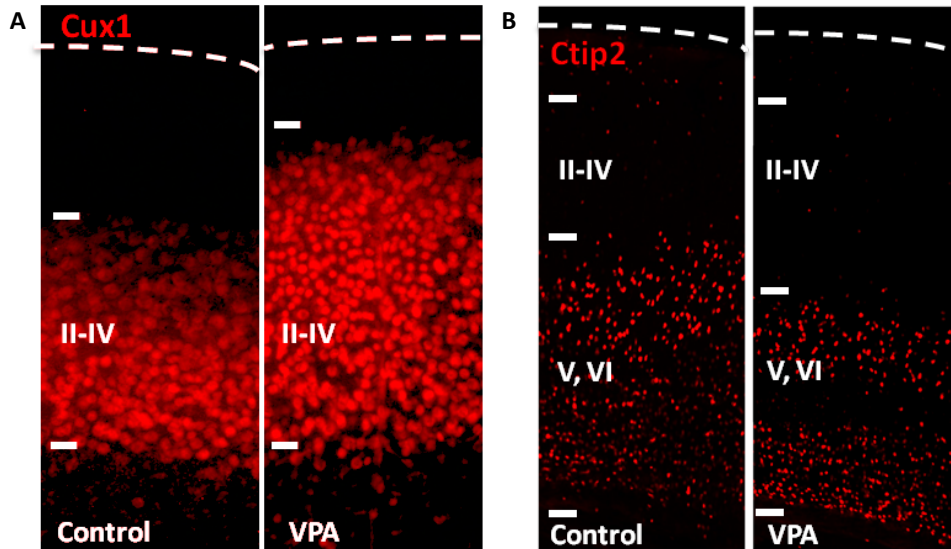
59

Fig. 21. Cortical laminarization is perturbed in VPA-treated mice. (A-B) The thickness of superficial layer (II-IV) marker Cux1 (A) and deep layer (V-VI) marker Ctip2 (B) were increase and decrease, respectively, in VPA-treated mice on P7.

III.6. Histone acetylation in late gestational NSCs are higher that in midgestational ones

Based on above results of mESC-derived NPCs and embryonic cortex NSCs after VPA treatment, increasing histone acetylation by means of HDAC inhibition is important for the generation of superficial layer neurons. However, it is not clear whether an increase of histone acetylation is indeed can be observed in NSCs *in vivo* when NSCs make a transition from producing deep-layer to superficial-layer neurons. To examine this question, I checked the level of acetylated histone H3 (AcH3) in Nestin-positive NSCs on E11.5 and E16.5, where NSCs can only produce deep-layer and superficial-layer neurons, respectively. I found that AcH3-immunoreactive signal was higher in NSCs of E16.5 than those of E11.5 (Fig. 22), suggesting the important role of histone acetylation in the generation of superficial-layer neurons.
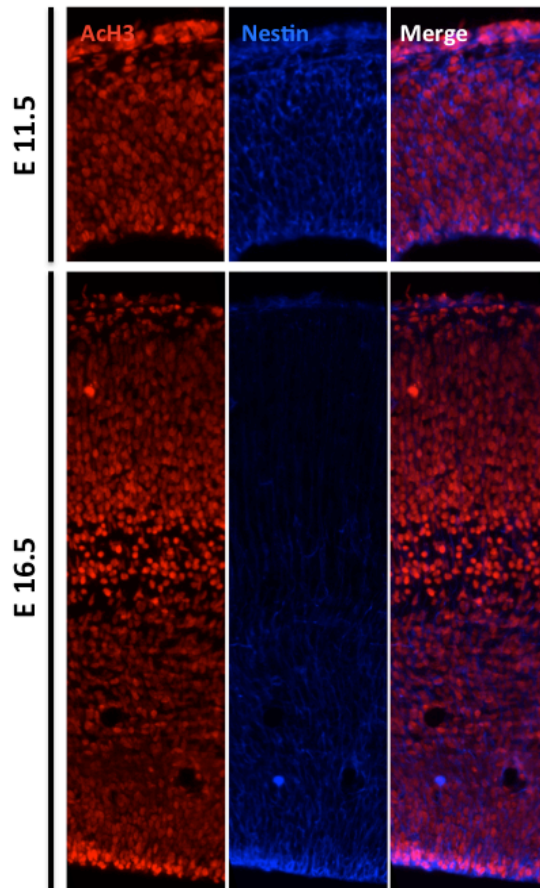
Fig. 22. Histone acetylation in NSCs is increasing during cortical development. Immunostaining of E11.5 and E16.5 mice cortex showed that expression of acetylated histone H3 (red) was higher in E16.5 Nestin (blue)-positive NSCs.

III.7. VPA treatment affects the size of brain parts

Having observed that cortical laminar positioning of cells which were born on E14.5 were changed and there were differences in laminar density between superficial layer and deep layer, I checked a possibility that VPA treatment alters brain parts size. Using modified geometric morphometrics protocols (Juliandi et al., 2008, 2010c), I found that forebrain size of VPA-treated mice was bigger on E15.5 but progressively become smaller after they were born (Fig. 23A). Specific brain parts, such as hippocampus and dentate gyrus, also smaller when observed on P56 in VPA-treated mice (Fig. 23B). This can be explain by

61

the fact that on embryonic stages, VPA treatment enhances neurogenesis which might lead to the expansion of forebrain size. Meanwhile, NSCs proliferation and number were reduced by VPA treatment. These reductions could lead to the lower production of neural cell types after VPA treatment was diminished. In support of this notion, the absolute BrdU-positive cell number on P7, after single pulse labeling on E14.5, was lower in VPA-treated mice (Fig. 23C). Moreover, using the same labeling, the absolute BrdU-positive cell number in the dentate gyrus of VPA-treated mice on P56 was also lower than that of control mice (Fig. 23D). Therefore, it is likely that NSCs in VPA-treated mice generated fewer neural cell types after VPA-treatment, which later caused smaller forebrain, hippocampus, and dentate gyrus.

To exclude the possibility that VPA selectively causes apoptosis in deep layer neuron-producing NSCs or other neural cell types, thereby resulting the decrease of brain parts size postnatally, I counted the number of activated Caspase 3 (Casp3)-positive cells on E15.5 and P7 cortices. There was no significant difference between VPA-treated and control mice for both timepoints (Fig. 24). Thefore, the observed size and density differences in VPA-treated mice were not attributable to apoptosis in specific cell types.
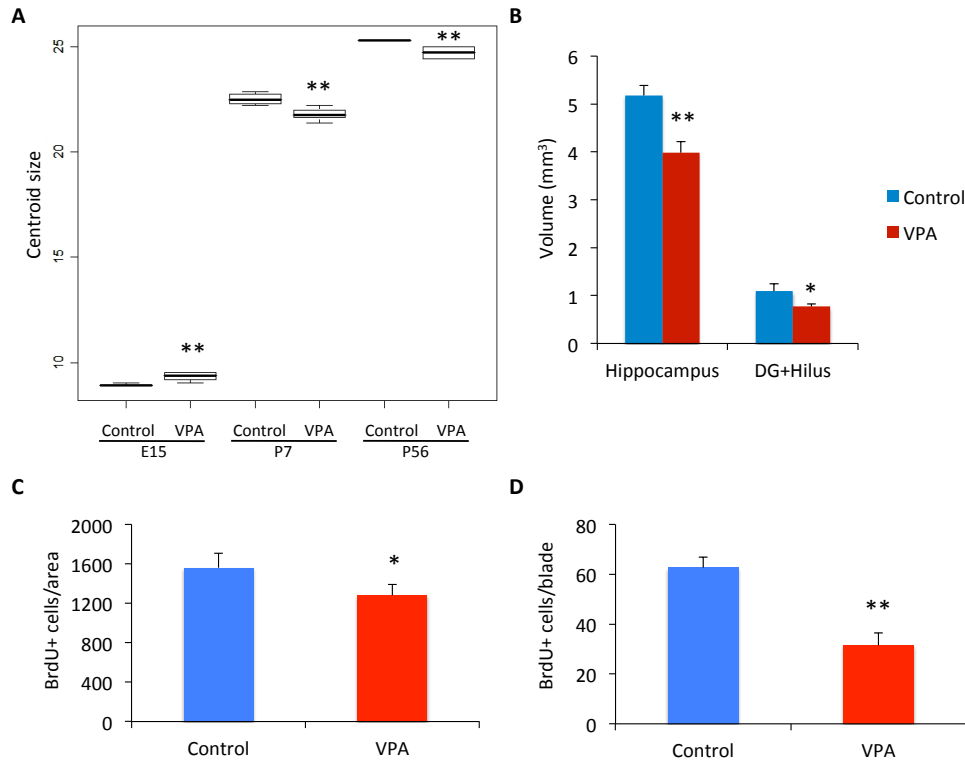
Fig. 23. VPA-treated mice have smaller brain parts size. (A) Forebrain size, as measure by centroid size, on E15.5, P7, and P56. (B) Hippocampus and dentate gyrus+hilus volume at P56. (C-D) Absolute number of BrdU+ cells at P7 cortex (C) and P56 dentate gyrus. * $P < 0.05$, ** $P < 0.001$ (Student t-test).
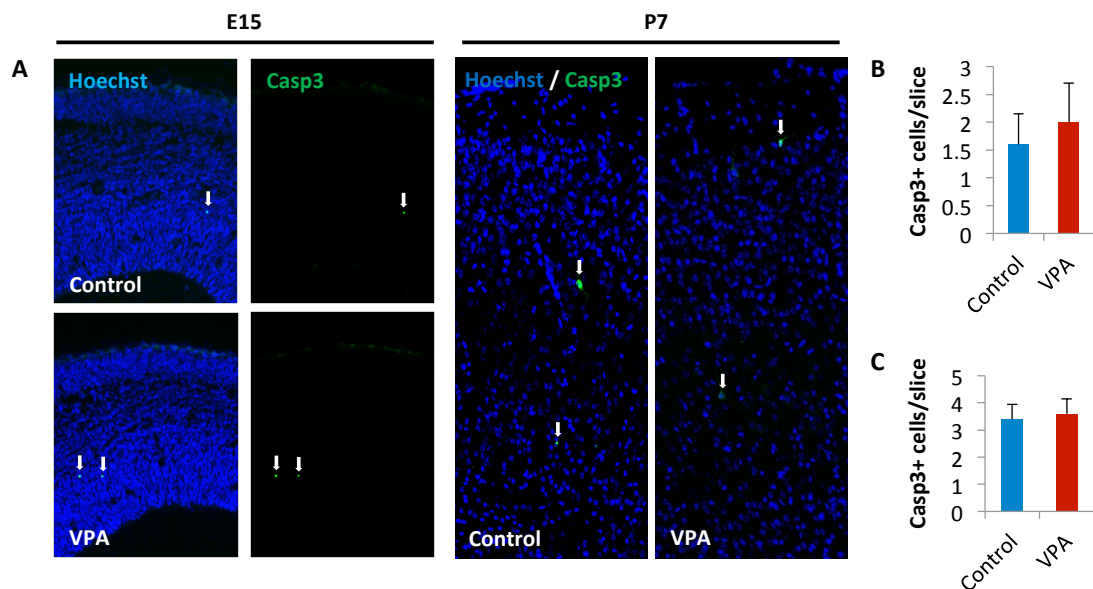

Fig. 24. VPA does not affect apoptosis program. (A) Apoptosis (cell death) program was not affected as shown by immunostaining of activated caspase-3 (Casp3) on E15.5 and P7. (B-C) Quantification of dying cells (Casp3+) on E15.5 (B) and P7 (C).

III.8. VPA-treated mice have a deficiency in learning and memory

In order to investigate whether the changes caused by embryonic treatment of VPA could caused any behavioral alterations, we conducted several behavioral tests on 12-13 weeks old male mice. We found that VPA-treated mice performance were poor, mainly in the tests that assessed learning and memory behavior, which were the contextual/cued fear conditioning and Y-maze alternation tests (Table 1, Fig. 25). One of the brain part which responsible for these learning and memory test is hippocampus. It has been reported that adult NSCs in the dentate gyrus (DG) of hippocampus have a functional role in learning and memory processes by undergo neurogenesis to generate adult born neural cells which later integrate into the existing neural circuit (Ramirez-Amaya et al., 2006; Zhao et al., 2008).

Table 1. List of tests used in this study to assess behavioral alterations on 12-13 weeks of age, after embryonic treatment of VPA on E12.5-14.5

Test name	Behavior assessed	Results
Open field	general activity level, gross locomotor activity, exploration habits	total distance[2], centre time[1], move episode[1], distance per movement[2]
Light/dark transition	anxiety-like	dark distance[3], dark time[1], transition[2], light distance[1], light time[1], latency to enter light[1]
Elevated plus maze	anxiety-like	total distance[2], open time[1], close time[1], open entry[1], close entry[2], total entry[1]
Pre-pulse inhibition	sensorimotor gating	pre 90db/120db[1], pre 95db/120db[2]
Tail suspension	depression	immobility time[1]
Contextual/cued fear conditioning	learning and memory	conditioning[3], contextual[3], cued[3]
Y-maze alternation	learning and memory	correct alternation[3]

[1] not significantly different, [2] $P < 0.05$, [3] $P < 0.01$ (Student's t-test)
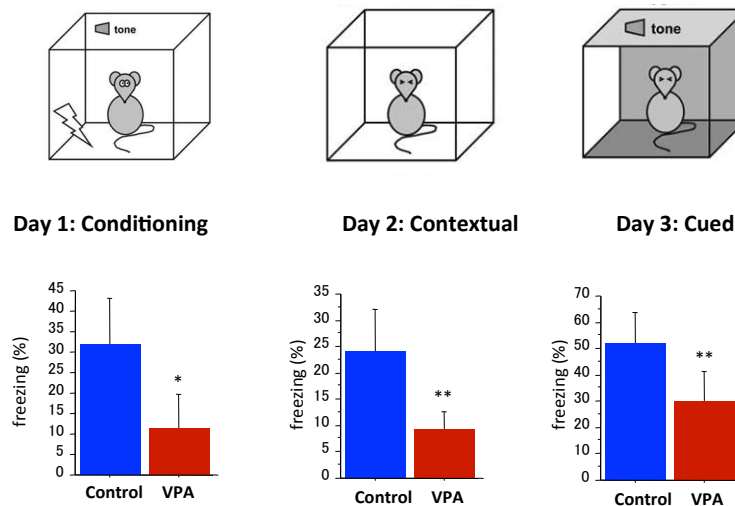
Fig. 25. The contextual/cued fear conditioning tests. Tests were done by placing a mouse into a new box on day 1 of the test. Mouse was presented with a tone for 30 sec and at the end of this tone, a mild electrical foot shock was given. This treatment was repeated 3 times (conditioning). On day 2, mouse was put back in the same box as day 1 but without any tone or foot shock. On day 3, mouse was put into a different box and presented with the same tone as day 1, but again without foot shock. VPA-treated mice had less freezing behavior compared to control which indicates that they have a difficulty to learn and memoryze the association between box, tone, and foot shock. * $P < 0.05$, ** $P < 0.01$ (Student t-test).

III.9. VPA-treated mice have a impaired neurogenesis in dentate gyrus

Having found earlier that the volume of hippocampus and dentate gyrus were smaller in VPA-treated mice (Fig. 23B), I further investigated whether granule cell layer (GCL) volume and granule cell absolute number in the dentate gyrus were also affected. These two parameters have been reported to influence the function of hippocampus in regulating learning and memory (Kempermann et al., 1997; van Praag et al., 1999a, 1999b). I found that the GCL volume and granule cell number were smaller in VPA-treated mice (Fig. 26). These reductions could be resulted from the different rate of proliferation and differentiation of NSCs in DG of VPA-treated mice, as they showed fewer generated neural cells after they were born (Fig. 23C,D).
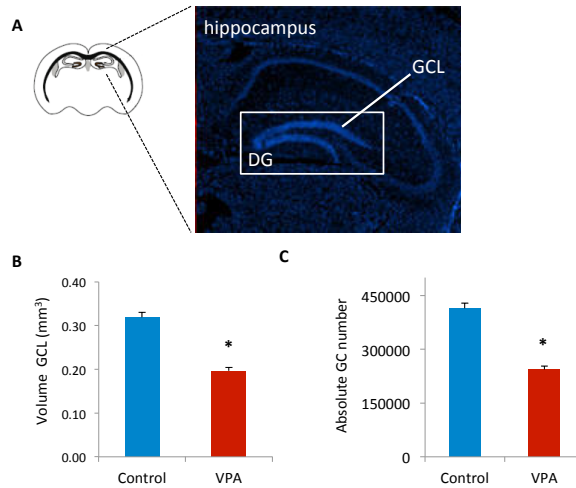
Fig. 26. VPA-treated mice have smaller granule cell layer. (A) Hippocampal formation. White boxed area is dentate gyrus (DG) and white line pointed granule cell layer (GCL). (B) Volume of GCL. (C) Quantification of granule cell number in GCL. * $P < 0.001$ (Student t-test).

In order to confirm that proliferation and differentiation of adult hippocampal NSCs are indeed reduced by embryonic VPA treatment, I performed 7 day-BrdU injection to label proliferating NSCs in DG of VPA-treated and control mice (Fig. 27A). Mice were then sacrificed one day and 4 weeks after the last BrdU injection to analyze NSCs proliferation and differentiation, respectively. The number of BrdU-positive cells in VPA-treated mice on both time points was lower than control (Fig. 27B,C). To confirm these results, I checked also the number of proliferating cells by using immunostaining of Ki67. As observed in experiment 1 day after the last BrdU injection, the number of proliferating Ki67-positive cells was also lower in VPA-treated mice (Fig. 28).

Next, I traced the fate of the labeled BrdU-positive cells 4 weeks after the last BrdU injection (Fig. 27A). I found a reduction of BrdU-positive cells which differentiated into NeuN-positive neurons and S100β-positive astrocytes in VPA-treated mice (Fig. 29A). These findings might be due to that the BrdU-positive cells died during the 4 weeks before

sacrificed. However, based on the results of active caspase3-staining (Fig. 24), this possibilty is unlikely. In fact, the survival rate of BrdU-positive cells in VPA-treated mice was higher than control (Fig. 29B). Therefore, BrdU-positive cells in VPA-treated mice might have differentiate to another cell types or become more quiescent. To check which of these possibilities reflect the fact found in VPA-treated mice, I investigated the fate of BrdU-positive cells by using another cell type markers. I discovered that in VPA-treated mice, higher percentage of BrdU-positive cells were still expressing Sox2 (NSCs marker) and Ki67 (proliferation marker) even 4 weeks after the last BrdU injection (Fig. 30A-C). When I looked at BrdU-positive cells in mice which were sacrificed 1 day after the last BrdU injection, the number of BrdU/Ki67-positive cells was also higher in VPA-treated mice (Fig. 30D). Together, these results suggest that VPA-treated mice have an impaired neurogenesis because of their adult NSCs become more quiescent.
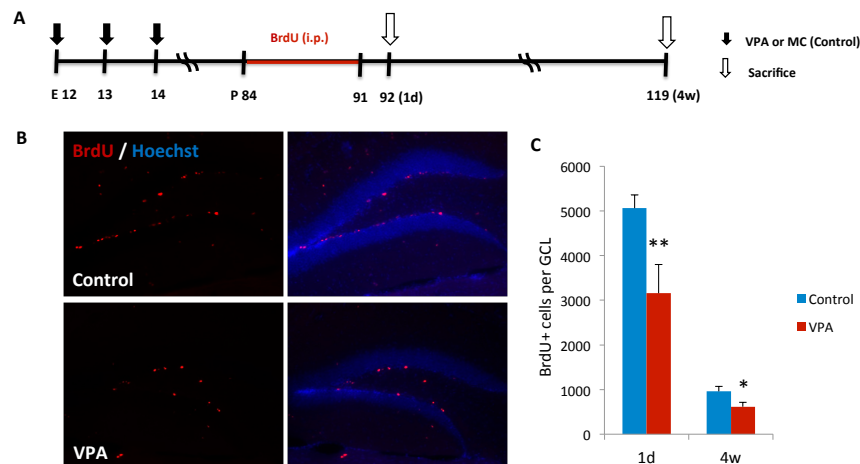

Fig. 27. VPA-treated mice have fewer proliferating cells in adult DG. (A) VPA or MC (Control) was orally administered to pregnant mice from E12.5 until E14.5. BrdU was injected once a day for 7 days starting at P84. Mice were sacrificed one day (1d) and 4 weeks (4w) after the last BrdU injection. (B-C) Immunostaining of 1d (B) and quantification (C) of BrdU+ cells at dentate gyrus show that VPA-treated mice have fewer proliferating cells. * $P < 0.05$, ** $P < 0.001$ (Student t-test).
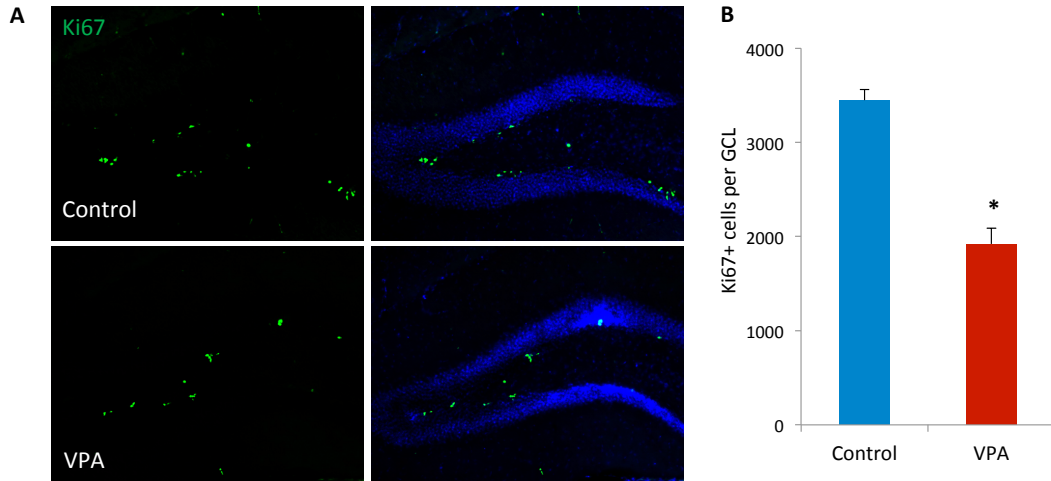
Fig. 28. VPA-treated mice have fewer Ki67+ proliferating cells in adult DG. (A-B) Immunostaining with Ki67 (A) and quantification of Ki67+ cells in DG (B). * $P < 0.001$ (Student t-test).
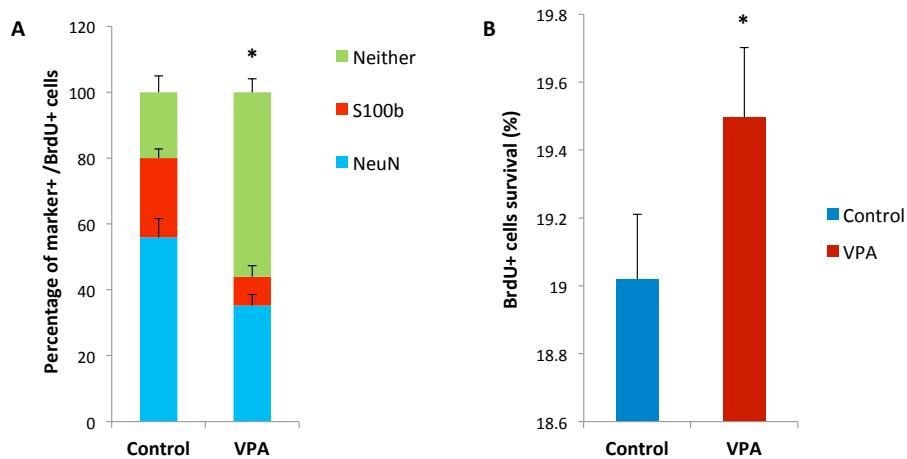

Fig. 29. Reduce neural differentiation in VPA-treated mice. (A) Quantification of newly generated NeuN+ neurons and S100b+ astrocytes show reduced differentiation of NSCs at DG of VPA-treated mice, 4 weeks after the last 7 days BrdU injection. (B) VPA-treated mice have a higher surviving BrdU+ cells, 4 weeks after the last 7 days BrdU injection. * $P < 0.001$ (Student t-test).
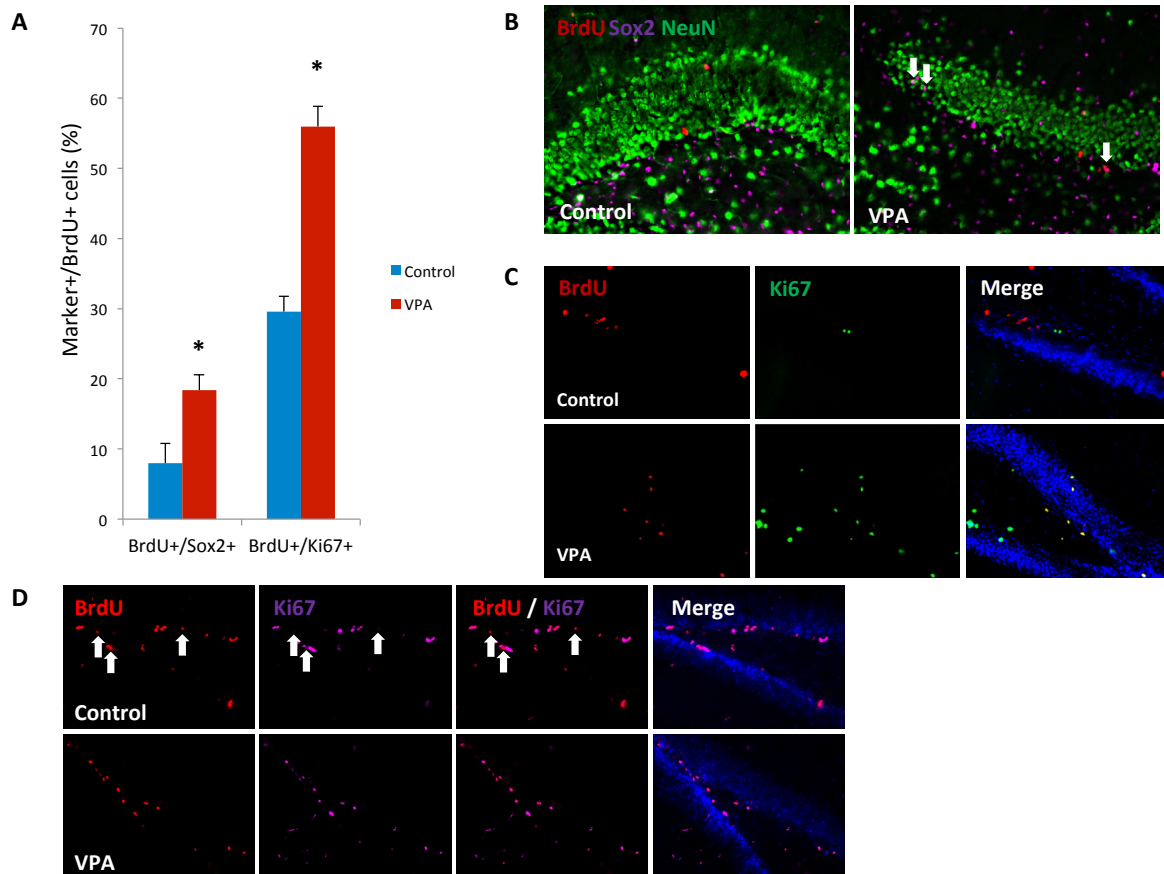
68

Fig. 30. NSCs in VPA-treated mice were more quiescent. (A-C) Quantification of BrdU+ cells which were remained as NSCs (Sox2+) and proliferating cells (Ki67+), 4 weeks after the last 7 days BrdU injection (A), and its representative immunostaining images (B-C). (D) Immunostaining for BrdU+ cells which were still proliferating (Ki67+), 1 day after the last 7 days BrdU injection. White arrow indicate BrdU+ cells which already exit cell cycle (non proliferative). * $P < 0.001$ (Student t-test).

III.10. Running recovers impaired neurogenesis and behavior of VPA-treated mice

Several studies have reported that voluntary running can increase adult neurogenesis in the dentate gyrus of hippocampus (van Praag et al., 1999a, 1999b). Given that VPA-treated mice have an impaired neurogenesis, I asked whether voluntary running can recovers this deficiency.

I set up running wheel in the cage of control and VPA-treated mice directly after they were weaned (P28). After they reached 12 weeks of age, I repeated the same BrdU

injection experiment conducted earlier to VPA-treated mice (Fig. 27). As expected, I observed an increase number of BrdU-positive cells in VPA-treated mice with running wheel (VPA+RW), 1 day (Fig. 31) and 4 weeks after the last BrdU injection (Fig. 32). This is an indication that voluntary running increase the proliferation and survival of NSCs in the DG of hippocampus, as already being reported for normal mice. To check whether the recovery of neurogenesis in VPA-treated mice could improve the learning and memory behaviors, we conducted again the same tests for assessing learning and memory we used earlier (Fig. 25). We found that voluntary running could help mice to perform better in almost every tests being conducted, except for the contextual associative test (Fig. 33). These results suggest that the increasing neurogenesis caused by running can recovers some learning and memory deficiencies in VPA-treated mice.
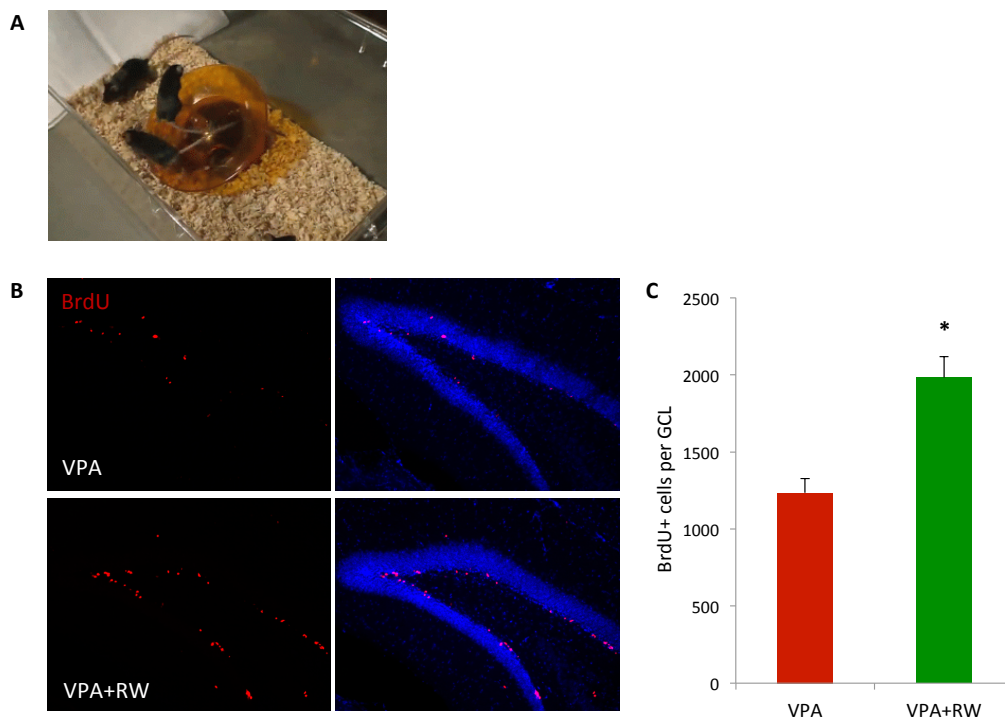

Fig. 31. Voluntary running increases proliferating cell number in VPA-treated mice. (A) Mice were freely run after they were being weaned on P28. (B-C) Immunostaining of BrdU+ cells (B) and its quantification (C), 1 day after the last 5 days BrdU injection. * $P < 0.001$ (Student t-test).
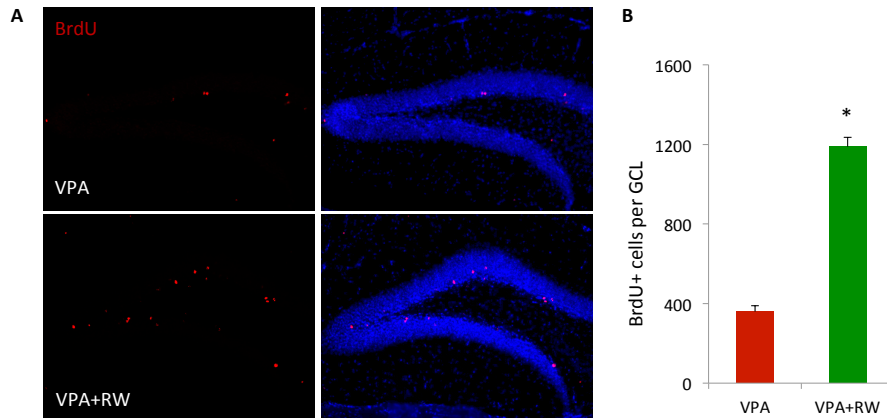
Fig. 32. Voluntary running increases the number of surviving BrdU+ cell in VPA-treated mice. (A-B) Immunostaining of BrdU+ cells (A) and its quantification (B), 4 weeks after the last 5 days BrdU injection. $* P < 0.001$ (Student t-test).
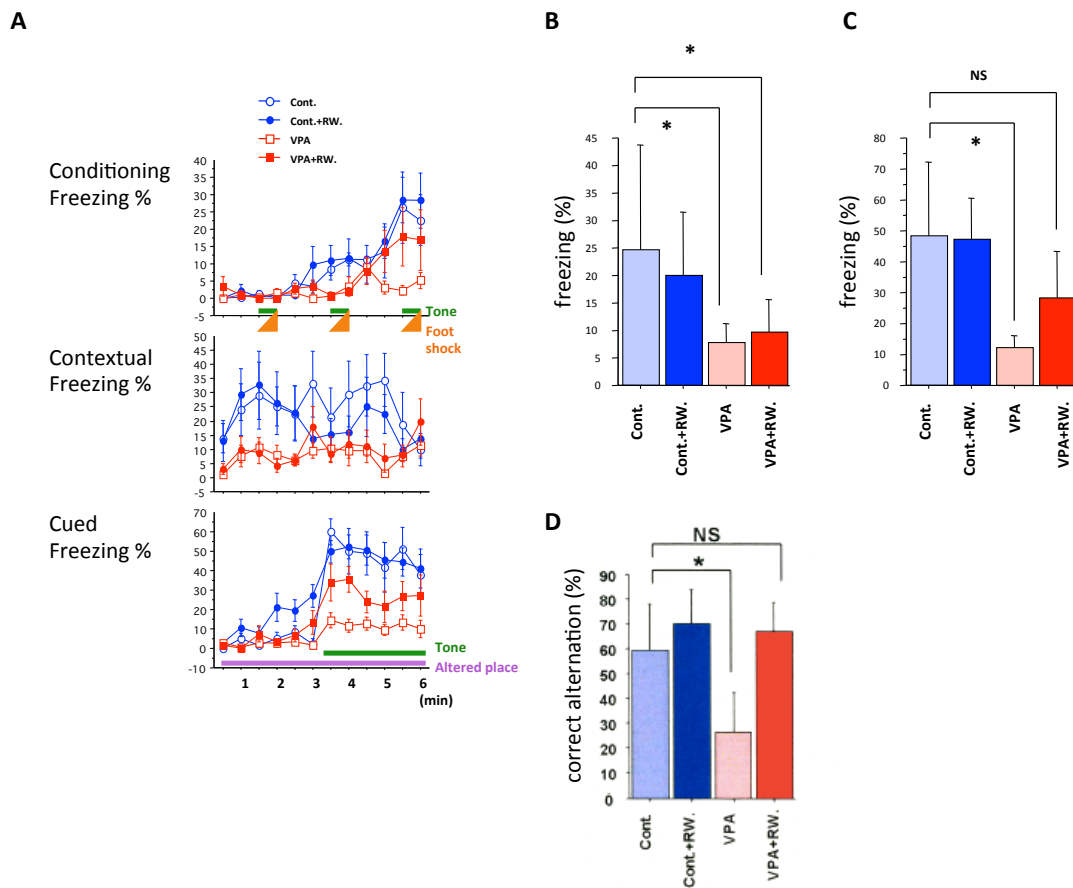
Fig. 33. Voluntary running recovers deficiencies in some learning and memory tests. (A-C) Quantification of freezing in contextual/cued fear conditioning test as a timelines (A), and means in contextual (B) and cued test (C). (D) Quantification of correct alternation in Y-maze alternation test. $* P < 0.001$, NS = not significant (Student t-test).

III.11. Running ameliorates disrupted neuronal morphology in VPA-treated mice

In order to become functional, neurons generated by NSCs in the DG of hippocampus have to undergo maturation which involves processes such as migration from subgranular zone (SGZ) into GCL, and extension and branching of dendrites into molecular layer. To check the migration of neurons generated from NSCs in DG during developmental stage, I injected BrdU on E14.5 and analyzed the position of labeled cells on P56 in GCL (Fig. 34A). As can be observed from in the immunostaining and quantification of BrdU-positive cells, VPA-treated mice have a higher percentage of E14.5-born cells which were migrated into upper granular zone (UGZ) area (Fig. 34B,C). Meanwhile, the absolute number of BrdU-positive cells was lower in all GCL areas (Fig. 34B,D). These results indicated that VPA treatment during embryonic stage enhanced the neurogenesis of DG cells-producing NSCs and later these NSCs generated fewer neural cell types after VPA treatment diminished, as already observed also earlier for NSCs in the cortical area (Section III.4 and Fig. 23).

Because embryonic neurogenesis was enhanced by VPA but I observed some deficiencies in behavior, I examined a possibility that the generated neurons have abnormal morphology. Using Golgi-Cox staining, I found that GC neurons in the DG of VPA-treated mice have a fewer dendrite branching (Fig. 35A,B). These neurons were also more oriented to the non-molecular layer area which might cause impairment in their functions (Fig. 35B,C). Interestingly, both of these deficiencies in VPA-treated mice can be recovered by voluntary running (Fig. 35). Running also increase the thickness of GCL in both control and VPA-treated mice, probably due to its simultaneous effect in increasing adult neurogenesis (Fig. 31).

Golgi-Cox staining labels neurons which were born on both embryonic and

postnatal stages. In order to investigate whether embryonic VPA-treatment could affect neurons which were born postnatally, long after VPA treatment was terminated, I checked the morphology of DCX-positive immature neurons. DCX-positive immature neurons in DG could already possess dendrite processes to the molecular layer. In VPA-treated mice though, these dendrite processes were less obvious compared with control mice (Fig. 36). In agreement with earlier results using Golgi-Cox staining above, running could ameliorate the orientation of dendrite processes in VPA-treated mice (Fig. 36). Taken together these results show that running can recovers disrupted neuronal morphology of VPA-treated mice.
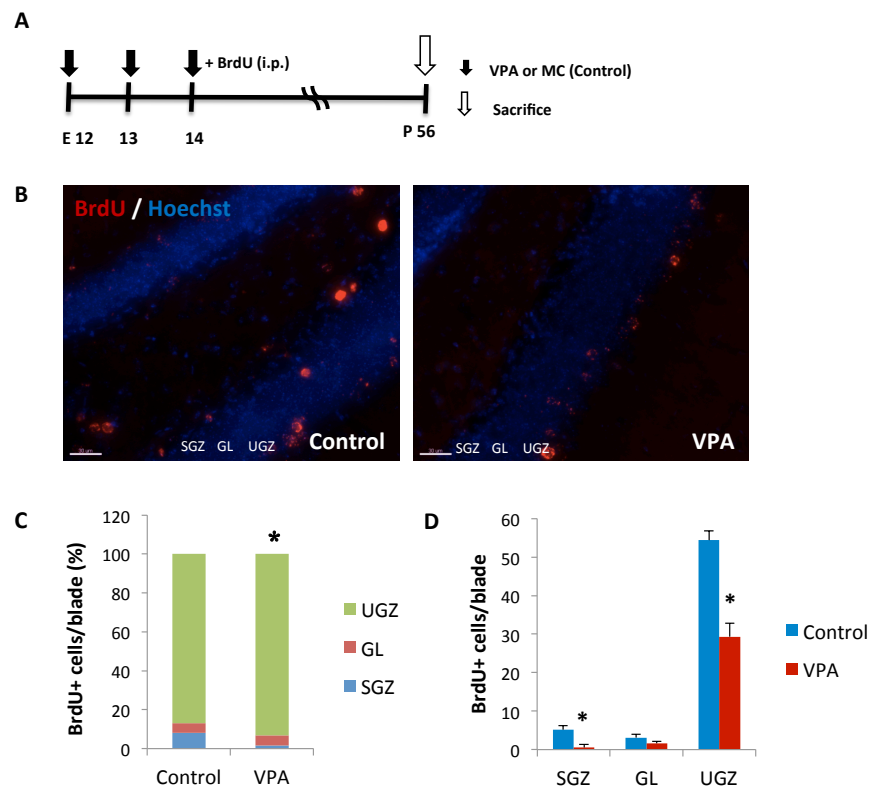
Fig. 34. VPA enhances neurogenesis of DG neuron-producing NSCs. (A) VPA or MC (Control) was orally administered to pregnant mice from E12.5 until E14.5. BrdU was injected on E14.5 and mice were sacrificed on P56. (B-D) Immunostaining (B) and quantification of BrdU+ cells (C-D) show enhanced neurogenesis of NSCs in VPA-treated mice which were proliferating on E14.5. * $P < 0.001$ (Student t-test).
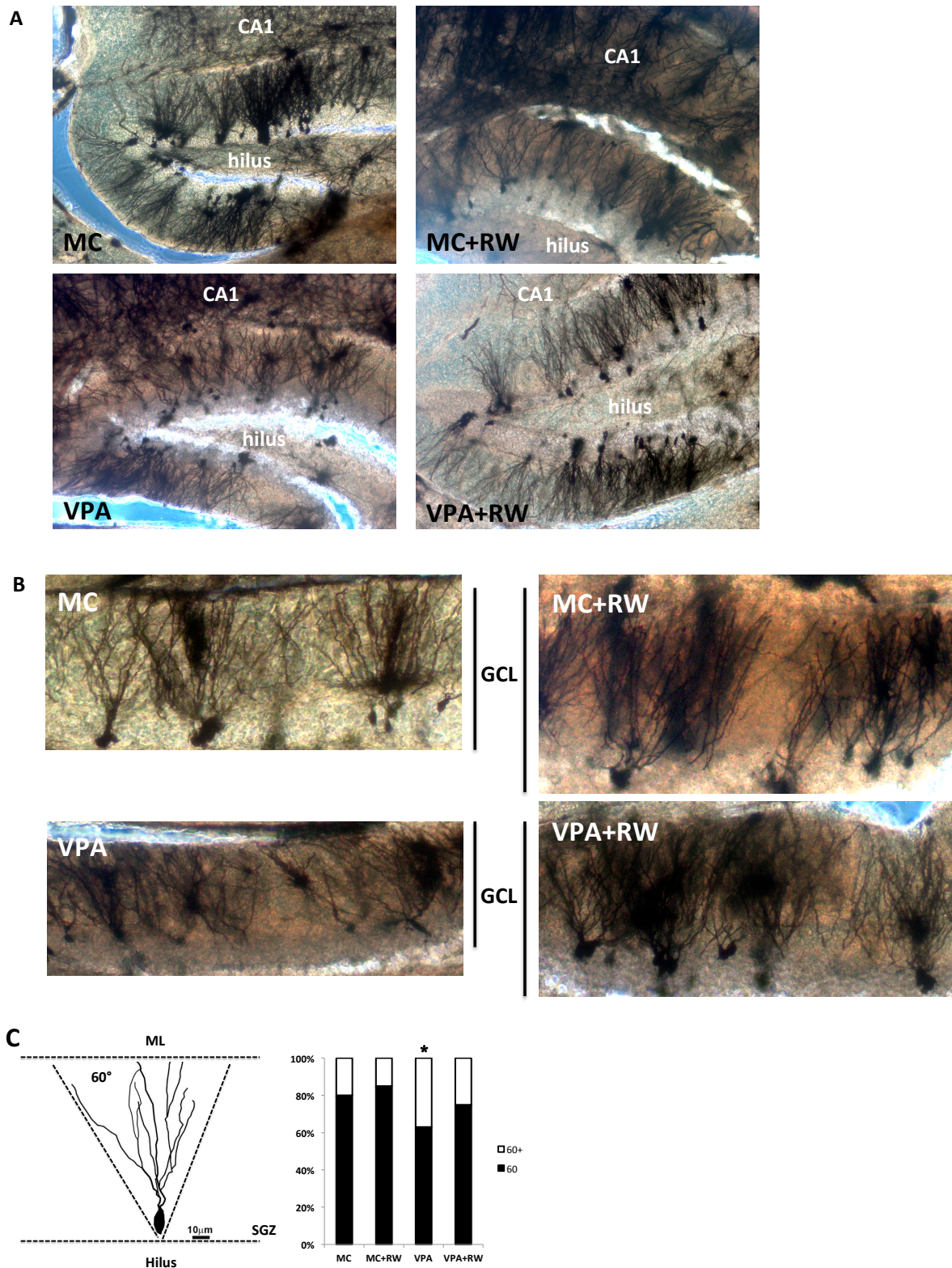
Fig. 35. Running recovers disrupted neuronal morphology of VPA-treated mice. (A-B) Golgi-Cox staining of DG area (A) and its higher magnification in GCL area (B). (C) Quantification of dendrite orientation in GCL. Dendrites were designated as ML-oriented (60) if they falled under 60 degree area which was drawed vertically from hilus to ML. Others were designated as non ML-oriented (60+). * $P < 0.001$ (Student t-test).
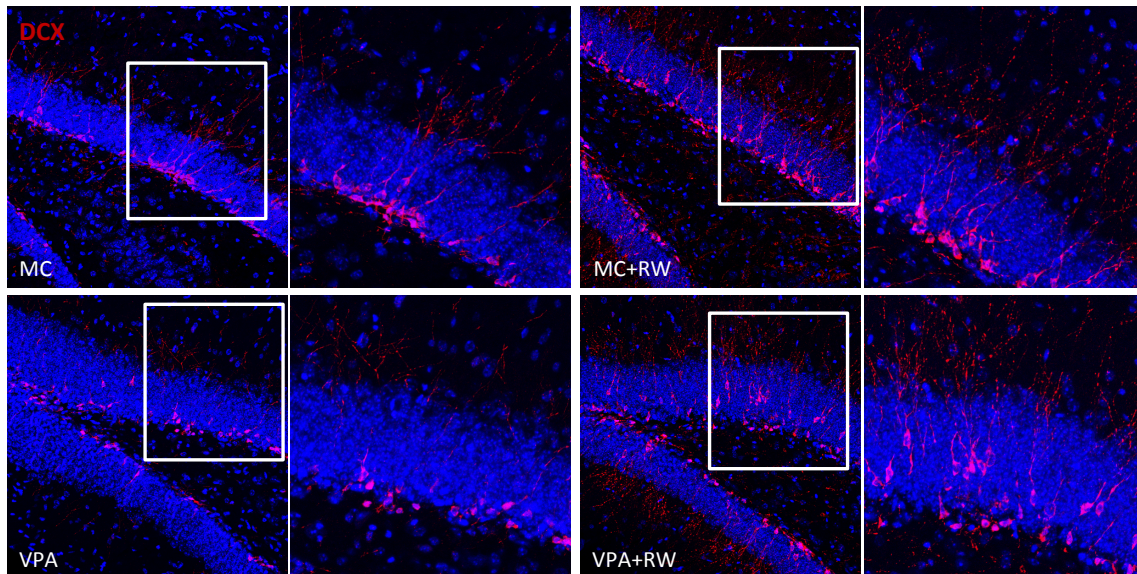
Fig. 36. Running recovers disrupted morphology of immature neurons in VPA-treated mice. Adult born DCX-positive immature neurons in VPA-treated mice have a less dendrite processes to the ML. This can be recovered by voluntary running.

III.12. VPA-treated mice have lower GABA receptor-mediated depolarization

In order to understand the electrophysiology of neurons in hippocampus region of VPA-treated mice, we used a combination of conventional electrophysiological methods with voltage-sensitive dye (VSD) imaging (Tominaga & Tominaga, 2010). We found that in control mice the tetanic stimulation could induce long-lasting depolarization and progressive decrease in individual excitatory postsynaptic potentials (EPSPs) of CA1 and mossy fiber area, but not in DG (Fig. 37A). Both of these effects were suppressed by picrotoxin (Pitx), a $GABA_A$ receptor antagonist (Fig. 37B). Interestingly, although we could observed the same depolarization and EPSPs in VPA-treated mice, the addition of Pitx did not suppressed any of these effects in CA1 and mossy fiber area like in control mice (Fig. 37). These results suggest

that in VPA-treated mice, the GABA receptor-mediated depolarization was lower than control mice, and it might contribute to the deficiencies that I found earlier above.
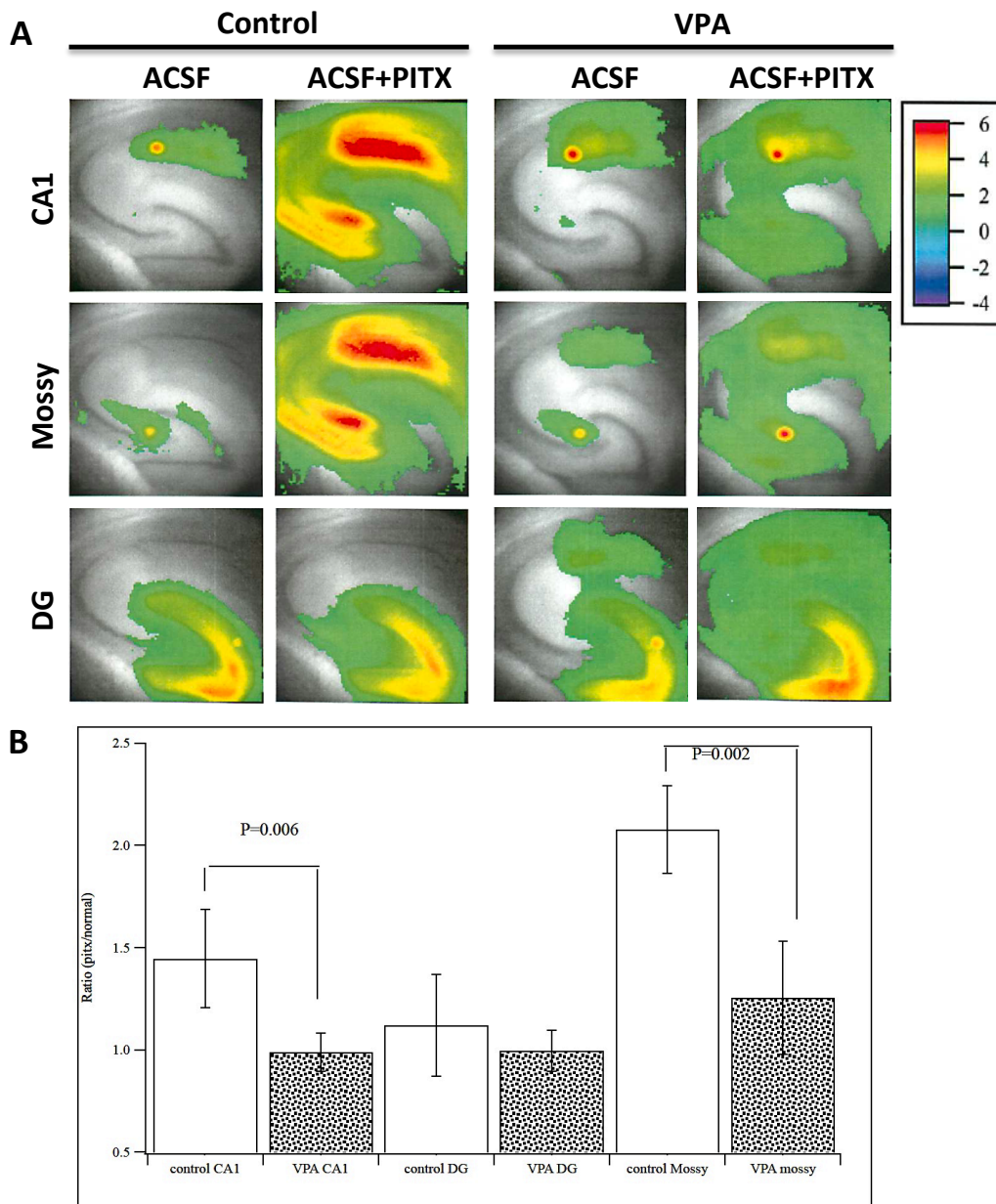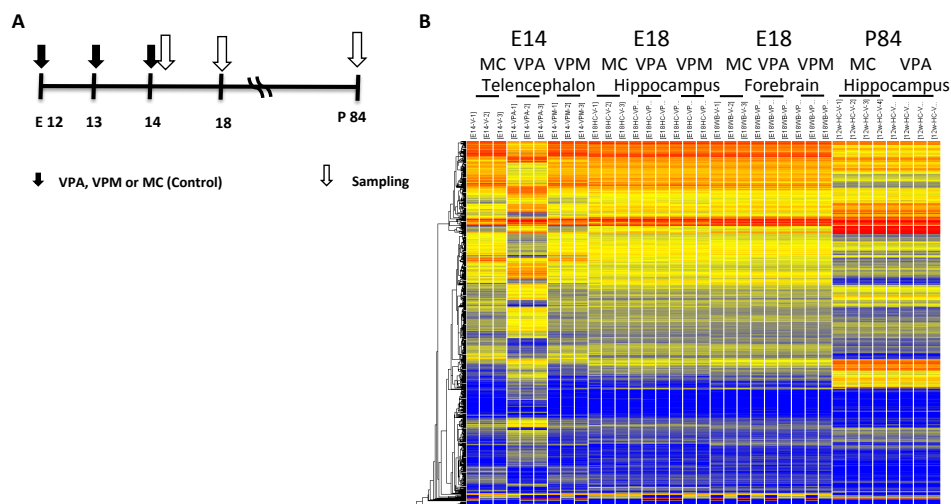

Fig. 37. GABA receptor-mediated depolarization is lower in VPA-treated mice. (A-B) Visualization (A) and quantification (B) of VSD imaging results of hippocampal area. ACSF = artificial cerebrospinal fluid, PITX = picrotoxin.

III.13. VPA changes global gene expression profile

In order to verify molecular mechanisms that caused the deficiencies in VPA-treated mice, we prepared RNA samples from mice treated with methylcellulose (Control), VPA, or valpromide (VPM) from E12.5 to E14.5 (Fig. 38A). VPM is an analog drug of VPA, which also have antiepileptic but lack of HDAC inhibition properties. We then did microarray analysis to see global gene expression profile 3 h after the last VPA treatment on E14.5, E18.5, and P84 (Fig. 38A). We found that on E14.5, global gene expression in telencephalon was change significantly by VPA, but not by VPM (Fig. 38B). On E18.5 and P84, this global change was diminished in cortex and hippocampus, as gene expression in VPA-treated mice returned to the same level as control mice (Fig. 38B). Nevertheless, some genes still showed significant different expression level at these time points. These results suggest that VPA treatment might cause all the deficiencies being observed earlier by changing the global gene expression through its HDAC inhibition properties, and this change only occurred transiently while VPA was being given to the mice.

Fig. 38. VPA changes global gene expression profile. (A) Timeline of VPA treatment and sample preparation for microarray analysis. (B) Hierarchical gene clustering of gene expression level.

III.14. VPA might causes deficiencies in cortex and hippocampus through *Fezf2* downregulation

Next, I tried to reveal the mechanisms that might caused the deficiencies in cortex and hippocampus development of VPA-treated mice. I screened the list of all genes which were changed by VPA treatment but neither by VPM nor MC from the above microarray analysis, to identify genes which have been reported to affect both cortical and hippocampal development. I found out one of such gene, zinc finger transcription factor *Fezf2*, which was downregulated by VPA treatment (Fig. 39A). To confirm this result, we conducted quantitative RT-PCR analysis of mESC-derived NPCs at differentiation day 12 (6 h after VPA treatment). We used cells from this culture system because it gave us more homogenous population of NSCs compared to direct isolation of NSCs from E14.5 forebrain. We found that in this system *Fezf2* was also to be down regulated by VPA treatment (Fig. 39B). *Fezf2* has been reported to play an important role in the specification of cortical neurons, in particular deep-layer neurons (Chen et al., 2008; Leone et al., 2008). This is in accordance to the earlier results above showing that VPA induced higher generation of superficial-layer neurons and suppresed generation of deep-layer neurons. Previous study also suggested that *Fezf1*$^{-/-}$*Fezf2*$^{-/-}$ mice has a severe phenotypes in the hippocampus, such as extensive reduction of CA3 region and loss of DG (Hirata et al., 2006). Therefore, it is conceivable that the down regulation of *Fezf2* in VPA-treated mice causes the smaller size of hippocampus and DG on postnatal stage and also contributes to the impairment of adult neurogenesis.
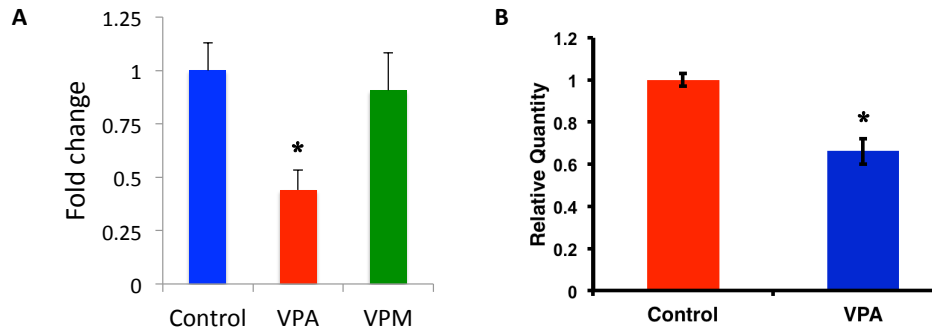
78

Fig. 39. The expression of *Fezf2* is down regulated by VPA. (A) Microarray data of E14.5 telencephalon (3 h after the last VPA treatment). (B) Quantitative PCR of mESC-derived NSCs at differentiation day 12 (6 h after VPA treatment). * $P < 0.001$ (Student t-test).

IV. Discussion

IV.1. The regulation of cortical NSCs development by HDAC inhibition

The brains of mammals differ in many aspects from those of other vertebrates. Most striking among the features that mammals have acquired during evolution are the increased size and complexity of the cerebral cortex, the largest brain structure where many of the higher cognitive functions reside (Finlay & Darlington, 1995; Hill & Walsh, 2005). The mammalian cerebral cortex is highly organized, with a six-layered structure that contains early-born or deep-layer (layer I, V-VI) and superficial-layer neurons (layer II-IV) that are produced in an orderly inside-out fashion (Molyneaux et al., 2007). The increased size and complexity partly reflect the overrepresentation of superficial-layer neurons, which are very abundant in primates, and especially so in human (Marin-Padilla, 1992). These cortical neurons are mainly of two types: pyramidal projection neurons, which mostly originate from NSCs of the dorsolateral wall of the telenchepalon (Molyneaux et al., 2007), and interneurons, which originate from the ventral telenchepalon during embryonic development (Wonders & Anderson, 2006).

Inhibition of HDAC activity by VPA, a widely used anticonvulsant and mood-stabilizing drug, has been shown to drive mESCs to differentiate into the ectodermal lineage at the expense of mesodermal and endodermal lineages (Murabe et al., 2007). This ectodermal lineage differentiation is further biased in favor of neuronal rather than glial fates by the VPA treatment (Murabe et al., 2007). Prior to this finding in mESCs, we and others (Hsieh et al., 2004; Balasubramaniyan et al., 2006) had also found a similar tendency for neuronal over glial fate preference when we cultured NSCs in the presence of HDAC

inhibitors such as VPA and trichostatin A. However, the types of neurons produced in these studies were not examined in detail.

In the present study, I have demonstrated that transient HDAC inhibition by VPA in 46C mESC-derived NPCs and mid-gestational NSCs enhances their neuronal differentiation (Figs. 11D,E, 16, 34). This has been reported previously in several studies using different types of NSCs (Hsieh et al., 2004; Murabe et al., 2007; Yu et al., 2008). Using an mESC culture system that can specifically produce and recapitulate the generation of cortical-layer neurons (Gaspard et al., 2008, 2009) and *in vivo* study, I further showed that the enhanced neurogenesis after VPA treatment includes a higher proportion of superficial-layer neurons (Cux1+) (Figs. 13B,D, 21A), accompanied by a decreasing proportion of early-born or deep-layer neurons (reelin+, Ctip2+) (Figs. 13A,C, 21B). Therefore, it is conceivable that VPA enhances the temporal progression of some of deep-layer-producing NSCs into superficial-layer-producing NSCs during the time when VPA was being supplied to the culture and animal. The residual NSCs retained this temporal progression even when VPA was withdrawn, because we still observed the same proportion of all cortical markers even at differentiation day 21, 7 days after VPA treatment was terminated in the culture (Fig. 14), and very few E14.5 labeled BrdU-positive cells occupied deep layer cortical area after postnatal day (Fig. 20).

In embryonic cortex, VPA enhances neurogenesis by producing higher number of proliferating IPCs (Fig. 18) which will mainly differentiated into superficial layer neurons (Tarabykin et al., 2001). At the same time, VPA represses proliferation of the residual NSCs (Fig. 19A,B) which caused the reduction of NSCs number (Fig. 16) and generated neural cell

types afterward (Fig. 23C,D). These reductions resulted in a smaller brain and its parts on postnatal day (Fig. 23A,B).

Elucidating the mechanisms that lead to the enhanced progression of NSCs from producing deep-layer neurons to producing superficial-layer neurons after transient VPA treatment is an important challenge for future study. It has been proposed that the zinc-finger transcription factor *Fezf2*, which acts upstream of *Ctip2*, plays an important role in the specification of deep-layer neurons (Chen et al., 2008; Leone et al., 2008). VPA might repress *Fezf2* directly or indirectly in our mESCs culture system (Fig. 39B), which could in turn decrease the generation of deep-layer neurons and release the inhibition of upper-layer neuron production. This scenario is plausible, since VPA treatment of mouse embryos also reduces levels of *Fezf2* mRNA in the forebrain (Fig. 39A), and there was an increase of Tbr1-positive cells in mESCs culture after VPA treatment (data not shown). It has been reported recently that Tbr1 can act as a direct transcriptional repressor for *Fezf2* (Han et al., 2011). The downregulation of *Fezf2* might release the inhibition of *Satb2* which can promotes superficial layer neuronal identity (Leone et al., 2008), and somehow by unknown mechanisms, induces the expression of another superficial layer neurons gene *Cux1*. Figure 40 depicted my current model about regulation of cortical NSCs by VPA.

My results suggest that histone acetylation plays important roles in the production of superficial-layer neurons in an adherent monolayer system of mESCs, and in embryonic cortex (Fig. 22). Similar efficient production of superficial-layer neurons from mESCs was also recently reported in a study of modified embryoid body (EB) formation (Eiraku et al., 2008). It is tempting to hypothesize that in the EB, high levels of histone acetylation occur and persist until late differentiation to help ensure the generation of superficial layer neurons.

82

Nevertheless, generation of cortical neurons from human (h)ESCs using the same EB method was skewed toward deep-layer identity (Eiraku et al., 2008), and both mESCs and hESCs failed to recapitulate the same inside-out pattern of cortical neurogenesis observed in the developing cortex (Au & Fishell, 2008; Gaspard & Vanderhaeghen, 2010). It will be of interest to explore the effects of increasing histone acetylation by VPA treatment on the production of superficial-layer neurons in hESCs, and whether histone acetylation plays a role in the inside-out mode of cortical neurogenesis.
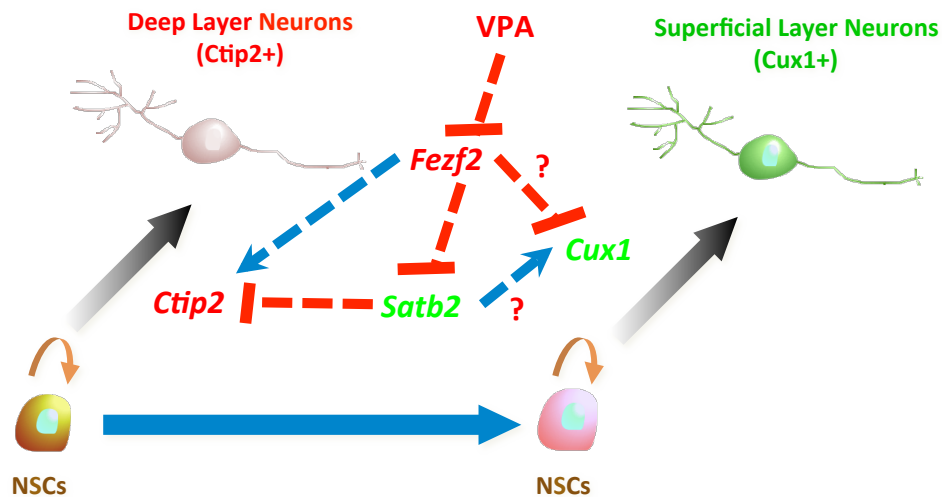
Fig. 40. Hypothetical model of cortical NSCs regulation by VPA. VPA treatment might repress *Fezf2* directly or indirectly which could in turn decrease the generation of Ctip2+ deep-layer neurons and release the inhibition of Cux1+ upper-layer neuron production.

IV.2. Adult neurogenesis and behavior after prenatal HDAC inhibition

VPA is an established drug for epilepsy. Previous studies have found that taking VPA during early pregnancy can lead to severe developmental defects to the embryo (DiLiberti et al., 1984; Nau et al., 1991), so that it must not be taken at this period. Nevertheless, it can be prescribed at later periods where VPA is considered to be safe. The

effect of VPA during later pregnancy period is elusive, and children of mothers who take VPA at this period show no significant defects during their development.

In the present study, I found that mice treated with VPA during mid-gestation (which is consider to be safe period) have an impaired adult neurogenesis in the DG of hippocampus (Fig. 27). The adult NSCs are less proliferative and more slowly differentiated into neural lineages (quiescent). This might be resulted from the persistent effect on repressing proliferation that VPA possesses, so that even long after VPA treatment, the residual NSCs still have lower proliferation rate. As a consequence, the absolute number of proliferating and differentiating NSCs in DG are lower in VPA-treated mice, which then caused the deficiencies in learning and memory (Table 1; Fig. 25). Previous studies have already reported that adult NSCs proliferation and differentiation in DG are important for learning and memory (Zhao et al., 2008). Moreover, recent study showed that although children from mother who took VPA during their pregnancy looks normal from outside, but they have significantly lower IQ than ordinary children (Meador et al., 2009).

Interestingly, voluntary running can increase the proliferation and differentiation of adult NSCs in DG of VPA-treated mice (Figs. 31, 32), as already reported previously for normal untreated mice (van Praag et al., 1999a, 1999b). Moreover, voluntary running can also recover the disrupted neuronal morphology of VPA-treated mice (Figs. 35, 36), in which together with the increasing adult neurogenesis, may ameliorate the deficit in learning and memory (Fig. 33). Figure 41 summarized findings and current model about adult neurogenesis in VPA-treated mice in this study.

The mechanisms of how voluntary running can recover impaired adult neurogenesis and disrupted neuronal morphology in VPA-treated mice remain elusive. Previous studies

have reported that voluntary running can increase the level of BDNF in the DG but not in other areas in the hippocampus (Farmer et al., 2004). BNDF has been suggested to have an important role in adult neurogenesis, neuronal maturation and dendrite branching (Tolwani et al., 2002; Bekinschtein et al., 2011; Stranahan, 2011). It is tempting to hypothesize that voluntary running may also increase the level of BDNF or enhances the BDNF pathway of VPA-treated mice in this study, thus leads to the recovery of adult neurogenesis and neuronal morphology of VPA-treated mice. This will be an interesting avenue to be explored in the future study.
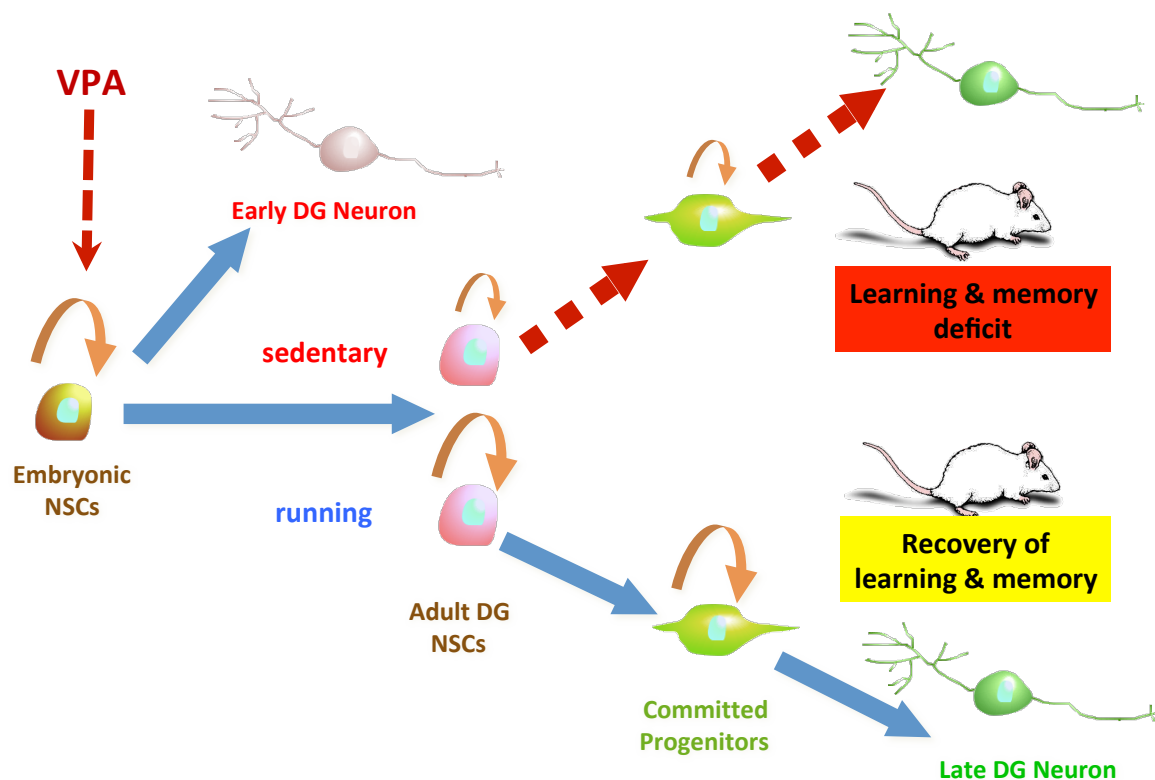
Fig. 41. Summary and model of adult neurogenesis after prenatal HDAC inhibition. VPA treatment induces neurogenesis of embryonic NSCs to produce early DG neurons of hippocampus. On postnatal, the residual NSCs become less proliferative and the adult neurogenesis is impaired, which lead to the deficiency in learning and memory. Voluntary running recovers NSCs proliferation and adult neurogenesis which in turn also recovers learning and memory.

IV.3. Concluding remarks

It is now well established that histone modification including histone acetylation, plays a substantial role in the differentiation of NSCs. However, our understanding about the mechanisms of how histone acetylation regulates NSCs differentiation is still in its infancy and many interesting avenues remain to be explored. For example, it is unclear why a global increase of histone acetylation, which occurs after treatment with HDAC inhibitors such as VPA, upregulates only specific genes such as neuronal genes in NSCs. Could this be due to a unique subunit composition of HDAC-containing chromatin remodeling complexes at the promoters of neuronal genes? If so, what are these subunits and what are their specific features? How are different molecules and signaling pathways that affect histone acetylation and chromatin structure integrated to promote NSCs differentiation? Given the potential of NSCs to treat neurological diseases and dysfunctions, and the use of HDAC inhibitors for treating CNS disorders and diseases, answers to these and other outstanding questions are eagerly awaited.

V. Acknowledgements

VI. References

Abranches, E., Silva, M., Pradier, L., Schulz, H., Hummel, O., Henrique, D., and Bekman, E. (2009). Neural differentiation of embryonic stem cells *in vitro*: a road map to neurogenesis in the embryo. PLoS One 4, e6286.

Aimone J. B., Deng, W., and Gage, F. H. (2010). Adult neurogenesis: integrating theories and separating functions. Trends Cogn Sci 14, 325-337.

Arlotta, P., Molyneaux, B. J., Chen, J., Inoue, J., Kominami, R., and Macklis, J. D. (2005). Neuronal subtype-specific genes that control corticospinal motor neuron development in vivo. Neuron 45, 207-221.

Au, E., and Fishell, G. (2008). Cortex shatters the glass ceiling. Cell Stem Cell 3, 472-474.

Azuara, V., Perry, P., Sauer, S., Spivakov, M., Jørgensen, H. F., John, R. M., Gouti, M., Casanova, M., Warnes, G., Merkenschlager, M., and Fisher, A. G. (2006). Chromatin signatures of pluripotent cell lines. Nat Cell Biol 8, 532-538.

Balasubramaniyan, V., Boddeke, E., Bakels, R., Küst, B., Kooistra, S., Veneman, A., and Copray, S. (2006). Effects of histone deacetylation inhibition on neuronal differentiation of embryonic mouse neural stem cells. Neuroscience 143, 939-951.

Ballas, N., Grunseich, C., Lu, D. D., Speh, J. C., and Mandel, G. (2005). REST and its corepressors mediate plasticity of neuronal gene chromatin throughout neurogenesis. Cell 121, 645-657.

Ballas, N., Lioy, D. T., Grunseich, C., and Mandel, G. (2009). Non-cell autonomous influence of MeCP2-deficient glia on neuronal dendritic morphology. Nat Neurosci 12, 311-317.

Barnabe-Heider, F., Wasylnka, J. A., Fernandes, K. J., Porsche, C., Sendtner, M., Kaplan, D. R., and Miller, F. D. (2005). Evidence that embryonic neurons regulate the onset of cortical gliogenesis via cardiotrophin-1. Neuron 48, 253-265.

Bekinschtein, P., Oomen, C. A., Saksida, L. M., and Bussey, T. J. (2011). Effects of environmental enrichment and voluntary exercise on neurogenesis, learning and memory, and pattern separation: BDNF as a critical variable? Semin Cell Dev Biol 22, 536-542.

Bernstein, B. E., Mikkelsen, T. S., Xie, X., Kamal, M., Huebert, D. J., Cuff, J., Fry, B., Meissner, A., Wernig, M., Plath, K., Jaenisch, R., Wagschal, A., Feil, R., Schreiber, S. L., and Lander, E. S. (2006). A bivalent chromatin structure marks key developmental genes in embryonic stem cells. Cell 125, 315-326.

Bestor, T. H. (2000). The DNA methyltransferases of mammals. Hum Mol Genet 9,

2395-2402.

Bonni, A., Sun, Y., Nadal-Vicens, M., Bhatt, A., Frank, D. A., Rozovsky, I., Stahl, N., Yancopoulos, G. D., and Greenberg, M. E. (1997). Regulation of gliogenesis in the central nervous system by the JAK-STAT signaling pathway. Science 278, 477-483.

Burgold, T., Spreafico, F., De Santa, F., Totaro, M. G., Prosperini, E., Natoli, G., and Testa, G. (2008). The histone H3 lysine 27-specific demethylase Jmjd3 is required for neural commitment. PLoS One 3, e3034.

Bray, S. (1998). A Notch affair. Cell 93, 499-503.

Britanova, O., de Juan Romero, C., Cheung, A., Kwan, K. Y., Schwark, M., Gyorgy, A., Vogel, T., Akopov, S., Mitkovski, M., Agoston, D., Sestan, N., Molnár, Z., and Tarabykin, V. (2008). Satb2 is a postmitotic determinant for upper-layer neuron specification in the neocortex. Neuron 57, 378-392.

Campos, L. S., Duarte, A. J., Branco, T., and Henrique, D. (2001). mDll1 and mDll3 expression in the developing mouse brain: role in the establishment of the early cortex. J Neurosci Res 64, 590-598.

Cai, L., Morrow, E. M., and Cepko, C. L. (2000). Misexpression of basic helix-loop-helix genes in the murine cerebral cortex affects cell fate choices and neuronal survival. Development 127, 3021-3030.

Chen, B., Schaevitz, L. R., and McConnell, S. K. (2005). Fezl regulates the differentiation and axon targeting of layer 5 subcortical projection neurons in cerebral cortex. Proc Natl Acad Sci USA 102, 17184-17189.

Chen, B., Wang, S. S., Hattox, A. M., Rayburn, H., Nelson, S. B., and McConnell, S. K. (2008). The Fezf2-Ctip2 genetic pathway regulates the fate choice of subcortical projection neurons in the developing cerebral cortex. Proc Natl Acad Sci USA 105, 11382-11387.

Cheng, L. C., Pastrana, E., Tavazoie, M., and Doetsch, F. (2009). miR-124 regulates adult neurogenesis in the subventricular zone stem cell niche. Nat Neurosci 12, 399-408.

Ciccolini, F. (2001). Identification of two distinct types of multipotent neural precursors that appear sequentially during CNS development. Mol Cell Neurosci 17, 895-907.

Conaco, C., Otto, S., Han, J. J., and Mandel, G. (2006). Reciprocal actions of REST and a microRNA promote neuronal identity. Proc Natl Acad Sci USA 103, 2422-2427.

Conti, L., Pollard, S. M., Gorba, T., Reitano, E., Toselli, M., Biella, G., Sun, Y., Sanzone, S., Ying, Q. L., Cattaneo, E., and Smith, A. (2005). Niche-independent symmetrical self-renewal of a mammalian tissue stem cell. PLoS Biol 3, e283.

Coy, J. F., Sedlacek, Z., Bachner, D., Delius, H., and Poustka, A. (1999). A complex pattern of evolutionary conservation and alternative polyadenylation within the long 3"-untranslated region of the methyl-CpG-binding protein 2 gene (MeCP2) suggests a regulatory role in gene expression. Hum Mol Genet 8, 1253-1262.

Cross, S. H., Meehan, R. R., Nan, X., and Bird, A. (1997). A component of the transcriptional repressor MeCP1 shares a motif with DNA methyltransferase and HRX proteins. Nat Genet 16, 256-259.

Deng, W., Aimone, J. B., and Gage, F. H. (2008). New neurons and new memories: how does adult hippocampal neurogenesis affect learning and memory? Nat Rev Neurosci 11, 339-350.

DiLiberti, J. H., Farndon, P. A., Dennis, N. R., and Curry, C. J. (1984). The fetal valproate syndrome. Am J Med Genet 19, 473-481.

Dou, Y., Milne, T. A., Tackett, A. J., Smith, E. R., Fukuda, A., Wysocka, J., Allis, C. D., Chait, B. T., Hess, J. L., and Roeder, R. G. (2005). Physical association and coordinate function of the H3 K4 methyltransferase MLL1 and the H4 K16 acetyltransferase MOF. Cell 121, 873-885.

Efroni, S., Duttagupta, R., Cheng, J., Dehghani, H., Hoeppner, D. J., Dash, C., Bazett-Jones, D. P., Le Grice, S., McKay, R. D., Buetow, K. H., Gingeras, T. R., Misteli, T., and Meshorer, E. (2008). Global transcription in pluripotent embryonic stem cells. Cell Stem Cell 2, 437-447.

Eiraku, M., Watanabe, K., Matsuo-Takasaki, M., Kawada, M., Yonemura, S., Matsumura, M., Wataya, T., Nishiyama, A., Muguruma, K., and Sasai, Y. (2008). Self-organized formation of polarized cortical tissues from ESCs and its active manipulation by extrinsic signals. Cell Stem Cell 3, 519-532.

Englund, C., Fink, A., Lau, C., Pham, D., Daza, R.A., Bulfone, A., Kowalczyk, T., and Hevner, R.F. (2005). Pax6, Tbr2, and Tbr1 are expressed sequentially by radial glia, intermediate progenitor cells, and postmitotic neurons in developing neocortex. J Neurosci 25, 247–251.

Ernst, P., Wang, J., Huang, M., Goodman, R. H., and Korsmeyer, S. J. (2001). MLL and CREB bind cooperatively to the nuclear coactivator CREB-binding protein. Mol Cell Biol 21, 2249-2258.

Fan, G., Martinowich, K., Chin, M. H., He, F., Fouse, S. D., Hutnick, L., Hattori, D., Ge, W., Shen, Y., Wu, H., ten Hoeve, J., Shuai, K., and Sun, Y. E. (2005). DNA methylation controls the timing of astrogliogenesis through regulation of JAK-STAT signaling. Development 132, 3345-3356.

Farmer, J., Zhao, X., van Praag, H., Wodtke, K., Gage, F. H., and Christie, B. R. (2004). Effects of voluntary exercise on synaptic plasticity and gene expression in the dentate gyrus of adult male Sprague-Dawley rats in vivo. Neuroscience 124, 71-79.

Finlay, B. L., and Darlington, R. B. (1995). Linked regularities in the development and evolution of mammalian brains. Science 268, 1578-1584.

Fujita, S. (1963). The matrix cell and cytogenesis in the developing central nervous system. J Comp Neurol 120, 37-42.

Fujita, S. (1986). Transitory differentiation of matrix cells and its functional role in the morphogenesis of the developing vertebrate CNS. Curr Top Dev Biol 20, 223-242.

Fujita, S. (2003). The discovery of the matrix cell, the identification of the multipotent neural stem cell and the development of the central nervous system. Cell Struct Funct 28, 205-228.

Fukuda, S., Kato, F., Tozuka, Y., Yamaguchi, M., Miyamoto, Y., and Hisatsune, T. (2003). Two distinct subpopulations of nestin-positive cells in adult mouse dentate gyrus. J Neurosci 23, 9357-9366.

Garcia, A. D., Doan, N. B., Imura, T., Bush, T. G., and Sofroniew, M. V. (2004). GFAP-expressing progenitors are the principal source of constitutive neurogenesis in adult mouse forebrain. Nat Neurosci 7, 1233-1241.

Gaspard, N., Bouschet, T., Hourez, R., Dimidschstein, J., Naeije, G., van den Ameele, J., Espuny-Camacho, I., Herpoel, A., Passante, L., Schiffmann, S. N., Gaillard, A., and Vanderhaeghen, P. (2008). An intrinsic mechanism of corticogenesis from embryonic stem cells. Nature 455, 351-357.

Gaspard, N., Bouschet, T., Herpoel, A., Naeije, G., van den Ameele, J., and Vanderhaeghen, P. (2009). Generation of cortical neurons from mouse embryonic stem cells. Nat Protoc 4, 1454-1463.

Gaspard, N., and Vanderhaeghen, P. (2010). Mechanisms of neural specification from embryonic stem cells. Curr Opin Neurobiol 20, 37-43.

Gorski, J. A., Talley, T., Qiu, M., Puelles, L., Rubenstein, J. L., and Jones, K. R. (2002). Cortical excitatory neurons and glia, but not GABAergic neurons, are produced in the Emx1-expressing lineage. J Neurosci 22, 6309-6314.

Goto, K., Numata, M., Komura, J. I., Ono, T., Bestor, T. H., and Kondo, H. (1994). Expression of DNA methyltransferase gene in mature and immature neurons as well as proliferating cells in mice. Differentiation 56, 39-44.

Gould, E., Beylin, A., Tanapat, P., Reeves, A., and Shors, T. J. (1999). Learning enhances adult neurogenesis in the hippocampal formation. Nat Neurosci 2, 260-265.

Grewal, S. I., and Moazed, D. (2003). Heterochromatin and epigenetic control of gene expression. Science 301, 798-802.

Guillemot, F. (2007). Spatial and temporal specification of neural fates by transcription factor codes. Development 134, 3771-3780.

Gundersen, H. J., Bagger, P., Bendtsen, T. F., Evans, S. M., Korbo, L., Marcussen, N., Møller, A., Nielsen, K., Nyengaard, J. R., Pakkenberg, B., Sørensen, F. B., Vesterby, A., and West, M. J. (1988). The new stereological tools: dissector, fractionator, nucleator, and point sampled intercepts and their use in pathological research and diagnosis. Acta Pathol Microbiol Immunol Scand 96, 857-881.

Han, W., Kwan, K. Y., Shim, S., Lam, M. M., Shin, Y., Xu, X., Zhu, Y., Li, M., and Sestan, N. (2011). TBR1 directly represses Fezf2 to control the laminar origin and development of the corticospinal tract. Proc Natl Acad Sci USA 108, 3041-3046.

Hatada, I., Namihira, M., Morita, S., Kimura, M., Horii, T., and Nakashima, K. (2008). Astrocyte-specific genes are generally demethylated in neural precursor cells prior to astrocytic differentiation. PLoS One 3, e3189.

He, L., and Hannon, G. J. (2004). MicroRNAs: small RNAs with a big role in gene regulation. Nat Rev Genet 5, 522-531.

Higashi, M., Maruta, N., Bernstein, A., Ikenaka, K., and Hitoshi, S. (2008). Mood stabilizing drugs expand the neural stem cell pool in the adult brain through activation of notch signaling. Stem Cells 26, 1758-1767.

Hill, R. S., and Walsh, C. A. (2005). Molecular insights into human brain evolution. Nature 437, 64-67.

Hillman, C. H., Erickson, K. I., and Kramer, A. F. (2008). Be smart, exercise your heart: exercise effects on brain and cognition. Nat Rev Neurosci 9, 58-65.

Hirabayashi, Y., Suzki, N., Tsuboi, M., Endo, T. A., Toyoda, T., Shinga, J., Koseki, H., Vidal, M., and Gotoh, Y. (2009). Polycomb limits the neurogenic competence of neural precursor cells to promote astrogenic fate transition. Neuron 63, 600-613.

Hirata, T., Nakazawa, M., Muraoka, O., Nakayama, R., Suda, Y., and Hibi, M. 2006. Zinc-finger genes Fez and Fez-like function in the establishment of diencephalon subdivisions. Development 133, 3993–4004.

Hsieh, J., Nakashima, K., Kuwabara, T., Mejia, E., and Gage, F. H. (2004). Histone deacetylase inhibition-mediated neuronal differentiation of multipotent adult neural progenitor cells. Proc Natl Acad Sci USA 101, 16659-16664.

Hsieh, J., and Gage, F. H. (2005). Chromatin remodeling in neural development and plasticity. Curr Opin Cell Biol 17, 664-671.

Humphrey, G. W., Wang, Y. H., Hirai, T., Padmanabhan, R., Panchision, D. M., Newell, L. F., McKay, R. D., and Howard, B. H. (2008). Complementary roles for histone deacetylases 1, 2, and 3 in differentiation of pluripotent stem cells. Differentiation 76, 348-356.

Jaenisch, R., and Bird, A. (2003). Epigenetic regulation of gene expression: how the genome integrates intrinsic and environmental signals. Nat Genet 33(Suppl.), 245-254.

Jessberger, S., Nakashima, K., Clemenson, G. D. Jr., Mejia, E., Mathews, E., Ure, K., Ogawa, S., Sinton, C. M., Gage, F. H., and Hsieh, J. (2007). Epigenetic modulation of seizure-induced neurogenesis and cognitive decline. J Neurosci 27, 5967-5975.

Juliandi, B., Suryobroto, B., and Perwitasari-Farajallah, D. (2008). The ischial callosities of Sulawesi macaques. Am J Primatol 71, 1021-1031.

Juliandi, B., Abematsu, M., and Nakashima, K. (2010a). Epigenetic regulation in neural stem cell differentiation. Dev Growth Differ 52, 493-504.

Juliandi, B., Abematsu, M., and Nakashima, K. (2010b). Chromatin remodeling in neural stem cell differentiation. Curr Opin Neurobiol 20, 408-415.

Juliandi, B., Suryobroto, B., and Perwitasari-Farajallah D. (2010c). Shape quantification of Sulawesi macaques ischial callosity. Primates Res 26 (Supp.), 26.

Jung, B. P., Zhang, G., Ho W., Francis, J., and Eubanks, J. H. (2002). Transient forebrain ischemia alters the mRNA expression of methyl DNA-binding factors in the adult rat hippocampus. Neuroscience 115, 515-524.

Jung, G. A., Yoon, J. Y., Moon, B. S., Yang, D. H., Kim, H. Y., Lee, S. H., Bryza, V., Arenas, E., and Choi, K. Y. (2008). Valproic acid induces differentiation and inhibition of proliferation in neural progenitor cells via the beta-catenin-Ras-ERK-p21$^{Cip/WAF1}$ pathway. BMC Cell Biol 9, 66.

Kanno, J., Aisaki, K., Igarashi, K., Nakatsu, N., Ono, A., Kodama, Y., and Nagao, T. (2006). "Per cell" normalization method for mRNA measurement by quantitative PCR and microarrays. BMC Genomics 7:64.

Kanold, P. O., and Shatz, C. J. (2006). Subplate neurons regulate maturation of cortical inhibition and outcome of ocular dominance plasticity. Neuron 51, 627-638.

Kawaguchi, A., Ikawa, T., Kasukawa, T., Ueda, H. R., Kurimoto, K., Saitou, M., and Matsuzaki, F. (2008). Single-cell gene profiling defines differential progenitor subclasses in mammalian neurogenesis. Development 135, 3113-3124.

Kazantsev, A. G., and Thompson, L. M. (2008). Therapeutic application of histone deacetylase inhibitors for central nervous system disorders. Nat Rev Drug Discov 7, 854-868.

Keller, G. (2005). Embryonic stem cell differentiation: emergence of a new era in biology and medicine. Genes Dev 19, 1129-1155.

Kempermann, G., Kuhn, H. G., and Gage, F. H. (1997). More hippocampal neurons in adult mice living in an enriched environment. Nature 386, 493-495.

Kempermann, G., Jessberger, S., Steiner, B., and Kronenberg, G. (2004). Milestones of neuronal development in the adult hippocampus. Trends Neurosci 27, 447-452.

Kempermann, G. (2006). Adult Neurogenesis. (New York: Oxford University Press).

Kishi, N., and Macklis, J. D. (2004). MECP2 is progressively expressed in post-migratory neurons and is involved in neuronal maturation rather than cell fate decisions. Mol Cell Neurosci 27, 306-321.

Kohyama, J., Kojima, T., Takatsuka, E., Yamashita, T., Namiki, J., Hsieh, J., Gage, F. H., Namihira, M., Okano, H., Sawamoto, K., and Nakashima, K. (2008). Epigenetic regulation of neural cell differentiation plasticity in the adult mammalian brain. Proc Natl Acad Sci USA 105, 18012-18017.

Krichevsky, A. M., Sonntag, K. C., Isacson, O., and Kosik, K. S. (2006). Specific microRNAs modulate embryonic stem cell-derived neurogenesis. Stem Cells 24, 857-864.

Lau, P., Verrier, J. D., Nielsen, J. A., Johnson, K. R., Notterpek, L., and Hudson, L. D. (2008). Identification of dynamically regulated microRNA and mRNA networks in developing oligodendrocytes. J Neurosci 28, 11720-11730.

Leasure, J. L., and Decker, L. (2009). Social isolation prevents exercise-induced proliferation of hippocampal progenitor cells in female rats. Hippocampus 19, 907-912.

Leone, D. P., Srinivasan, K., Chen, B., Alcamo, E., and McConnell, S. K. (2008). The determination of projection neuron identity in the developing cerebral cortex. Curr Opin Neurobiol 18, 28-35.

Lewis, J. D., Meehan, R. R., Henzel, W. J., Maurer-Fogy, I., Jeppesen, P., Klein, F., and Bird, A. (1992). Purification, sequence, and cellular localization of a novel chromosomal protein that binds to methylated DNA. Cell 69, 905-914.

Lillien, L., and Raphael, H. (2000). BMP and FGF regulate the development of EGF-responsive neural progenitor cells. Development 127, 4993-5005.

Lim, D. A., Huang, Y. C., Swigut, T., Mirick, A. L., Garcia-Verdugo, J. M., Wysocka, J., Ernst, P., and Alvarez-Buylla, A. (2009). Chromatin remodelling factor Mll1 is essential for neurogenesis from postnatal neural stem cells. Nature 458, 529-533.

Louvi, A., and Artavanis-Tsakonas, S. (2006). Notch signaling in vertebrate neural development. Nat Rev Neurosci 7, 93-102.

Lundkvist, J., and Lendahl, U. (2001). Notch and the birth of glial cells. Trends Neurosci 24,

492-494.

Lunyak, V. V., Burgess, R., Prefontaine, G. G., Nelson, C., Sze, S. H., Chenoweth, J., Schwartz, P., Pevzner, P. A., Glass, C., Mandel, G., and Rosenfeld, M. G. (2002). Co-repressor-dependent silencing of chromosomal regions encoding neuronal genes. Science 298, 1747-1752.

Lunyak, V. V., and Rosenfeld, M. G. (2005). No rest for REST: REST/NRSF regulation of neurogenesis. Cell 121, 499-501.

Lytle, J. R., Yario, T. A., and Steitz, J. A. (2007). Target mRNAs are repressed as efficiently by microRNA-binding sites in the 5' UTR as in the 3' UTR. Proc Natl Acad Sci USA 104, 9667-9672.

Ma, D. K., Guo, J. U., Ming, G. L., and Song, H. (2009). DNA excision repair proteins and Gadd45 as molecular players for active DNA demethylation. Cell Cycle 8, 1526-1531.

MacDonald, J. L., and Roskams, A. J. (2008). Histone deacetylases 1 and 2 are expressed at distinct stages of neuro-glial development. Dev Dyn 237, 2256-2267.

MacDonald, J. L., Gin, C. S., and Roskams, A. J. (2005). Stage-specific induction of DNA methyltransferases in olfactory receptor neuron development. Dev Biol 288: 461-473.

Makeyev, E. V., Zhang, J., Carrasco, M. A., and Maniatis, T. 2007. The microRNA miR-124 promotes neuronal differentiation by triggering brain-specific alternative pre-mRNA splicing. Mol Cell 27, 435-448.

Marin, O., and Rubenstein, J. L. (2001). A long, remarkable journey: tangential migration in the telencephalon. Nat Rev Neurosci 2, 780-790.

Marin-Husstege, M., Muggironi, M., Liu, A., and Casaccia-Bonnefil, P. (2002). Histone deacetylase activity is necessary for oligodendrocyte lineage progression. J Neurosci 22, 10333-10345.

Marin-Padilla, M. (1992). Ontogenesis of the pyramidal cell of the mammalian neocortex and developmental cytoarchitectonics: a unifying theory. J Comp Neurol 321, 223–240.

Massague, J. (2000). How cells read TGF-beta signals. Nat Rev Mol Cell Biol 1, 169-178.

Meador, K. J., Baker, G. A., Browning, N., Clayton-Smith, J., Combs-Cantrell, D. T., Cohen, M., Kalayjian, L. A., Kanner, A., Liporace, J. D., Pennel, P. B., Privitera, M., Loring, D. W., and NEAD Study Group. (2009). Cognitive function at 3 years of age after fetal exposure to antiepileptic drugs. N Engl J Med 360, 1597-1605.

Meshorer, E., Yellajoshula, D., George, E., Scambler, P. J., Brown, D. T., and Misteli, T. (2006). Hyperdynamic plasticity of chromatin proteins in pluripotent embryonic

stem cells. Dev Cell 10, 105-116.

Meshorer, E., and Misteli, T. (2006). Chromatin in pluripotent embryonic stem cells and differentiation. Nat Rev Mol Cell Biol 7, 540-546.

Mikkelsen, T. S., Ku, M., Jaffe, D. B., Issac, B., Lieberman, E., Giannoukos, G., Alvarez, P., Brockman, W., Kim, T. K., Koche, R. P., Lee, W., Mendenhall, E., O'Donovan, A., Presser, A., Russ, C., Xie, X., Meissner, A., Wernig, M., Jaenisch, R., Nusbaum, C., Lander, E. S., and Bernstein, B. E. (2007). Genome-wide maps of chromatin state in pluripotent and lineage-committed cells. Nature 448, 553-560.

Miller, R. H. (1996). Oligodendrocyte origins. Trends Neurosci 19, 92-96.

Milne, T. A., Briggs, S. D., Brock, H. W., Martin, M. E., Gibbs, D., Allis, C. D., and Hess, J. L. (2002). MLL targets SET domain methyltransferase activity to Hox gene promoters. Mol Cell 10, 1107-1117.

Molyneaux, B. J., Arlotta, P., Menezes, J. R. L., Macklis, J. D. (2007). Neuronal subtype specification in the cerebral cortex. Nat Rev Neurosci 8, 427-437.

Murabe, M., Yamauchi, J., Fujiwara, Y., Hiroyama, M., Sanbe, A., and Tanoue, A. (2007). A novel embryotoxic estimation method of VPA using ES cells differentiation system. Biochem Biophys Res Commun 352, 164-169.

Naka, H., Nakamura, S., Shimazaki, T., and Okano, H. (2008). Requirement for COUP-TFI and II in the temporal specification of neural stem cells in central nervous system development. Nat Neurosci 11, 1014-1023.

Nakashima, K., Wiese, S., Yanagisawa, M., Arakawa, H., Kimura, N., Hisatsune, T., Yoshida, K., Kishimoto, T., Sendtner, M., and Taga, T. (1999a). Developmental requirement of gp130 signaling in neuronal survival and astrocyte differentiation. J Neurosci 19, 5429-5434.

Nakashima, K., Yanagisawa, M., Arakawa, H., Kimura, N., Hisatsune, T., Kawabata, M., Miyazono, K., and Taga, T. (1999b). Synergistic signaling in fetal brain by STAT3-Smad1 complex bridged by p300. Science 284, 479-482.

Nakayama, K., Nagase, H., Hiratochi, M., Koh, C. S., and Ohkawara, T. (2008). Similar mechanisms regulated by gamma-secretase are involved in both directions of the bi-directional Notch-Delta signaling pathway as well as play a potential role in signaling events involving type 1 transmembrane proteins. Curr Stem Cell Res Ther 3, 288-302.

Namihira, M., Nakashima, K., and Taga, T. (2004). Developmental stage dependent regulation of DNA methylation and chromatin modification in a immature astrocyte specific gene promoter. FEBS Lett 572, 184-188.

Namihira, M., Kohyama, J., Abematsu, M., and Nakashima, K. (2008). Epigenetic mechanisms regulating fate specification of neural stem cells. Phil Trans R Soc B 363, 2099-2109.

Namihira, M., Kohyama, J., Semi, K., Sanosaka, T., Deneen, B., Taga, T., and Nakashima, K. (2009). Committed neuronal precursors confer astrocytic potential on residual neural precursor cells. Dev Cell 16, 245-255.

Nan, X., Campoy, F. J., and Bird, A. (1997). MeCP2 is a transcriptional repressor with abundant binding sites in genomic chromatin. Cell 88, 471-481.

Nau, H., Hauck, R. S., and Ehlers, K. (1991). Valproic acid-induced neural tube defects in mouse and human: aspects of chirality, alternative drug development, pharmacokinetics and possible mechanisms. Pharmacol Toxicol 69, 310-321.

Noctor, S. C., Flint, A. C., Weissman, T. A., Dammerman, R. S., and Kriegstein, A. R. (2001). Neurons derived from radial glial cells establish radial units in neocortex. Nature 409, 714-720.

Noctor, S. C., Martínez-Cerdeño, V., Ivic, L., and Kriegstein, A. R. (2004). Cortical neurons arise in symmetric and asymmetric division zones and migrate through specific phases. Nat Neurosci 7, 136-144.

Noctor, S. C., Martinez-Cerdeño, V., and Kriegstein, A. R. (2008). Distinct behaviors of neural stem and progenitor cells underlie cortical neurogenesis. J Comp Neurol 508, 28-44.

Nye, J. S., and Kopan, R. (1995). Developmental signaling.Vertebrate ligands for Notch. Curr Biol 5, 966-969.

Okada, Y., Matsumoto, A., Shimazaki, T., Enoki, R., Koizumi, A., Ishii, S., Itoyama, Y., Sobue, G., and Okano, H. (2008). Spatio-temporal recapitulation of central nervous system development by murine ES cell-derived neural stem/progenitor cells. Stem Cells 26, 3086-3098.

Okano, H., and Temple, S. (2009). Cell types to order: temporal specification of CNS stem cells. Curr Opin Neurobiol 19: 1-8.

Okano, M., Bell, D. W., Haber, D. A., and Li, E. (1999). DNA methyltransferases Dnmt3a and Dnmt3b are essential for de novo methylation and mammalian development. Cell 99, 247-257.

Orom, U. A., Nielsen, F. C., and Lund, A. H. (2008). MicroRNA-10a binds the 5' UTR of ribosomal protein mRNAs and enhances their translation. Mol Cell 30, 460-471.

Packer, A. N., Xing, Y., Harper, S. Q., Jones, L., and Davidson, B. L. (2008). The bifunctional microRNA miR-9/miR-9* regulates REST and CoREST and is

downregulated in Huntington's disease. J Neurosci 28, 14341-14346.

Pevny, L. H., Sockanathan, S., Placzek, M., and Lovell-Badge, R. (1998). A role for SOX1 in neural determination. Development 125, 1967-1978.

Qian, X., Shen, Q., Goderie, S. K., He, W., Capela, A., Davis, A. A., and Temple, S. (2000). Timing of CNS cell generation: a programmed sequence of neuron and glial cell production from isolated murine cortical stem cells. Neuron 28, 69-80.

Rajan, P., and McKay, R. D. (1998). Multiple routes to astrocytic differentiation in the CNS. J Neurosci 18, 3620-3629.

Ramirez-Amaya, V., Marrone, D. F., Gage, F. H., Worley, P. F., and Barnes C. A. (2006). Integration of new neurons into functional neural networks. J Neurosci 26, 12237-12241.

Rana, T. M. (2007). Illuminating the silence: understanding the structure and function of small RNAs. Nat Rev Mol Cell Biol 8, 23-36.

Rice, J. C., and Allis, C. D. (2001). Histone methylation versus histone acetylation: new insights into epigenetic regulation. Curr Opin Cell Biol 13, 263-273.

Robertson, K. D., and Wolffe, A. P. (2000). DNA methylation in health and disease. Nat Rev Genet 1, 11-19.

Seri, B., Garcia-Verdugo, J. M., McEwen, B. S., and Alvarez-Buylla, A. (2001). Astrocytes give rise to new neurons in the adult mammalian hippocampus. J Neurosci 21, 7153-7160.

Setoguchi, H., Namihira, M., Kohyama, J., Asano, H., Sanosaka, T., and Nakashima, K. (2006). Methyl-CpG binding proteins are involved in restricting differentiation plasticity in neurons. J Neurosci Res 84, 969-979.

Shahbazian, M. D., Antalffy, B., Armstrong, D. L., and Zoghbi, H. Y. (2002). Insight into Rett syndrome: MeCP2 levels display tissue- and cell-specific differences and correlate with neuronal maturation. Hum Mol Genet 11, 115-124.

Shen, S., Li, J., and Casaccia-Bonnefil, P. (2005). Histone modifications affect timing of oligodendrocyte progenitor differentiation in the developing rat brain. J Cell Biol 169, 577-589.

Shi, Y., Lie, D. C., Taupin, P., Nakashima, K., Ray, J., Yu, R. T., Gage, F. H., and Evans, R. M. (2004). Expression and function of orphan nuclear receptor TLX in adult neural stem cells. Nature 427, 78-83.

Shibata, M., Kurokawa, D., Nakao, H., Ohmura, T., and Aizawa, S. (2008). MicroRNA-9 modulates Cajal-Retzius cell differentiation by supressing Foxg1 expression in mouse medial pallium. J Neurosci 28, 10415-10421.

Shimozaki, K., Namihira, M., Nakashima, K., and Taga, T. (2005). Stage- and site-specific DNA demethylation during neural cell development from embryonic stem cells. J Neurochem 93, 432-439.

Simpson, P. (1995). Developmental genetics. The Notch connection. Nature 375, 736-737.

Smirnova, L., Gräfe, A., Seiler, A., Schumacher, S., Nitsch, R., and Wulczyn, F. G. (2005). Regulation of miRNA expression during neural cell specification. Eur J Neurosci 21, 1469-1477.

Snyder, J. S., Glover, L. R., Sanzone, K. M., Kamhi, J. F., and Cameron, H. A. (2009). The effects of exercice and stress on the survival and maturation of adult-generated granule cells. Hippocampus 19, 898-906.

Song, M. R., and Ghosh, A. (2004). FGF2-induced chromatin remodeling regulates CNTF-mediated gene expression and astrocyte differentiation. Nat Neurosci 7, 229-235.

Squire, L. R. (1992). Memory and the hippocampus: a synthesis from findings with rats, monkeys, and humans. Psychol Rev 99, 195-231.

Stahl, N., and Yancopoulos, G. D. (1994). The tripartite CNTF receptor complex: activation and signaling involves components shared with other cytokines. J Neurobiol 25, 1454-1466.

Steiner, B., Zurborg, S., Hörster, H., Fabel, K., and Kempermann, G. (2008). Differential 24 h responsiveness of Prox1-expressing precursor cells in adult hippocampal neurogenesis to physical activity, environmental enrichment, and kainic acid-induced seizures. Neuroscience 154, 521-529.

Strahl, B. D., and Allis, C. D. (2000). The language of covalent histone modifications. Nature 403, 41-45.

Stranahan, A. M. (2011). Physiological variability in brain-derived neurotrophic factor expression predicts dendritic spine density in the mouse dentate gyrus. Neurosci Lett 495, 60-62.

Suh, H., Consiglio, A., Ray, J., Sawai, T., D'Amour, K. A., and Gage, F. H. (2007). In vivo fate analysis reveals the multipotent and self-renewal capacities of Sox2+ neural stem cells in the adult hippocampus. Cell Stem Cell 1, 515-528.

Suh, H., Deng, W., and Gage, F. H. (2009). Signaling in adult neurogenesis. Annu Rev Cell Dev Biol 25, 253-275.

Sun, Y., Nadal-Vicens, M., Misono, S., Lin, M. Z., Zubiaga, A., Hua, X., Fan, G., and Greenberg, M. E. (2001). Neurogenin promotes neurogenesis and inhibits glial differentiation by independent mechanisms. Cell 104, 365-376.

Takizawa, T., Nakashima, K., Namihira, M., Ochiai, W., Uemura, A., Yanagisawa, M., Fujita, N., Nakao, M., and Taga, T. (2001). DNA methylation is a critical cell-intrinsic determinant of astrocyte differentiation in the fetal brain. Dev Cell 1, 749-758.

Tanemura, K., Murayama, M., Akagi, T., Hashikawa, T., Tominaga, T., Ichikawa, M., Yamaguchi, H., and Takashima, A. (2002). Neurodegeneration with tau accumulation in a transgenic mouse expressing V337M human tau. J Neurosci 22, 133-141.

Tarabykin, V., Stoykova, A., Usman, N., and Gruss, P. (2001). Cortical upper layer neurons derive from subventricular zone as indicated by Svet1 gene expression. Development 128, 1983-1993.

Tatebayashi, Y., Miyasaka, T., Chui, D. H., Akagi, T., Mishima, K., Iwasaki, K., Fujiwara, M., Tanemura, K., Murayama, M., Ishiguro, K., Planel, E., Sato, S., Hashikawa, T., and Takashima, A. (2002). Tau filament formation and associative memory deficit in aged mice expressing mutant (R406W) human tau. Proc Natl Acad Sci USA 99, 13896-13901.

Temple, S. (2001). The development of neural stem cells. Nature 414, 112-117.

Tolwani, R. J., Buckmaster, P. S., Varma, S., Cosgaya, J. M., Wu, Y., Suri, C., and Shooter, E. M. (2002). BDNF overexpression increases dendrite complexity in hippocampal dentate gyrus. Neuroscience 114, 795-805.

Tominaga, T., and Tominaga, Y. 2010. GABA$_A$ receptor-mediated modulation of neuronal activity propagation upon tetanic stimulation in rat hippocampal slices. Eur J Physiol 460, 875-889.

Tropepe, V., Sibilia, M., Ciruna, B. G., Rossant, J., Wagner, E. F., and van der Kooy, D. (1999). Distinct neural stem cells proliferate in response to EGF and FGF in the developing mouse telencephalon. Dev Biol 208, 166-188.

Tsujimura, K., Abematsu, M., Kohyama, J., Namihira, M., and Nakashima, K. (2009). Neuronal differentiation of neural precursor cells is promoted by the methyl-CpG binding protein MeCP2. Exp Neurol. 219, 104-111.

van Praag, H., Kempermann, G., and Gage, F. H. (1999a). Running increases cell proliferation and neurogenesis in the adult mouse dentate gyrus. Nat Neurosci 2, 266-270.

van Praag, H., Christie, B. R., Sejnowski, T. J., and Gage, F. H. (1999b). Running enhances neurogenesis, learning, and long-term potentiation in mice. Proc Natl Acad Sci USA 96, 13427-13431.

van Praag, H., Kempermann, G., and Gage, F. H. (2000). Neural consequences of

environmental enrichment. Nat Rev Neurosci 1, 191-198.

van Praag, H., Shubert, T., Zhao, C., and Gage, F. H. (2005). Exercice enhances learning and hippocampal neurogenesis in aged mice. J Neurosci 25, 8680-8685.

van Praag, H. (2009). Exercise and the brain: something to chew on. Trends Neurosci 32, 283-290.

Visvanathan, J., Lee, S., Lee, B., Lee, J. W., and Lee, S. K. (2007). The microRNA miR-124 antagonizes the anti-neural REST/SCP1 pathway during embryonic CNS development. Genes Dev 21, 744-749.

Wallberg, A. E., Pedersen, K., Lendahl, U., and Roeder, R. G. (2002). p300 and PCAF act cooperatively to mediate transcriptional activation from chromatin templates by notch intracellular domains in vitro. Mol Cell Biol 22, 7812-7819.

Williams R. W., and Rakic, P. (1988). Three-dimensional counting: an accurate and direct method to estimate numbers of cells in sectioned material. J Comp Neurol 278, 344-352.

Wonders, C. P., and Anderson, S. A. (2006). The origin and specification of cortical interneurons. Nat Rev Neurosci 7, 687-696.

Wood, H. B., and Episkopou, V. (1999). Comparative expression of the mouse Sox1, Sox2 and Sox3 genes from pre-gastrulation to early somite stages. Mech Dev 86, 197-201.

Xia, Z. B., Anderson, M., Diaz, M. O., and Zeleznik-Le, N. J. (2003). MLL repression domain interacts with histone deacetylases, the polycomb group proteins HPC2 and BMI-1, and the corepressor C-terminal-binding protein. Proc Natl Acad Sci USA 100, 8342-8347.

Ye, F., Chen, Y., Hoang, T. N., Montgomery, R. L., Zhao, X., Bu, H., Hu, T., Taketo, M. M., van Es, J. H., Clevers, H., Hsieh, J., Bassel-Duby, R., Olson, E. N., and Lu, Q. R. (2009). HDAC1 and HDAC2 regulate oligodendrocyte differentiation by disrupting the β-catenin-TCF interaction. Nat Neurosci 12, 829-838.

Yeo, M., Lee, S. K., Lee, B., Ruiz, E. C., Pfaff, S. L., and Gill, G. N. (2005). Small CTD phosphatases function in silencing neuronal gene expression. Science 307, 596-600.

Ying, Q. L., and Smith, A. G. (2003). Defined conditions for neural commitment and differentiation. Methods Enzymol 365, 327-341.

Ying, Q. L., Stavridis, M., Griffiths, D., Li, M., and Smith, A. (2003). Conversion of embryonic stem cells into neuroectodermal precursors in adherent monoculture. Nat Biotechnol 21, 183-186.

Yoder, A. J., Walsh, C. P., and Bestor, T. H. (1997). Cytosine methylation and the ecology of

intragenomic parasites. Trends Genet 13, 335-340.

Yoo, C. B., and Jones, P. A. (2006). Epigenetic therapy of cancer: past, present and future. Nat Rev Drug Discov 5, 37-50.

Yoon, K. J., Koo, B. K., Im S. K., Jeong, H. W., Ghim, J., Kwon, M. C., Moon, J. S., Miyata, T., and Kong, Y. Y. (2008). Mind bomb 1-expressing intermediate progenitors generate notch signaling to maintain radial glial cells. Neuron 58, 519-531.

Yu, I. T., Park, J. Y., Kim, S. H., Lee, J. S., Kim, Y. S., and Son, H. (2009). Valproic acid promotes neuronal differentiation by induction of proneural factors in association with H4 acetylation. Neuropharmacology 56, 473-480.

Zhao, C., Guan, W., and Pleasure, S. J. (2006). A transgenic marker mouse line labels Cajal-Retzius cells from the cortical hem and thalamocortical axons. Brain Res 1077, 48-53.

Zhao, C., Deng, W., and Gage, F. H. (2008). Mechanisms and functional implications of adult neurogenesis. Cell 132, 645-660.

Zhao, C., Sun, G., Li, S., and Shi, Y. (2009). A feedback regulatory loop involving microRNA-9 and nuclear receptor TLX in neural stem cell fate determination. Nat Struct Mol Biol 16, 365-371.

Zhao, X., Ueba, T., Christie, B. R., Barkho, B., McConnell, M. J., Nakashima, K., Lein, E. S., Eadie, B. D., Willhoite, A. R., Muotri, A. R., Summers, R. G., Chun, J., Lee, K. F., and Gage F. H. (2003). Mice lacking methyl-CpG binding protein 1 have deficits in adult neurogenesis and hippocampal function. Proc Natl Acad Sci USA 100, 6777-6782.